

The Role of Cardiac Myocyte Dimensions in the Transition from Hypertensive Hypertrophy to Cardiac Dilatation

Raúl José Correia

Dissertation submitted to the Faculty of Health Sciences, University of the
Witwatersrand, Johannesburg, in fulfilment of the requirements for the degree of
Master of Science in Medicine

Johannesburg, 2010

DECLARATION

I, Raúl José Correia declare that this dissertation is my own, unaided work. It is being submitted for the degree of Master of Science in Medicine, in the Faculty of Medicine, University of the Witwatersrand, Johannesburg. The work contained in this thesis has not been submitted before for any degree or examination in this university, or any other university.

.....

RAÚL JOSÉ CORREIA

..... day of, 2010

I certify that the studies contained in this thesis have the approval of the Animal Ethics Committee of the University of the Witwatersrand, Johannesburg. The ethics approval numbers are: 97:44:5, 99:01:2b, 2002:37:5, 2002:39:5 and 2006:41:05.

.....

RAÚL JOSÉ CORREIA

..... day of, 2010

.....

ANGELA J. WOODIWISS (Supervisor)

.....

GAVIN R. NORTON (Supervisor)

Dedication:
For my parents,
Augusto and Jeanette
de Paiva Correia

PUBLICATIONS AND PRESENTATIONS

Data presented in this dissertation have been published in a manuscript of which I am third author, namely,

Veliotes DGA, Norton GR, Correia RJ, Strijdom H, Badenhorst D, Brooksbank R & Woodiwiss AJ (2010). Impact of aldosterone receptor blockade on the deleterious effects of adrenergic activation in hypertensive rats. *J Cardiovasc Pharmacol* **56**, 203-211.

In addition data presented in this dissertation have been presented in the form of an oral presentation, as well as in a poster at the 33rd Meeting of the Physiology Society of Southern Africa Conference in Cape Town, September 2005. The titles of these presentations were,

Correia RJ, Norton GR & Woodiwiss AJ. Cardiomyocyte lengthening does not contribute to the development of cardiac dilatation (oral presentation)

Woodiwiss A, Correia R, Norton G, Muller C & Strijdom H. Determination of cardiomyocyte length using flow cytometry (poster presentation)

ABSTRACT

The progression from compensated cardiac hypertrophy to decompensation and cardiac failure is accompanied by cardiac dilatation. As cardiac failure has a poor prognosis, it is imperative to prevent the progression to cardiac dilatation and heart failure. In this regard, an understanding of the mechanisms of cardiac dilatation is vital to guide optimal therapy to prevent heart failure. Although a number of factors have been shown to contribute to the development of cardiac dilatation, to date the role of alterations in cardiac myocyte dimensions remains unclear. Hence, the aim of the current study was to determine whether changes in cardiac myocyte dimensions contribute to the process of cardiac dilatation.

Methods: Two models of cardiac dilatation in pressure-overload induced cardiac hypertrophy were assessed. One model was a natural progression model, in which 18 spontaneously hypertensive rats (SHR), were assessed at 23 months of age (an age when left ventricular hypertrophy is noted to have progressed to left ventricular decompensation, dilatation and heart failure in approximately 50% of rats). The second model, a pharmacological model, was induced in 14 month old SHR (n=9) by chronic beta-adrenoreceptor activation [0.02mg/kg isoproterenol (ISO) twice daily for 4.5 months]. Chronic beta-adrenoreceptor activation in SHR, enhances the progression from compensated left ventricular hypertrophy to left ventricular dilatation. Nine normotensive Wistar Kyoto (WKY) rats were the controls for both models. Left ventricular dilatation was defined as an increase in left ventricular radius determined at controlled filling pressures using piezo-electric transducers. The classification of rats as being in heart failure was based upon the presence of pleuropericardial effusions and / or atrial thrombi. Cardiac myocytes were isolated and dimensions determined using both light microscopy and flow cytometry.

Results: Left ventricular radius was increased in SHR-Failure compared to SHR-Non-Failure ($p<0.01$), and in SHR-ISO compared to SHR-Control (saline administration) ($p<0.01$), hence confirming the presence of cardiac dilatation in both models. Although, cardiac myocyte length

was increased in all SHR groups compared to WKY ($p < 0.001$), no differences were observed between SHR-Failure and SHR-Non-Failure, or between SHR-ISO and SHR-Control. No differences in cell length:width ratios or in cell widths were evident between the groups. The flow cytometry data confirmed the results obtained for cardiac myocyte lengths using microscopy. Moreover, a linear correlation ($r = 0.46$, $p = 0.002$) between flow cytometry and microscopy cardiac myocyte lengths was observed. Importantly, no relationships were evident between left ventricular radius and cardiac myocyte length ($r = 0.12$, $p = 0.42$ and $r = 0.14$, $p = 0.35$ for microscopic and flow cytometry lengths respectively).

Conclusion: The results from the present study show that although pressure-overload hypertrophy is associated with lengthening of cardiac myocytes, no further changes occur with cardiac dilatation. Hence, alterations in cardiac myocyte dimensions do not contribute to the development of cardiac dilatation in pressure-overload models.

ACKNOWLEDGEMENTS

I am grateful for the assistance of the Central Animal Services of the University of the Witwatersrand. I would like to thank Mr Ernest Somya and Dr Oleg Osadchii for their invaluable assistance. I would also like to thank Prof. A Woodiwiss and Prof. G Norton for their guidance.

Funding for these studies was obtained from grants awarded to Prof. A Woodiwiss from the South African National Research Foundation, and to Prof. G Norton from the Medical Research Council of South Africa. The Cardiovascular Pathophysiology and Genomics Research Unit, the School of Physiology and Faculty of Health Sciences of the University of the Witwatersrand also supported these studies.

TABLE OF CONTENTS

<i>Declaration</i>	ii
<i>Dedication</i>	iii
<i>Publications and Presentations</i>	iv
<i>Abstract</i>	v
<i>Acknowledgements</i>	vii
<i>Table of Contents</i>	viii
<i>List of Figures</i>	x
<i>List of Tables</i>	xi
<i>Abbreviations</i>	xii
<i>Preface</i>	xiv
CHAPTER 1	1
1.0 INTRODUCTION	2
1.1 CARDIAC DILATATION AND HEART FAILURE	4
1.1.1 Definition of Cardiac Dilatation	6
1.1.2 Appropriate Measurements of Cardiac Dilatation	6
1.1.3 Role of Cardiac Dilatation in the Development of Heart Failure	9
1.1.4 How Does Cardiac Dilatation Produce Pump Dysfunction?	11
1.2 MEDIATORS OF CARDIAC HYPERTROPHY AND ADVERSE CARDIAC REMODELLING	13
1.2.1 Role of Neurohormones in Compensatory Cardiac Hypertrophy and the Progression to Cardiac Decompensation and Heart Failure	14
1.2.1.1 Role of the Sympathetic Nervous System	15
1.2.1.2 Role of the Renin-Angiotensin-Aldosterone System	18
1.2.2 Role of Growth Factors and Inflammatory Cytokines	19
1.2.3 Role of Stretch Receptors (Cardiac Myocyte Stretch)	20
1.3 PROPOSED MECHANISMS OF COMPENSATORY CARDIAC HYPERTROPHY	20
1.3.1 Role of Collagen and Interstitial Changes	20
1.3.2 Role of Cardiac Myocyte Hypertrophy Due to Increases in Cell Width	21
1.4 PROPOSED MECHANISMS OF ADVERSE CARDIAC REMODELLING	22
1.4.1 Role of Collagen and Interstitial Changes	23
1.4.2 Role of Cardiac Myocyte Apoptosis and Necrosis	24
1.4.3 Role of Cardiac Myocyte Hypertrophy Due to Increases in Cell Length	25
1.4.3.1 Are Changes in Cardiac Dimensions Associated with Changes in Cardiac Myocyte Length?	25
1.4.3.1.1 Data from Human Studies	25
1.4.3.1.2 Data from Animal Experimental Models	29
1.5 PROBLEM STATEMENT AND STUDY OBJECTIVES	35
CHAPTER 2	39
2.0 METHODS	40
2.1 RAT STRAINS AND GROUPS	40
2.1.1 Natural Progression Model	43
2.1.2 Pharmacological Model	43
2.2 SYSTOLIC BLOOD PRESSURE	44
2.3 LEFT VENTRICULAR GEOMETRY	44
2.3.1 Identification of Failure and Non-Failure Rats	48
2.4 TISSUE SAMPLING	49
2.5 MYOCYTE ISOLATION	50
2.6 LIGHT MICROSCOPY	52
2.7 FLOW CYTOMETRY	56

2.8 STATISTICAL ANALYSES	57
CHAPTER 3	62
3.0 RESULTS	63
3.1 LEFT VENTRICULAR GEOMETRY	63
3.1.1 Natural Progression Model	63
3.1.1.1 Body and Tissue Weights and Blood Pressures	63
3.1.1.2 LV Dimensions	63
3.1.2 Pharmacological Model	66
3.1.2.1 Body and Tissue Weights	66
3.1.2.2 LV Dimensions	68
3.2 MYOCYTE DIMENSIONS	68
3.2.1 Natural Progression Model	68
3.2.1.1 Light Microscopy	68
3.2.1.2 Flow Cytometry	71
3.2.2 Pharmacological Model	74
3.2.2.1 Light Microscopy	75
3.2.2.2 Flow Cytometry	78
3.3 CORRELATIONS	78
3.3.1 Left Ventricular End Diastolic Radius and Cardiac Myocyte Length	78
3.3.2 Cardiac Myocyte Lengths Obtained Using Light Microscopy versus Flow Cytometry	78
3.3.3 Left Ventricular Weight (mg/100g Body Weight) versus Cardiac Myocyte Length	82
CHAPTER 4	84
4.0 DISCUSSION	85
CHAPTER 5	94
5.0 REFERENCES	95
APPENDICES (Animal Ethics Screening Committee Clearance Certificates)	116

LIST OF FIGURES

Figure	Page
<u>Chapter 1</u>	
1.1 Example of a right-shift in the diastolic pressure-volume relationship	7
1.2 Example of changes in the Frank-Starling relationship	12
1.3 Schematic representation showing possible mechanisms of cardiac dilatation	16
1.4 Schematic representation of the factors known to contribute to cardiac dilatation	37
<u>Chapter 2</u>	
2.1 Flow chart detailing the groups of rats	42
2.2 Intraventricular pressure monitoring and piezo-electric ultrasonic transducers	46
2.3 Example of recordings of left ventricular external diameter measurements	47
2.4 Examples of isolated cardiac myocytes	53
2.5 Photograph of digital camera and microscope	54
2.6 An example of striations of an isolated cardiac myocyte	55
2.7 Flow cytometer	58
2.8 Example of flow cytometer dot plot	59
2.9 Diagrammatic representation of a cardiac myocyte in the path of the flow cytometer laser beam	60
2.10 Plot of cardiac myocyte counts versus time of flight	61
<u>Chapter 3</u>	
3.1 Left ventricular end diastolic radius – pressure relations in the natural progression model	65
3.2 Left ventricular end diastolic wall thickness to radius ratio – pressure relations in the natural progression model	67
3.3 Left ventricular end diastolic radius – pressure relations in the pharmacological model	69
3.4 Left ventricular end diastolic wall thickness to radius ratio – pressure relations in the pharmacological model	70
3.5 Cardiac myocyte lengths and frequency distribution of cardiac myocyte lengths in the natural progression model	72
3.6 Cardiac myocyte widths and length to width ratios in the natural progression model	73
3.7 Cardiac myocyte lengths as assessed by flow cytometry in the natural progression model	74
3.8 Cardiac myocyte lengths and frequency distribution of cardiac myocyte lengths in The pharmacological model	76
3.9 Cardiac myocyte widths and length to width ratios in the pharmacological model	77
3.10 Cardiac myocyte lengths as assessed by flow cytometry in the pharmacological model	79
3.11 Linear correlation analyses between left ventricular end diastolic radius and cardiac myocyte length	80
3.12 Linear correlation analysis between cardiac myocyte length measured using light microscopy and flow cytometry	81
3.13 Linear correlation analyses between left ventricular weight normalised to 100g body weight and cardiac myocyte length as assessed by light microscopy and flow cytometry	83

LIST OF TABLES

Table	Page
<u>Chapter 1</u>	
1.1 Summary of human data addressing possible association of cardiac remodelling with alterations in myocyte morphology	26
1.2 Summary of data from animal experimental models addressing possible association of cardiac remodelling with alterations in myocyte morphology	30
<u>Chapter 3</u>	
3.1 Body and tissue weights in the natural progression model and in the pharmacological model	64

ABBREVIATIONS

ACE – Angiotensin-converting enzyme

AESC – Animal ethics screening committee

ANOVA – Analysis of variance

ATP – Adenosine triphosphate

CaCl₂ – Calcium chloride

cAMP – Cyclic adenosine monophosphate

CAS – Central animal service

CHF – Congestive heart failure

CO₂ – Carbon dioxide

EDP – End-diastolic ventricular pressure

EDV – End-diastolic ventricular volume

ESV - End-systolic ventricular volume

HEPES- (4-(2-hydroxyethyl)-piperazine-1-ethanesulfonic acid hemisodium salt

HOCM –Hypertrophic obstructive cardiomyopathy

h/r – relative wall thickness; i.e. LVED wall thickness to LVED radius ratio

IDCM - Idiopathic dilated cardiomyopathy

ISO - Isoproterenol

KCl – Potassium chloride

KH₂PO₄ – Potassium dihydrogen phosphate

LV – Left ventricle

LVAD – Left ventricular assist device

LVDP – Left ventricular diastolic pressure

LVED – Left ventricular end-diastolic

LVEDh – Left ventricular end-diastolic wall thickness

LVEDP – Left ventricular end-diastolic pressure

LVEDr – Left ventricular end-diastolic radius

LVEF – Left ventricular ejection fraction

LVextD – Left ventricular external diameter

MI – Myocardial infarction

MgCl₂ – Magnesium chloride

NaCl – Sodium chloride

NaOH – Sodium hydroxide

O₂ - Oxygen

PNS – Parasympathetic nervous system

PSS - Physiological saline solution

RAAS – Renin-angiotensin-aldosterone system

SBP – Systolic blood pressure

SEM – Standard error of the mean

SHHF – Spontaneously hypertensive heart failure

SHR – Spontaneously hypertensive rat

SNS – Sympathetic nervous system

TNF- α - Tumour Necrosis Factor- α

WKY - Wistar-Kyoto

PREFACE

Cardiovascular disease is one of the leading causes of morbidity and mortality in all parts of the world today. Almost all forms of cardiovascular disease progress to heart failure, which is the terminal endpoint of cardiovascular diseases. Hence, the progression to heart failure needs to be prevented. Chronic cardiovascular disease is initially accompanied by cardiac hypertrophy which is considered compensatory in that cardiac wall stress is maintained within normal levels; however compensatory cardiac hypertrophy progresses to cardiac decompensation and heart failure, a state in which cardiac wall stress is elevated. The increase in cardiac wall stress is primarily due to enlargement of the cardiac chamber volume and thinning of the cardiac chamber wall, a process termed detrimental cardiac remodelling or dilatation. As cardiac failure has a poor prognosis, it is imperative to prevent the progression to cardiac dilatation and heart failure. In this regard, an understanding of the mechanisms of cardiac dilatation is vital to guide optimal therapy to prevent heart failure.

The mechanisms by which the cardiac tissue remodels to cause the dilatation are the topic of much debate. Both changes in the cardiac interstitium as well as changes in the cardiac myocytes are believed to play a role. In previous studies, adverse cardiac remodelling has been associated with increased cardiac interstitial fibrosis, but of the non-cross-linked form; cardiac myocyte apoptosis and necrosis; as well as cardiac myocyte hypertrophy due to changes in cell length. Although, some consensus has been reached regarding the role of the cardiac interstitium and cardiac myocyte death (apoptosis or necrosis); to date the role of alterations in the dimensions of cardiac myocytes remains unclear.

Although, cardiac dilatation is thought to be mediated by increases in the length of cardiac myocytes, not all studies support this hypothesis. Indeed, although some studies show that increases in cardiac myocyte length are associated with increases in cardiac chamber dimensions or heart failure; a number of other studies show no relationship. Furthermore, data from

intervention studies failed to show changes in cardiac dimensions in parallel with changes in cardiac myocyte length. A number of reasons may explain the controversial results regarding the role of alterations in cardiac myocyte length in cardiac dilatation.

Firstly, in some studies the increased cardiac myocyte length in patients with heart failure compared to healthy controls could be as a consequence of the differences in body weight and hence left ventricular (LV) weight between these two groups. The differences in body weight were due to a greater proportion of males in the heart failure group compared to the control group.

Secondly, as the phase of the cardiac cycle determines cardiac chamber dimensions and cardiac myocyte length, possible differences between the heart failure and control groups in the phase of the cardiac cycle at the time of cardiac arrest may account for the differences in cardiac chamber diameter and cardiac myocyte length observed between these two groups in some human studies.

Thirdly, in a number of studies in spontaneously hypertensive heart failure (SHHF) rats showing an association between cardiac myocyte length and cardiac chamber dimension, the animals in heart failure were significantly older than the control animals. As LV weight increases with age in hypertensive rats, and cardiac myocyte length is strongly associated with age and LV weight, the increases in cardiac myocyte length observed in the rats in heart failure may reflect age induced changes, rather than an association with adverse chamber remodelling (cardiac dilatation) and the development of heart failure.

Fourthly, other than the studies in SHHF rats, no other studies have made direct comparisons of animals with cardiac pathology which have heart failure to animals with the same cardiac pathology but without heart failure. However, as discussed the increased cardiac myocyte length in SHHF rats may reflect increased age and hence increased LV weight compared to controls, rather than increased cardiac dimensions. Indeed, it has been shown that cardiac myocyte lengthening increased with age and occurred well before the development of heart failure in SHHF rats. Although the latter study suggests that changes in cardiac myocyte length are not responsible for

the development of heart failure, no measurements of cardiac dimensions were made in this study. To my knowledge no study to date has compared age-matched animals with the same cardiac pathology which have heart failure to those without heart failure.

Lastly, the use of load dependent measures of cardiac chamber dimensions (echocardiography *in vivo*) in the presence of increased preloads may also contribute to the controversy. In this regard cardiac myocyte lengthening occurs as a consequence of the stretching of cardiac myocytes during increased preloads (filling volume or pressure). Moreover, when pulmonary capillary wedge pressure was normalised as a consequence of LV assist device support, a normalisation of both LV end diastolic diameter and cardiac myocyte length has been reported.

Moreover, data from various intervention studies failed to show changes in cardiac dimensions in parallel with changes in cardiac myocyte length and hence the results of these studies do not support a role of changes in cardiac myocyte length in cardiac dilatation. Indeed, if increases in cardiac myocyte length were causally related to adverse cardiac remodelling, a reduction in cardiac myocyte length should be accompanied by a decrease in cardiac chamber dimensions. However, these intervention data need to be interpreted with caution in view of the use of load dependent measures of cardiac dimensions in these studies.

The data to date provides no clear conclusion as to the possible role of cardiac myocyte length in adverse chamber remodelling. Hence, the aim of the current study was to determine whether changes in cardiac myocyte length contribute to the progression from compensatory cardiac hypertrophy to adverse chamber remodelling (cardiac dilatation) as measured using load independent methods in rats with heart failure compared to those not in heart failure.

CHAPTER 1

1.0 INTRODUCTION

One of the leading causes of morbidity and mortality in all parts of the world today is cardiovascular disease (American Heart Association, 2010). Over 80 million adults (more than one in three), in America alone have some form of cardiovascular disease (American Heart Association, 2010). Moreover, cardiovascular disease accounts for 16,7 million of deaths (29.2%) worldwide per annum (Frey *et al.*, 2004). In South Africa, cardiovascular disease was reported to account for ~90 to 100 deaths per 100 000 population in 2006 (Mayosi *et al.*, 2009). In addition, of the total cases reported on in a cardiology unit, at a hospital that services an urban developing community in South Africa, 43% were *de novo* presentations of heart failure (Stewart *et al.*, 2008). Importantly, almost all forms of cardiovascular disease progress to heart failure, which is the terminal endpoint of cardiovascular diseases. Hence, the progression to heart failure needs to be prevented.

In order to adequately prevent morbidity and mortality from heart failure, an understanding of the mechanisms underlying the progression to heart failure are paramount. In this regard a number of different models of heart failure have been investigated. A major predictor of progressive heart disease and an adverse prognosis is cardiac hypertrophy (Levy *et al.*, 1990). Although, cardiac hypertrophy is initially a compensatory response to alterations in loading conditions (Grossman *et al.*, 1975), prolonged hypertrophy ultimately leads to cardiac dilatation (increase in cardiac chamber dimensions), heart failure and subsequent death (Bing *et al.*, 1995; Inoko *et al.*, 1994; Lorell 1997; Spann *et al.*, 1967). Factors which have been associated with the development of cardiac dilatation and heart failure (decompensation) in various models of cardiac hypertrophy, include unfavourable changes in the cardiac interstitium; enhanced cardiac myocyte apoptosis and necrosis; realignment of cardiac

myocytes within the ventricular walls (myocardial slippage) expression of foetal genes; and alterations in cardiac myocyte dimensions (Cohn *et al.*, 2000; Ferrari *et al.*, 2009; Frigerio & Roubina, 2005; Remme 2003). These changes occur in response to sustained pathological stress signals such as neurohumoral activation, the release of growth factors and inflammatory cytokines, and mechanical stretch (Cohn *et al.*, 2000; Ferrari *et al.*, 2009; Frigerio & Roubina, 2005; Remme 2003). These pathological signals are termed the mediators of adverse cardiac remodelling.

Despite a plethora of studies investigating the various factors associated with the development of heart failure, the role of alterations in cardiac myocyte dimensions in the progression from compensatory cardiac hypertrophy to cardiac dilatation is unclear. In this regard, compensatory cardiac hypertrophy is generally associated with increases in cardiac myocyte width (Onodera *et al.*, 1998; Zierhut *et al.*, 1991); whereas alterations in cardiac myocyte length are thought to contribute to cardiac dilatation (Gerdes 2002). However, most studies showing increases in cardiac myocyte length in association with increases in left ventricular (LV) dimensions have used load dependent measures of cardiac chamber dimensions (Chen *et al.*, 2010; Gerdes *et al.*, 2010; Kajstura *et al.*, 1995; Tamura *et al.*, 1998; Wang *et al.*, 1999; Yarbrough *et al.*, 2010). Thus whether cardiac dilatation has indeed occurred in these studies is debatable. Moreover, although in some studies increases in load dependent measures of cardiac chamber diameter are associated with increases in cardiac myocyte dimensions (Gerdes *et al.*, 2010; Janczewski *et al.*, 2003; Kajstura *et al.*, 1995; Schultz *et al.*, 2007; Tamura *et al.*, 1998; Toischer *et al.*, 2010; Wang *et al.*, 1999); other studies fail to show such relationships (Li *et al.*, 2010; Schultz *et al.*, 2007; Tamura *et al.*, 2000; Yarbrough *et al.*, 2010). Nevertheless, an understanding of the role of cardiac myocyte hypertrophy in cardiac dilatation is essential to guide choices of optimal therapy to prevent

the progression from compensatory hypertrophy to decompensation.

Hence, the aim of my studies was to determine the role of alterations in cardiac myocyte dimensions in the progression from concentric cardiac hypertrophy to cardiac dilatation. As the most prevalent form of heart failure is that associated with hypertensive heart disease (Remme *et al.*, 2003), I chose to assess two models of cardiac dilatation in spontaneously hypertensive rats (SHR) with cardiac hypertrophy. Therefore, in the present chapter of my dissertation, I will discuss the role of cardiac dilatation in the development of heart failure and the importance of defining cardiac dilatation using load independent measurements. I will then review the literature on the factors (mediators and mechanisms) associated with the development of cardiac hypertrophy and the progression to decompensation and heart failure, with specific reference to the controversial role of alterations in cardiac myocyte dimensions.

1.1 CARDIAC DILATATION AND HEART FAILURE

In response to chronic elevations in cardiac wall stress (increases in loading conditions, such as chronic hypertension or post myocardial infarction), the heart undergoes hypertrophy (thickening of the ventricular wall) in an attempt to normalise wall stress. According to the law of La Place, wall tension or stress, is proportional to the product of pressure (P) and radius (r) and inversely proportional to wall thickness (h). Hence, an increased wall thickness in cardiac hypertrophy maintains a normal wall stress in the presence of increments in either pressure or volume (radius) within the cavity (Grossman *et al.*, 1975). This process, termed compensatory cardiac hypertrophy, is generally associated with adequate cardiac systolic function, and a normal or increased ventricular wall thickness to radius ratio (Janicki *et al.*, 2004). However, diastolic function may be decreased due to the restriction of ventricular

filling by a thickened ventricular wall (Kai *et al.*, 2005; Norton *et al.*, 1993). The development of compensatory hypertrophy is due to the load-induced activation of various mediators which initiate cellular, molecular and genetic processes.

As will be discussed in more detail later, persistent activation of these mediators over time, and consequently alterations in cellular, molecular and genetic processes eventually leads to cardiac decompensation (Remme, 2003). Cardiac decompensation is associated with a reduced ventricular wall thickness to radius ratio, ventricular enlargement and depressed cardiac systolic function (Janicki *et al.*, 2004). This process of adverse cardiac remodelling (reduced ventricular wall thickness to radius ratio and ventricular enlargement), also termed cardiac dilatation, progresses with time to heart failure. Hence, cardiac dilatation is an important negative prognostic factor in patients with heart failure (Cohn *et al.*, 2000; Udelson *et al.*, 2002). Moreover, even in asymptomatic subjects without a prior history of heart failure, LV dilatation is associated with an increased risk of the development of heart failure (Vasan *et al.*, 1997). It is therefore important to understand how cardiac remodelling contributes to the development of heart failure.

One of the limitations of many studies assessing the role of cardiac remodelling in heart failure, and the mechanisms thereof, is the inability to define cardiac dimensions in a load-independent model. In this regard, increases in cardiac filling volumes (increased preloads) would manifest as increased cardiac dimensions. Moreover, increases in cardiac afterload (increased cardiac wall stress as discussed above) would reduce stroke volume thereby increasing ventricular volumes at the end of systole, which would also manifest as increased cardiac dimensions. Hence, the correct definition of cardiac remodelling is an increase in cardiac diameter, or a decrease in the wall thickness to radius ratio, at a given filling volume.

Therefore, before discussing the impact of cardiac dilatation on cardiac function and the development of heart failure, I will first discuss in more detail the definition of cardiac dilatation and appropriate measurements thereof.

1.1.1 Definition of Cardiac Dilatation

Cardiac chamber dilatation is defined as an increase in chamber cavity volume or dimension as a consequence of a right shift in the diastolic pressure-volume relationship (Figure 1.1). Importantly, cardiac dilatation is not an increase in only the chamber cavity volume, as this may result from an enhanced blood volume or venous return (increased preload) without necessarily being accompanied by a right shift in the diastolic pressure-volume relationship. In addition, cardiac dilatation is not a right shift in the diastolic pressure-volume relationship produced by alterations in the slope of this relationship. Changes in the slope of the cardiac diastolic pressure-volume relationship occur as a consequence of alterations in chamber stiffness, which are usually mediated by modifications in the material properties of the myocardium (Gilbert and Glantz, 1989). However, cardiac chamber dilatation is the consequence of a right shift in the diastolic pressure-volume relationship due to an increase in the volume intercept of this relationship (Gibbs *et al.*, 2004) (Figure 1.1).

1.1.2 Appropriate Measurements of Cardiac Dilatation

As increases in blood volume, venous return, and blood pressure (may decrease stroke volume); and decreases in cardiac contractility can result in increases in ventricular volumes, it is important that filling volumes are controlled when determining the relationship between diastolic pressure and volume. Hence, the *in vivo* assessment of the diastolic pressure-volume relationship using echocardiographic measures of cardiac dimensions is not appropriate. Indeed, blood volumes are related to body size, which may differ between for example

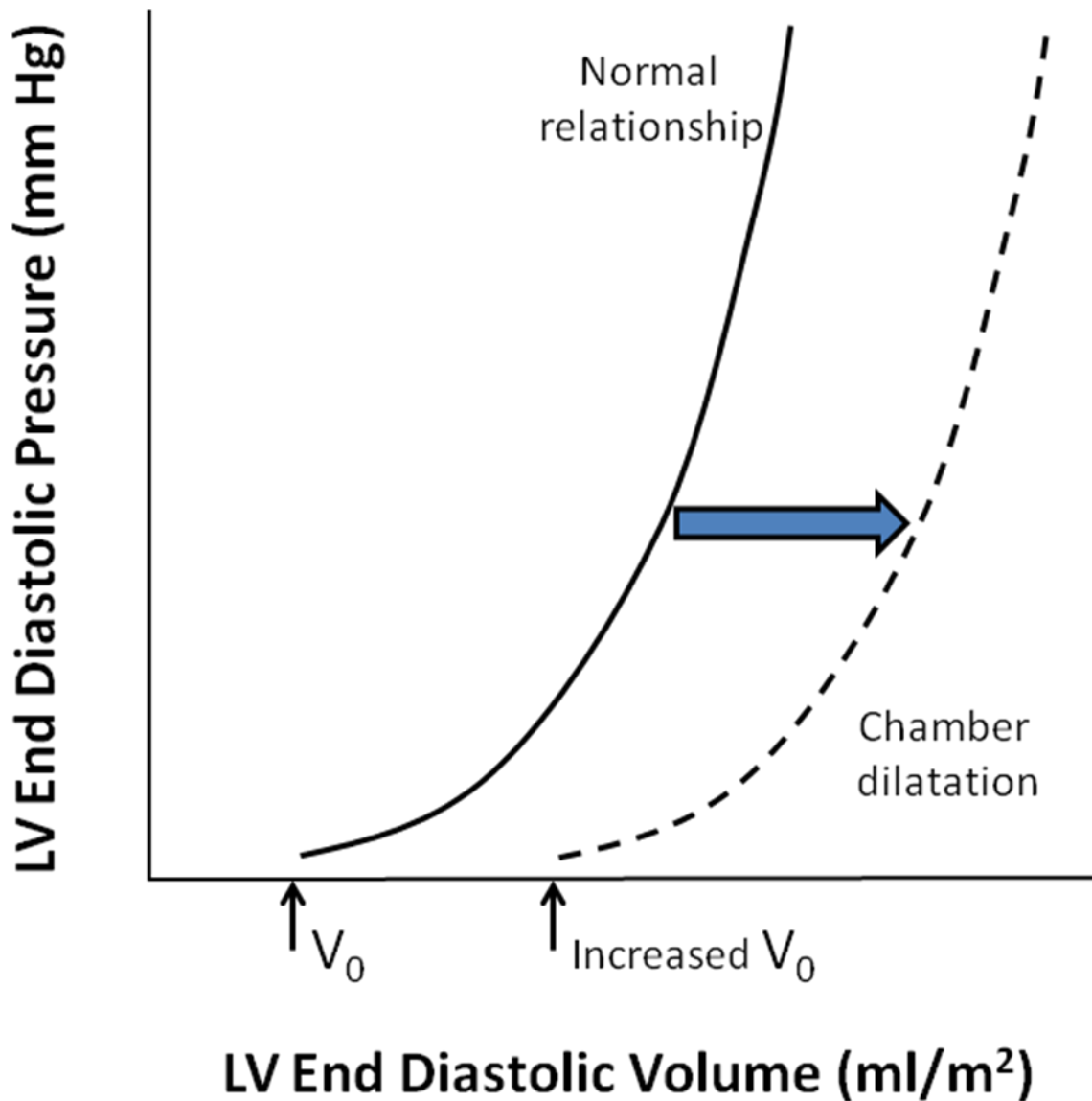


Figure 1.1 Example of a right-shift in the diastolic pressure-volume relationship

The normal diastolic pressure-volume relationship is indicated by the solid line, and a right shift in the pressure-volume relationship, indicative of cardiac dilatation, is indicated by the dashed line. The volume intercept [volume at which left ventricular (LV) end diastolic pressure equals zero (V_0)] is increased in the right shifted relationship.

normotensive and hypertensive rats (Badenhorst *et al.*, 2003a; Tsotetsi *et al.*, 2001; Veliotes *et al.*, 2005). In addition, increases in cardiac afterload, such as increases in blood pressure or peripheral resistance in hypertension, would reduce stroke volume and hence increase filling volumes (more blood is left behind at the end of systole). Moreover, the measurement of cardiac dimensions alone, without the measurement of the accompanying diastolic pressures is not appropriate. Indeed, as diastolic pressure increases, so does diastolic volume (Figure 1.1). Hence, increases in chamber dimensions may be a manifestation of increases in filling pressures (increased preload) rather than measures of true cardiac dilatation.

Nevertheless, many clinical and experimental studies have defined the presence of dilatation using non-invasive measurements such as echocardiography and ventriculography. Hence, whether cardiac dilatation was indeed present is questionable. Indeed increases in filling pressures were noted in many of these studies (Chen *et al.*, 2010; Gerdes *et al.*, 2010; Kajstura *et al.*, 1995; Tamura *et al.*, 1998; Wang *et al.*, 1999; Yarbrough *et al.*, 2010; Zefeiridis *et al.* 1998). Although in clinical studies there is no alternative to non-invasive measurements; of greater concern is the use of such measurements in terminal experimental studies. In this regard, in many animal based studies, the groups differ in age (Gerdes *et al.*, 1996; Tamura *et al.*, 1998). As age is associated with increased LV weight (Gerdes *et al.* 1996), and increased left ventricular weight is correlated with cardiac myocyte length (Campbell *et al.* 1991; Capasso *et al.* 1992), and age (Tamura *et al.*, 1998), any differences in cardiac dimensions could be attributed to differences in age and hence heart weight rather than true differences in the dimensions of the heart. In other words the increased left ventricular weight and hence cardiac myocyte length is likely to reflect growth effects during aging.

Therefore, in order to appropriately define the presence of cardiac dilatation, ventricular pressures need to be determined and ventricular filling volumes need to be controlled. In this manner the diastolic pressure-volume relationship can be constructed and hence the volume at which pressure is 0 mm Hg (ie. the volume intercept) can be determined. Importantly, very few studies have accurately defined dilatation using pressure-volume relationships. In this regard, no study assessing the role of cardiac myocyte dimensions in heart failure, has accurately defined the presence of dilatation.

1.1.3 Role of Cardiac Dilatation in the Development of Heart Failure

Initially it was thought that cardiac dilatation was a remodeling process that began in order to prevent the progressive increases in filling pressures associated with heart failure (Ertl *et al.*, 1991). In essence, it was believed that the decreased contractility in heart failure and hence increased filling volumes (Patterson and Adams, 1996), were necessary in order to maintain stroke volume via the Frank-Starling effect (Grossman *et al.*, 1975). However, the increased filling volumes would be accompanied by increases in filling pressures and hence pulmonary capillary hydrostatic pressures may be elevated resulting in pulmonary congestion. It was therefore believed that in order to accommodate enhanced filling volumes at normal filling pressures a right shift in the diastolic pressure-volume occurred.

However, more recently, cardiac dilatation has been shown to be a precursor of pump dysfunction and clinical heart failure (Gaudron *et al.*, 1993; Pfeffer *et al.*, 1992; Vasan *et al.*, 1997). In a 3 year prospective study in patients post myocardial infarction, those patients who had progressive dilatation also had a progressive decline in ejection fraction and an increase in pulmonary capillary wedge pressure (Gaudron *et al.*, 1993); whereas in those patients with no dilatation, LV ejection fraction did not decline and pulmonary wedge pressure remained

within normal values. Hence cardiac dilatation post myocardial infarction results in the development of heart failure. In addition, in an 11-year follow-up study of people who had not sustained a myocardial infarction and who did not have congestive heart failure at enrolment, increments in LV internal dimension increased the risk of development of congestive heart failure (adjusted hazard ratio of 1.47 for a one standard deviation increase in LV end diastolic diameter indexed for height) (Vasan *et al.*, 1997). Moreover, intervention studies have shown that the alleviation of LV enlargement post myocardial infarction prolongs survival and reduces mortality and morbidity due to major cardiovascular events (Pfeffer *et al.*, 1992; St John Sutton *et al.*, 1997). Hence, the process of cardiac dilatation has to be seen as a cause of heart failure as opposed to its consequence.

There are a number of additional observations which support the role of cardiac dilatation in the development of heart failure. Firstly, in the presence of compensatory cardiac hypertrophy (increases in wall thickness) in response to pressure overload, there is no evidence of systolic heart failure (Wang *et al.*, 1999; Onodera *et al.*, 1998; Woodiwiss *et al.*, 1995; Yousef *et al.*, 2000). Secondly, the neurohumoral factors that maintain systolic function in the hypertrophied heart, in the long-term are detrimental to the myocardium. Indeed, these neurohumoral factors promote cardiac dilatation and ultimately lead to systolic dysfunction (Woodiwiss *et al.*, 1995; Yousef *et al.*, 2000). Lastly, there is evidence to show that maladaptive changes in myocardial tissue occur long before symptoms of heart failure (Onodera *et al.*, 1998). Hence adverse cardiac remodelling, which consists of both macroscopic and microscopic changes in the myocardium, precedes heart failure and therefore contributes to, instead of results from, heart failure (Onodera *et al.*, 1998). The question of how cardiac dilatation produces pump dysfunction and heart failure therefore arises.

1.1.4 How Does Cardiac Dilatation Produce Pump Dysfunction?

Changes in pump function are best explained by the Frank-Starling relationship. Figure 1.2 illustrates the normal Frank-Starling relationship and the changes that occur in association with either an enhanced pump function or a decreased pump function. A left and upward shift of the curve compared to normal (an enhanced pump function) occurs when intrinsic myocardial contractility increases (such as in the presence of increased circulating catecholamines as may occur with exercise); or afterload decreases (such as following vasodilatation); or the relationship between wall thickness and internal radius increases (such as with compensatory cardiac hypertrophy). In contrast, displacement to the right and downward from the normal occurs when ventricular contractility is depressed; or afterload is increased; or the heart dilates as is the case in most forms of heart failure due to systolic functional abnormalities. Although the impact of changes in intrinsic myocardial contractility and the resistance to blood flow on systolic function, are relatively easy concepts to grasp, cardiac dilatation is sometimes a conceptually difficult issue. Hence, how does cardiac dilatation produce deleterious effects on pump function?

As chamber dilatation is associated with an increased cavity volume (and hence radius), and a reduced wall thickness, according to La Place's law, wall tension or stress (afterload) will be increased. As wall stress determines myocardial oxygen consumption, the myocardial oxygen demand-to-supply ratio may be increased in a dilated ventricle, and a demand-to-supply mismatch may subsequently decrease cardiac contraction. However, when systolic function was measured using a stress (or load)-independent measure of pump function (end systolic elastance) in an animal model of congestive cardiac failure and pump dysfunction associated with massive cardiac dilatation (Norton *et al.*, 2002), pump function was reduced without parallel changes in myocardial contractility. These data would suggest that a mechanism

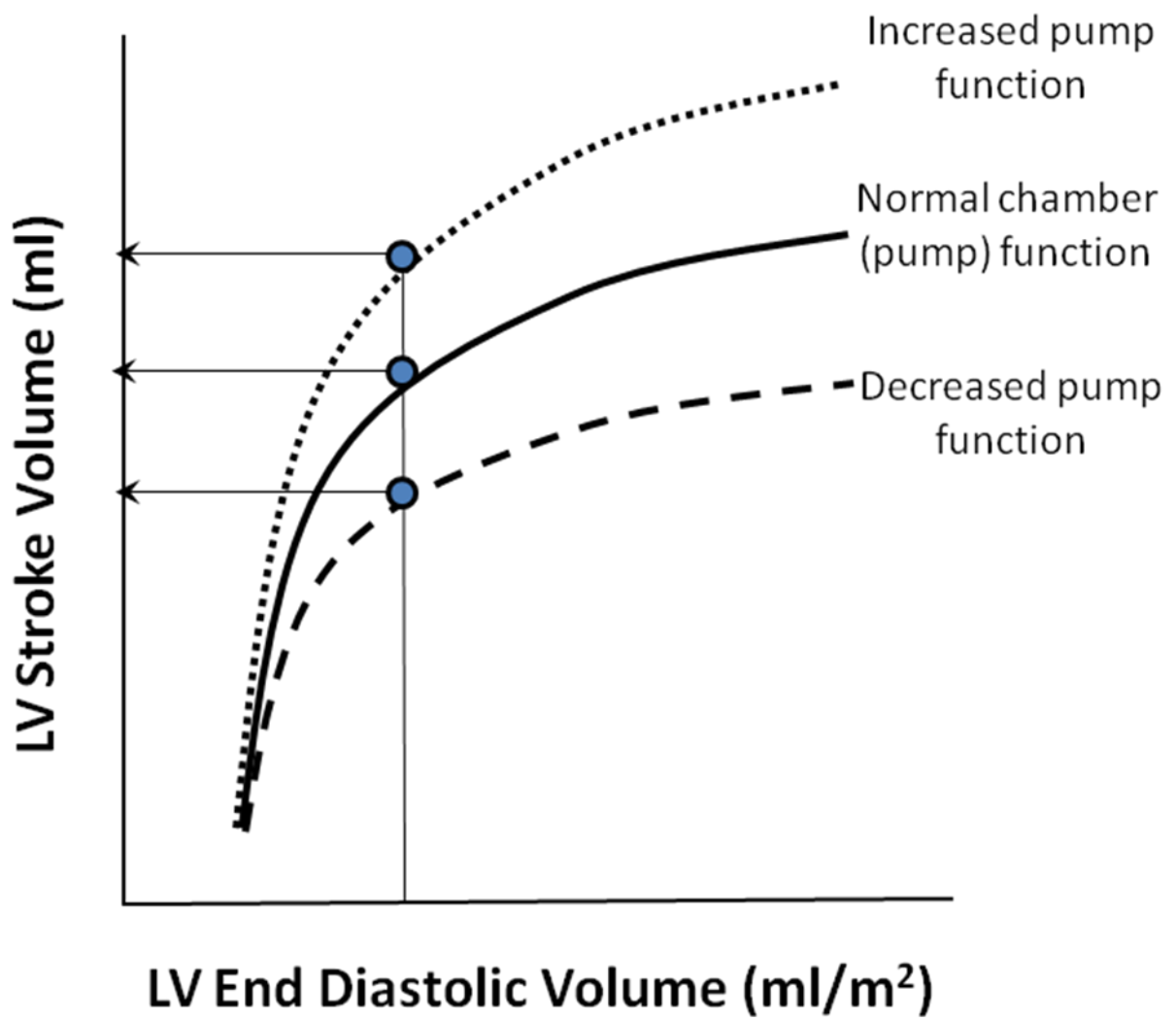


Figure 1.2 Example of changes in the Frank-Starling relationship

unrelated to stress or load-induced effects contributes to pump dysfunction in cardiac dilatation. It is possible that inappropriate force transduction occurs in dilated ventricles during myocyte contraction, which in-turn leads to pump dysfunction (Sallin 1969). Alternatively, in a dilated ventricle, larger chamber volumes may be required to produce cardiomyocyte stretch and hence to recruit the Frank-Starling effect. Indeed, when the structure of the ventricle changes, the mechanics of systolic output are affected, thus resulting in a low-output state (Laskey *et al.*, 1984; Cohn *et al.*, 2000).

Having established that cardiac dilatation is a cause rather than a consequence of pump dysfunction and heart failure; in order to reduce morbidity or mortality from progressive heart failure treatments which prevent or reverse adverse cardiac remodelling are required. The choice of effective therapy is based on the knowledge of the mediators and the mechanisms responsible for cardiac remodelling. I will therefore discuss what is known to date regarding the mediators of cardiac dilatation and the role of various potential mechanisms.

1.2 MEDIATORS OF CARDIAC HYPERTROPHY AND ADVERSE CARDIAC REMODELLING

The generally accepted theory is that the mediators responsible for compensatory cardiac hypertrophy, when sustained are ultimately responsible for the progression to adverse cardiac remodelling and heart failure. I will therefore discuss what is known regarding the mediators of compensatory hypertrophy as well as the how these factors are thought to mediate cardiac dilatation and the development of heart failure.

Compensatory cardiac hypertrophy and cardiac dilatation occur due to the independent and interactive effects of three extrinsic mediators on the heart, namely: (1) neurohormones; (2) growth factors and inflammatory cytokines; and (3) mechanical stretch receptors in the cell membranes, which activate signalling pathways intracellularly (Cohn *et al.*, 2000; Ferrari *et al.*, 2009; Frigerio & Roubina, 2005; Remme 2003).

These extrinsic mediators act via various intracellular pathways [mitogen activated protein (MAP) kinase; nuclear factor κ B; protein kinase B] to activate nuclear transcription, which leads to cellular hypertrophy, necrosis, apoptosis and fibrosis (Katz 2002; Opie *et al.*, 2006; Yousef *et al.*, 2000). The nature of the signalling stimulus is believed to determine which intracellular pathways are activated and hence whether compensatory cardiac hypertrophy or cardiac dilatation occurs (Ferrari *et al.*, 2009; Hill & Olson 2008; Opie *et al.*, 2006).

1.2.1 Role of Neurohormones in Compensatory Cardiac Hypertrophy and the Progression to Cardiac Decompensation and Heart Failure

Neurohormonal activation [activation of the sympathetic nervous system (SNS) and the renin-angiotensin-aldosterone system (RAAS)] is known to occur in response to increases in cardiac wall stress. Indeed, circulating concentrations of noradrenaline are increased in persons with hypertension and LV hypertrophy (Agabiti-Rosei *et al.*, 1987; Kelm *et al.*, 1996). In addition, the RAAS is activated in the hypertrophied and failing heart (Danser *et al.*, 1997; Iwai *et al.*, 1995). Initially, the increased activity of the SNS and RAAS occur in order to normalise wall stress and to preserve contractile performance; however continual activation of the SNS (Badenhorst *et al.*, 2003b; Gibbs *et al.*, 2004; Veliotes *et al.*, 2005) and

the RAAS (Mizuno *et al.*, 2001; Schunkert *et al.*, 1993) have been shown to induce cardiac dilatation and heart failure. Indeed, neurohumoral activation in heart failure (Hasking *et al.*, 1986), is a major factor responsible for the progression of heart failure (Bristow 1997; Cohn *et al.*, 1984).

1.2.1.1 Role of the Sympathetic Nervous System

Initially in compensatory hypertrophy, in response to increased catecholamines, the inotropy of the cardiac myocytes is increased through post receptor activation of adenylate cyclase and consequent increases in the intracellular concentration of the second messenger cyclic adenosine monophosphate (cAMP). This response will improve the cardiac output through an increased myocardial contraction. However, sustained elevations in catechoamines in the presence of increased pressure loads will increase myocardial oxygen demand (a consequence of increased inotrope as well as increased afterload, due to alpha adrenergic mediated vasoconstriction), which may outstrip myocardial oxygen supply, as increased vascularisation does not occur in parallel with myocardial hypertrophy (Weisman *et al.*, 1988). One of the consequences of oxygen demand-to-supply imbalance is tissue necrosis. As cardiac myocytes within the syncytium die, the viable cardiac myocytes within the syncytium are stretched hence possibly resulting in side-to-side slippage and ultimately cardiac dilatation (Figure 1.3). Indeed, myocyte slippage in end stage dilated cardiomyopathy has been well documented (Beltrami *et al.*, 1995; Linzbach 1960).

Sustained (or chronic) activation of the SNS not only induces cardiac myocyte death through hemodynamic mechanisms as described above, but also via direct mechanisms. Indeed, excessive concentrations of adrenergic agonists promote necrosis (Esler *et al.*, 1997) and apoptosis (Communal *et al.*, 1998; Singh *et al.*, 2001). Adrenergic-induced cardiac myocyte

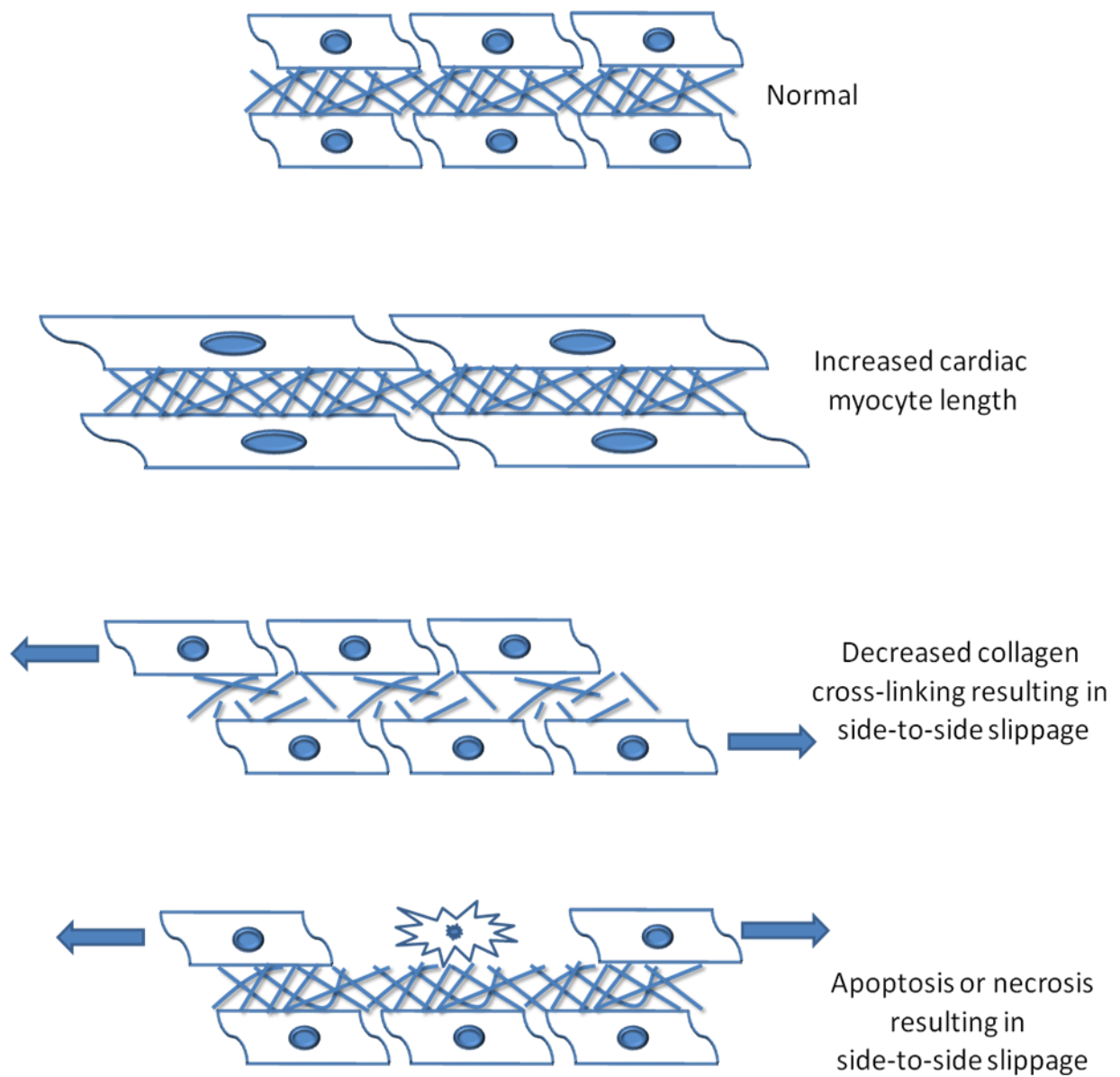


Figure 1.3 Schematic representation showing possible mechanisms of cardiac dilatation.

apoptosis is mediated via activation of β 1-adrenergic receptor cAMP-dependent protein kinase A and mitogen-activated protein kinase (MAPK) pathways. Adrenergic activation may also promote cardiomyocyte apoptosis indirectly via stimulation of the RAAS (see 1.2.1.2 below) or through increases in myocardial expression of inflammatory cytokines (see 1.2.2 below). Similar to necrosis the consequences of apoptosis are stretching of the viable cardiac myocytes within the syncytium are stretched hence possibly resulting in side-to-side slippage and ultimately cardiac dilatation (Figure 1.3). In addition to cardiac myocyte death, chronic β -adrenergic activation results in unfavourable alterations in the cardiac interstitium, which result in decreased tethering of the cardiac myocytes (Figure 1.3). Indeed, as will be discussed below (see 1.4.1) increases in the non-cross-linked collagen content of the myocardium have been demonstrated in association with cardiac dilatation after chronic administration of the β -adrenergic agonist isoproterenol (Woodiwiss *et al.*, 2001). Although, isoproterenol, has been shown to stimulate the activity of matrix metalloproteinases (MMPs) in isolated cardiac myocytes (Coker *et al.*, 2001), which would increase collagen turnover thereby reducing time available for cross-linking to occur (Woodiwiss *et al.*, 2001); it is more likely that the changes in the characteristics of myocardial collagen are mediated by activation of the RAAS, as the decreased collagen cross-linking could be prevented by both angiotensin-converting enzyme inhibitor administration (Woodiwiss *et al.*, 2001) as well as aldosterone receptor blockade (Veliotes *et al.*, 2005).

Although, adrenergic activation, together with activation of inflammatory cytokines, has been associated with cardiac myocyte hypertrophy (increased cell width) (Tarone & Lembo, 2003); to date there is no evidence to implicate adrenergic activation in promoting lengthening of cardiac myocytes.

Evidence of the potential role of activation of the SNS in mediating adverse cardiac remodelling is provided by the detection of substantially increased plasma concentrations of noradrenaline and adrenaline in patients with heart failure (Anand *et al.*, 2003; Cohn *et al.*, 1984; Francis *et al.*, 1993; Swedberg *et al.*, 1990), and the relationship of these concentrations to the severity of pump dysfunction (Kluger *et al.*, 1982) and heart failure (Sigurdsson *et al.*, 1994). Furthermore, a number of studies have demonstrated that β -adrenergic receptor blocking agents reduce cardiac cavity dimensions (Gerson *et al.*, 2002; Metra *et al.*, 2003; Packer *et al.*, 1996; Toyama *et al.*, 2003; Waagstein *et al.*, 1993a; Waagstein *et al.*, 1993b).

1.2.1.2 Role of the Renin-Angiotensin-Aldosterone System

Initially activation of the RAAS is compensatory in nature in that RAAS mediated fluid retention improves venous return and thus cardiac output (via the Frank-Starling effect). However sustained elevations in the RAAS are detrimental. Indeed, both angiotensin II and aldosterone have been shown to promote cardiac myocyte apoptosis (De Angelis *et al.*, 2002), and hence the potential for side-to-side slippage of cardiac myocytes (Figure 1.3).

Activation of the RAAS is also likely to play a role in the unfavourable changes in the characteristics of myocardial collagen, as decreased collagen cross-linking associated with cardiac dilatation could be prevented by both angiotensin-converting enzyme inhibitor administration (Woodiwiss *et al.*, 2001) as well as aldosterone receptor blockade (Veliotis *et al.*, 2005). In addition, angiotensin II and aldosterone have been shown to stimulate collagen synthesis (Brilla *et al.*, 1994).

Although, angiotensin II acting as a growth factor has been shown to mediate cardiac

myocyte hypertrophy by increasing cell width (Sadoshima *et al.*, 1997; Sernerer *et al.*, 1999), the role of the RAAS in cardiac myocyte lengthening is as yet unclear.

Nevertheless, the role of the RAAS in adverse cardiac remodelling is substantiated by intervention data showing reductions in cardiac dimensions following the administration of ACEI to patients in heart failure (Greenberg *et al.*, 1995; Konstam *et al.*, 1992).

1.2.2 Role of Growth Factors and Inflammatory Cytokines

Growth factors such as insulin-like growth factor are thought to mediate cellular hypertrophy via the protein kinase B pathway (Opie *et al.*, 2006). Activation of this pathway promotes cardiac myocyte growth (increased cell width) and inhibits apoptosis (Matsui & Rosenzweig, 2005). Hence, activation of insulin-like growth factor is important in mediating compensatory hypertrophy, but possibly plays no role in the transition to cardiac decompensation. In comparison transforming growth factor β , similar to angiotensin II, activates fibroblasts hence promoting collagen formation and fibrosis (Hein *et al.*, 2003; Kuwahara *et al.*, 2004). Increased fibrosis (as discussed below) is important in both compensatory hypertrophy and dilatation. Inflammatory cytokines, such as tumour necrosis factor α , seem to have a dual role. At low concentrations these cytokines mediate compensatory hypertrophy; whereas at high concentrations they may play a role in mediating cardiac dilatation and heart failure (Tarone & Lembo, 2003). Lastly, cardiac myocyte apoptosis may be promoted by increased myocardial expression of inflammatory cytokines as a consequence of adrenergic activation (Baumgarten *et al.*, 2000). However, intervention studies targeting inflammatory cytokines proved disappointing in patients with heart failure, in that no differences were observed in rates of death or hospitalisation due to chronic heart failure compared to placebo (Anker & Coats 2002).

1.2.3 Role of Stretch Receptors (Cardiac Myocyte Stretch)

The hypertrophy of cardiac myocytes is also regulated by stretch mediated by hemodynamic loading conditions (Russell *et al.*, 2010); in association with increased activation of the RAAS (Kudoh *et al.*, 1997; Sadoshima *et al.*, 1993. In this regard increases in ventricular volume (increased diastolic strain) are thought to be responsible for increases in cardiac myocyte length (Russell *et al.*, 2010); whereas increases in pressure (increased systolic stress) produce increases in cardiac myocyte width (Russell *et al.*, 2010). Consequently, compensated cardiac hypertrophy is associated with increases in cardiac myocyte width and cross-sectional area in proportion to increases in length (Onodera *et al.*, 1998; Zierhut *et al.*, 1991). In comparison, in the decompensated state, changes in cardiac myocyte length may exceed increments in cardiac myocyte width (Fedak *et al.*, 2005; Gerdes & Capasso 1995).

1.3 PROPOSED MECHANISMS OF COMPENSATORY CARDIAC HYPERTROPHY

Mechanisms of compensatory cardiac hypertrophy include changes in the cardiac interstitium as well as changes in the cardiac myocytes. In essence compensatory cardiac hypertrophy is associated with increased cardiac interstitial fibrosis, increased collagen cross-linking, as well as cardiac myocyte hypertrophy (increased cell width). These mechanisms will be discussed separately below.

1.3.1 Role of Collagen and Interstitial Changes

In compensatory cardiac hypertrophy, in response to increased angiotensin II, aldosterone, transforming growth factor β and noradrenaline, cardiac fibroblasts are activated (Hein *et al.*,

2003; Kuwahara *et al.*, 2004; Weber *et al.*, 1990; Weber *et al.*, 1993). Consequently, collagen synthesis is enhanced. In addition, matrix metalloproteinases (MMPs), which are responsible for collagen degradation (Gunasinghe *et al.*, 2001) are inhibited (Janicki *et al.*, 2004), hence collagen deposition exceeds collagen degradation. In addition, compensatory hypertrophy is associated with increased collagen cross-linking, mediated by increased activity of the cross-linking enzyme lysyl oxidase (Hermida *et al.*, 2009). As a consequence of increased fibrosis and collagen cross-linking, there is adequate tethering of cardiac myocytes to the interstitial matrix. Hence in the presence of increased loading conditions the structural morphology of the cardiac chamber is maintained.

1.3.2 Role of Cardiac Myocyte Hypertrophy Due to Increases in Cell Width

The initial response to high pressures in the cardiovascular system is cellular hypertrophy by means of increases in cardiac myocyte width, which result in increases in chamber wall thickness (Grossman *et al.*, 1975). In response to increased afterload (increased cardiac wall stress due to high pressures in the cardiovascular system), cardiac hypertrophy occurs in order to increase cardiac wall thickness and hence to decrease cardiac wall stress (via La Place's law) (Grossman *et al.*, 1975). In addition, cellular hypertrophy occurs in an attempt to relieve the heart of the raised filling pressures (increased preload) by increasing the output of the heart through an increased stroke volume or systolic function. The greater stroke volume is achieved by the increased muscle mass which generates a stronger muscle force. Katz *et al.* (2002), in a review article, refer to this process of hypertrophy by the heart and its myocytes as an attempt to '*grow their way out of trouble*'. In other words, in the presence of increased loading conditions, the ventricles need to grow (through hypertrophy) in order to reduce the loading conditions.

The initial response of cardiac muscle tissue to increased pressure load conditions is to increase cardiac myocyte width through parallel additions of cardiac myofilaments (Onodera *et al.*, 1998; Zierhut *et al.*, 1991), thus resulting in thickening of the myocardial wall. In models of pressure overload (hypertension), both Onodera *et al.* 1998 and Zierhut *et al.* 1991, showed that initially cardiac hypertrophy was accompanied by increases in cardiac myocyte width but not by changes in cardiac myocyte length. Hence, the initial response of the cardiac myocyte to augmented afterload is to increase in width but not in length (Onodera *et al.*, 1998; Zierhut *et al.*, 1991). As a consequence of increases in cardiac wall thickness subsequent to cellular hypertrophy, the luminal radius is reduced (Janicki *et al.*, 2004). An increase in the width of the ventricular wall with a concomitant reduction in the luminal radius is commonly referred to as concentric or compensatory hypertrophy (Janicki *et al.*, 2004). This initial form of hypertrophy in response to increased cardiovascular loading conditions is considered compensatory in nature (Janicki *et al.*, 2004).

1.4 PROPOSED MECHANISMS OF ADVERSE CARDIAC REMODELING

The mechanisms by which the cardiac tissue remodels to cause the dilatation are the topic of much debate. However, as with compensatory cardiac hypertrophy both changes in the cardiac interstitium as well as changes in the cardiac myocytes are believed to play a role. In essence adverse cardiac remodelling is associated with increased cardiac interstitial fibrosis, but of the non-cross-linked form; cardiac myocyte apoptosis and necrosis; as well as cardiac myocyte hypertrophy due to changes in cell length. These mechanisms will be discussed separately below.

1.4.1 Role of Collagen and Interstitial Changes

Sustained elevations in noradrenaline, angiotensin II, aldosterone and transforming growth factor β increase collagen synthesis (Boluyt *et al.*, 1995; Hein *et al.*, 2003; Weber & Brilla 1991; Weber *et al.*, 1993). However, sustained elevations in these neurohormones are also accompanied by increases in MMP activity (Banfi *et al.*, 2005; Mujundar & Tyagi, 1999; Spinale *et al.*, 1998). Therefore, both collagen synthesis and degradation are enhanced. Indeed, reductions in cardiac chamber dimensions following the use of LV assist devices are generally accompanied by increases rather than decreases in myocardial collagen concentrations (Li *et al.*, 2001; Scheinin *et al.*, 1992); whereas pacing-induced cardiac dilatation (Spinale *et al.*, 1991) and adrenergic-induced cardiac dilatation (Woodiwiss *et al.*, 2001) are accompanied by decreases in myocardial collagen concentrations. Hence, alterations in the characteristics of myocardial collagen, rather than in myocardial collagen concentrations, are more likely to contribute toward chamber dilatation.

As a consequence of enhanced collagen turnover (increased synthesis and degradation), the time available for collagen cross-linking to occur is decreased (Woodiwiss *et al.*, 2001). A reduction in collagen cross-linking reduces the capacity to tether cardiac myocytes (Li *et al.*, 2001; Mann & Spinale 1998), resulting in side-to-side slippage of cardiac myocytes and hence the development of cardiac dilatation (Olivetti *et al.*, 1990; Woodiwiss *et al.*, 2001) (Figure 1.3). Indeed, non cross-linked collagen is associated with cardiac dilatation and systolic dysfunction (Capasso *et al.*, 1989; Gunja-Smith *et al.*, 1996; Spinale *et al.*, 1996; Woodiwiss *et al.*, 2001).

In addition, non cross-linked collagen may be more susceptible to degradation by MMPs thus resulting in decreased tethering of cardiac myocytes and cardiac dilatation (Badenhorst *et al.*,

2003b; Woodiwiss *et al.*, 2001). Indeed, genetic decreases in the susceptibility of collagen to degradation, reduce the degree of dilatation which accompanies pressure-overload states (Papadimitriou *et al.*, 1974). In addition, increased myocardial expression and activation of MMPs has been demonstrated in patients with heart failure or in patients with a reduced systolic function and cardiac dilatation (Li *et al.*, 2001; Polyakova *et al.*, 2004; Reddy *et al.*, 2004; Spinale *et al.*, 2000; Spinale, 2002), and in animal models of pump dysfunction and cardiac dilatation (King *et al.*, 2003; Mukherjee *et al.*, 2003; Peterson *et al.*, 2001; Rohde *et al.*, 1999; Sakata *et al.*, 2004; Spinale *et al.*, 1998). Moreover, MMP inhibition attenuates left ventricular dilatation in animal models of pacing-induced heart failure (Spinale *et al.*, 1999), myocardial infarction (Mukherjee *et al.*, 2003; Rohde *et al.*, 1999) and heart failure in the spontaneously hypertensive rat (Peterson *et al.*, 2001); and a loss of MMP inhibitory control of MMPs, through a gene deletion of the tissue inhibitor of the matrix metalloproteinase-type 1 (TIMP-1), has been demonstrated to lead to ventricular dilatation in mice (Roten *et al.*, 2000).

1.4.2 Role of Cardiac Myocyte Apoptosis and Necrosis

Cardiac myocyte cell death may occur via an active, regulated, energy demanding process controlled by an inherited genetic program (Sabbah & Sharov, 1998) resulting in apoptosis. Alternatively cardiac myocyte death may occur via the unregulated process of necrosis (Kang & Izumo, 2000). Due to sustained increases in noradrenaline and angiotensin II, and the consequence of myocardial oxygen demand exceeding supply, necrosis and apoptosis of cardiac myocytes occurs. Cardiac myocyte death could reduce the capacity to tether cardiac myocytes hence promoting side-to-side slippage of cardiac myocytes (Figure 1.3). Hence, cardiac myocyte death mediated either by tissue apoptosis or necrosis may promote the development of cardiac dilatation (Yussman *et al.*, 2002). Indeed, cardiac dilatation occurs

following myocardial infarction and cellular necrosis (Anversa *et al.*, 1985; Zimmer *et al.*, 1990; Olivetti *et al.*, 1990).

1.4.3 Role of Cardiac Myocyte Hypertrophy Due to Increases in Cell Length

Although, cardiac dilatation is thought to be mediated by increases in the length of cardiac myocytes, not all studies support this hypothesis. Indeed, although some studies show that increases in cardiac myocyte length are associated with increases in cardiac chamber dimensions or heart failure (Beltrami *et al.*, 1994; Gerdes *et al.*, 1996; Gerdes *et al.*, 2010; Janczewski *et al.*, 2003; Kajstura *et al.*, 1995; Pangonyte *et al.*, 2008; Schultz *et al.*, 2007; Tamura *et al.*, 1998; Toischer *et al.*, 2010; Wang *et al.*, 1999; Zefeiridis *et al.*, 1998); a number of other studies show no relationship (Li *et al.*, 2010; Schultz *et al.*, 2007; Tamura *et al.*, 2000; Yarbrough *et al.*, 2010). Furthermore, data from intervention studies failed to show changes in cardiac dimensions in parallel with changes in cardiac myocyte length (Kuzman *et al.*, 2007; Li *et al.*, 2010; Schultz *et al.*, 2007; Tamura *et al.*, 2000). Therefore, it is important to discuss possible reasons for the controversial results regarding the possible role of alterations in cardiac myocyte length in cardiac dilatation.

1.4.3.1 Are Changes in Cardiac Dimensions Associated with Changes in Cardiac Myocyte Length?

1.4.3.1.1 Data From Human Studies:

Previous data obtained in human studies on the possible association between cardiac myocyte length and cardiac dimensions are summarised in Table 1. The data from human studies indicate that increases in cardiac myocyte length accompany increases in cardiac chamber

Table 1.1: Summary of human data addressing possible association of cardiac remodelling with alterations in myocyte morphology

Pathology/Model/Intervention	Measure of Cardiac Remodeling	Function / Presence of Heart Failure	Method of Cardiac Assessment	Myocyte Morphology	Method of Cell Measurement	Reference	My Interpretation
Cardiac transplantation in patients with congestive heart failure due to ischemic cardiomyopathy (males)	↑ transverse chamber diameter	Patients with congestive HF	Anatomical measurement	↑ length	Measurement of cells in histological sections	<i>Beltrami et al 1994</i>	↑ LVEDD associated with ↑ cell length in patients in HF, but assessments all anatomical
Cardiac transplantation in patients with congestive heart failure due to ischemic cardiomyopathy (males)	Not done	↓ EF	Echo (<i>in vivo</i>)	↑ length	Direct measurement of gluteraldehyde fixed freshly isolated myocytes	<i>Gerdes et al 1992</i>	↓ EF associated with ↑ cell length, but no LV dimension data. All patients were male & had higher body weight than controls (all females), hence ↑ cell length may be due to ↑ body weight and therefore ↑ heart weight in patients
Cardiac transplantation in patients with heart failure (12 ischemic & 18 nonischemic) (80% males versus 50% males in control group) LV assist device support in 10 patients with heart failure (80% males)	↑ LVEDD Normalisation of LVEDD	↑ PCWP Normalisation of PCWP	Echo (<i>in vivo</i>)	↑ length Normalisation of length	Direct measurement of gluteraldehyde fixed freshly isolated myocytes	<i>Zafeiridis et al 1998</i>	↑ LVEDD associated with ↑ cell length, but ↑ LVEDD is a preload induced effect (↑ PCWP). More patients were male & hence had higher body weight than controls, therefore ↑ cell length may be due to ↑ body weight and therefore ↑ heart weight in patients
Within 12 hours of MI in patients who died from first MI compared with patients who died after second or subsequent MI (males)	↑ endocardial surface area	No clinical symptoms of HF	Anatomical measurement	↑ length in both MI groups	Measurement of cells in histological sections	<i>Pangonyte et al 2008</i>	↑ cell length occurs during ischaemia and prior to MI and development of HF

↑, increase; ↓ decrease; echo, echocardiography; EF, ejection fraction; HF, heart failure; LV, left ventricle; LVEDD, left ventricular end diastolic diameter; PCWP, pulmonary capillary wedge pressure; ↑, ↓ and no change are in comparison to control group unless otherwise stated

diameter (Beltrami *et al.*, 1994; Pangonyte *et al.*, 2008; Zefeiridis *et al.*, 1998). However, it would be incorrect to draw a conclusion that adverse chamber remodelling (cardiac dilatation) is associated with increases in cardiac myocyte length, from this data for a number of reasons.

Firstly, in one these studies (Zefeiridis *et al.*, 1998), echocardiography *in vivo* was used to determine left ventricular end diastolic diameters and hence the cardiac chamber dimension measurements were load dependent. As increases in pulmonary capillary wedge pressure were noted in the patients in this study (Zefeiridis *et al.*, 1998), the increased chamber dimensions are likely to be due to increases in LV preload. In this regard, as discussed previously, cardiac myocyte lengthening occurs as a consequence of the stretching of cardiac myocytes during increased preloads (Ferrari *et al.*, 2009). Indeed, Zefeiridis *et al.* (1998) showed a normalisation of both LV end diastolic diameter and cardiac myocyte length, when pulmonary capillary wedge pressure was normalised as a consequence of LV assist device support. Left ventricular assist devices divert blood from the left atrium to the aorta, thereby removing the preload and afterload to the left ventricle. Hence these devices are used to provide haemodynamic support for patients with end-stage heart failure awaiting transplantation.

Secondly, in the study of Beltrami *et al.* (1994), the hearts were collected at autopsy for the control group and during cardiac transplantation for the heart failure group. Measurements of cardiac chamber dimensions and cardiac myocyte length were made anatomically; however no mention was made as to whether the hearts were arrested in diastole or systole. It is possible that during transplantation the hearts were arrested in diastole, as this was part of the surgical procedure at the time; whereas in the control group the phase of the cardiac cycle at the time of arrest was unknown as 70% of the control hearts were obtained from individuals in whom death was sudden due to traumatic injury. As the phase of the cardiac cycle

determines cardiac chamber dimensions and cardiac myocyte length, possible differences between the heart failure and control groups in the phase of the cardiac cycle at the time of cardiac arrest may have accounted for the differences in cardiac chamber diameter and cardiac myocyte length between these two groups.

Thirdly, in some studies the increased cardiac myocyte length in patients compared to controls could be as a consequence of the differences in body weight and hence LV weight between these two groups (Gerdes *et al.*, 1992; Zafeiridis *et al.*, 1998). Indeed, in one study all patients in heart failure were males; whereas all healthy controls were females (Gerdes *et al.*, 1992). As the males had greater body weights than the controls (Gerdes *et al.*, 1992), the increased cardiac myocyte length may be attributed to the greater body size in the males rather than to the presence of heart failure. Similarly, in another study the increased cardiac myocyte length in the patients compared to the controls may in part be attributed to the greater proportion of males in the heart failure group compared to the control group (Zafeiridis *et al.*, 1998).

Lastly, in a study assessing cardiac myocyte length and cardiac dimensions within 12 hours of death due to a first myocardial infarction compared to within 12 hours of death from a second or subsequent myocardial infarction, increases in cardiac myocyte length were noted in both groups with myocardial infarction compared to a control group who died from non-cardiovascular causes (Pangonyte *et al.*, 2008). Importantly neither of the myocardial infarction groups had clinical symptoms of heart failure. Therefore, from this study it can be concluded that increases in cardiac myocyte length occur during ischaemia before myocardial infarction and the development of heart failure.

Hence, from human studies published to date, the potential relationship between adverse chamber remodelling (cardiac dilatation) and cardiac myocyte length is unclear.

1.4.3.1.2 Data from Animal Experimental Models:

Previous data on the possible association between cardiac myocyte length and cardiac dimensions obtained from animal experimental models are summarised in Table 2. Although a number of studies have attempted to address the question of the relationship between cardiac myocyte length and cardiac dimensions in various animal experimental models; the data is controversial. Some studies show that increases in cardiac myocyte length are associated with increases in cardiac chamber dimensions or heart failure (Gerdes *et al.*, 1996; Gerdes *et al.*, 2010; Janczewski *et al.*, 2003; Kajstura *et al.*, 1995; Schultz *et al.*, 2007; Tamura *et al.*, 1998; Toischer *et al.*, 2010; Wang *et al.*, 1999); whereas a number of other studies show no relationship (Li *et al.*, 2010; Schultz *et al.*, 2007; Tamura *et al.*, 2000; Yarbrough *et al.*, 2010). As with the human studies, a number of possible reasons may explain the controversial data.

One of the reasons for the contrasting findings is the use of load dependent measures of cardiac chamber dimensions (echocardiography *in vivo*) in the presence of increased preloads (Chen *et al.*, 2010; Gerdes *et al.*, 2010; Kajstura *et al.*, 1995; Tamura *et al.*, 1998; Wang *et al.*, 1999; Yarbrough *et al.*, 2010). As discussed above with respect to human studies, the increased cardiac chamber diameters and cardiac myocyte length noted in these studies may be indicative of the increased preloads rather than the presence of adverse chamber remodelling (cardiac dilatation).

Secondly, in a number of studies showing an association between cardiac myocyte length and cardiac chamber dimension, the experimental animals (spontaneously hypertensive heart failure, SHHF rats) were from 12 to 16 months older than the control animals (Gerdes *et al.*, 1996; Tamura *et al.*, 1998). As LV weight increases with age in hypertensive rats (Gerdes *et*

Table 1.2: Summary of data from animal experimental models addressing possible association of cardiac remodelling with alterations in myocyte morphology

Pathology/Model/Intervention	Measure of Cardiac Remodeling	Function / Presence of Heart Failure	Method of Cardiac Assessment	Myocyte Morphology	Method of Cell Measurement	Reference	My Interpretation
Dogs with pacing-induced heart failure (gender not stated)	↑ chamber diameter	↑ LVEDP, ↓ LVSP	LV dimensions of cardiac rings following perfusion fixation at LVEDP measured <i>in vivo</i>	↑ length	Direct measurement of freshly isolated myocytes	<i>Kajstura et al. 1995</i>	As ↑ LVEDP in dogs with pacing-induced HF, ↑ LV dimensions likely to be due to ↑ preload
Rats genetically predisposed to developing heart failure with increasing age (spontaneously hypertensive heart failure, SHHF) (females)	Not done	Clinical signs of HF (dyspnoea, cyanosis), ↑ liver weight, ↑ lung wet weight, ↓ LV systolic pressure	Catheter plus pressure transducer (<i>in vivo</i>)	↑ length	Direct measurement of gluteraldehyde fixed freshly isolated myocytes	<i>Gerdes et al. 1996</i>	↑ cell length in rats in HF, but these rats were 12 months older than rats not in HF. As cardiac myocyte length is strongly correlated with age & LV weight, and LV weight ↑ with age in hypertensive rats; ↑ cell length possibly due to ↑ age & LV weight rather than ↑ LV dimensions
Rats genetically predisposed to developing heart failure with increasing age (spontaneously hypertensive heart failure, SHHF) (females)	Not done	No clinical signs of HF	Echo (<i>in vivo</i>)	↑ length	Direct measurement of gluteraldehyde fixed freshly isolated myocytes	<i>Onodera et al. 1998 (Gerdes laboratory)</i>	↑ cell length with age associated with ↑ heart weight/body weight with age in hypertensive rats without HF; therefore ↑ cell length possibly due to ↑ age & heart weight rather than ↑ LV dimensions

Pathology/Model/Intervention	Measure of Cardiac Remodeling	Function / Presence of Heart Failure	Method of Cardiac Assessment	Myocyte Morphology	Method of Cell Measurement	Reference	My Interpretation
Rats genetically predisposed to developing heart failure with increasing age (spontaneously hypertensive heart failure, SHHF) (females)	↑ chamber circumference	Clinical signs of HF (eg. dyspnoea, ascites, pleural effusion, pericardial effusion, cyanosis)	Anatomical measurement of chamber circumference in formalin fixed heart slices	↑ length	Direct measurement of gluteraldehyde fixed freshly isolated myocytes & myocytes isolated from formalin fixed tissue using potassium hydroxide	<i>Tamura et al. 1998 (Gerdes laboratory)</i>	↑ cell length in rats in HF, but these rats were 16 months older than rats not in HF. As cardiac myocyte length is strongly correlated with age & LV weight, and LV weight ↑ with age in hypertensive rats; ↑ cell length possibly due to ↑ age & LV weight rather than ↑ LV dimensions
Constriction of thoracic aorta in guinea pigs (males)	↑ LVEDD	↓ FS, ↓ EF, ↑ LVEDP	Echo (<i>in vivo</i>)	↑ length	Direct measurement of gluteraldehyde fixed freshly isolated myocytes	<i>Wang et al 1999 (Gerdes laboratory)</i>	As ↑ LVEDP in guinea pigs with ↓ FS & ↓ EF, ↑ LVEDD likely to be due to ↑ preload
Rats genetically predisposed to developing heart failure with increasing age (spontaneously hypertensive heart failure, SHHF) (females)	↑ LVEDD at 22 months	No change in FS	Echo (<i>in vivo</i>)	No change in length	Direct measurement of gluteraldehyde fixed freshly isolated myocytes	<i>Tamura et al. 2000 (Gerdes laboratory)</i>	Despite ↑ LVEDD at 22 months, no change in cell length observed, hence ↑ LV dimensions not associated with ↑ cell length
Angiotensin II type 1 receptor blocker administration to SHHF (females)	No change in LVEDD	No change in FS	Echo (<i>in vivo</i>)	↓ length			↓ cell length associated with ↓ heart weight /body weight but no change in LVEDD, suggests that ↑ cell length in SHHF is due to ↑ heart weight rather than ↑ LV dimensions

Pathology/Model/Intervention	Measure of Cardiac Remodeling	Function / Presence of Heart Failure	Method of Cardiac Assessment	Myocyte Morphology	Method of Cell Measurement	Reference	My Interpretation
Transgenic mice with cardiac specific overexpression of tumour necrosis alpha (results in the development of HF) (males compared to females)	↑ LVEDD only in males	↓ FS	Echo (<i>in vivo</i>)	↑ length in males & females	Direct measurement of freshly isolated myocytes	<i>Janczewski et al 2003</i>	In females, ↑ cell length but no change in LVEDD, hence ↑ cell length not associated with ↑ LVEDD
Cardiomyopathic hamsters (male)	↑ LVEDD	↓ EF	Echo (<i>in vivo</i>)	No change in length	Direct measurement of gluteraldehyde fixed freshly isolated myocytes	<i>Kuzman et al 2007 (Gerdes laboratory)</i>	Cell length not associated with LVEDD
L-thyroxine administration Diiodothyropropionic acid (thyroid hormone analogue) administration	Normalisation of LVEDD	↓ EF		No change in length			
Spontaneously hypertensive heart failure (SHHF) adult rats (females)	↑ LVEDD	↓ EF & ↓ FS	Echo (<i>in vivo</i>); catheter plus pressure transducer (<i>in vivo</i>)	↑ length	Direct measurement of gluteraldehyde fixed freshly isolated myocytes	<i>Schultz et al 2007 (Gerdes laboratory)</i>	↑ LVEDD, ↓ EF & ↓ FS associated with ↑ cell length
Long-term exercise (16 months) in SHHF adult rats	↑ LVEDD, and > in non-exercise SHHF	↓ EF & ↓ FS, and < in non-exercise SHHF; ascites in 42% of rats		↑ length, but not different from non-exercise SHHF			Despite greater ↑ LVEDD, ↓ EF, ↓ FS & presence of ascites, no difference in cell length compared to non-exercise SHHF
Myocardial infarction (MI) via left coronary artery ligation in adult rats (males compared to females)	↑ LVEDD	↓ FS & ↓ LV systolic pressure; ↑ LVEDP	Echo (<i>in vivo</i>); catheter plus pressure transducer (<i>in vivo</i>)	↑ length	Direct measurement of gluteraldehyde fixed freshly isolated myocytes	<i>Chen et al 2010 (Gerdes laboratory)</i>	↑ LVEDD, ↓ FS, ↓ LVSP & ↑ LVEDP associated with ↑ cell length; but ↑ LVEDD is a likely to be a preload induced effect
Myocardial infarction (MI) via left coronary artery ligation in adult mice (males)	↑ LVEDD	↓ FS	Echo (<i>in vivo</i>)	No change in length	Direct measurement of freshly isolated myocytes	<i>Li et al 2010</i>	↑ LVEDD not associated with ↑ cell length

Pathology/Model/Intervention	Measure of Cardiac Remodeling	Function / Presence of Heart Failure	Method of Cardiac Assessment	Myocyte Morphology	Method of Cell Measurement	Reference	My Interpretation
Intramyocardial delivery of mesenchymal stem cells to mice with MI	Prevention of ↑ LVEDD	Prevention of ↓ FS	Echo (<i>in vivo</i>)	↑ length	Direct measurement of freshly isolated myocytes	<i>Li et al 2010</i>	Normalisation of LVEDD associated with ↑ cell length
↑ preload via aortocaval shunt in adult mice (females)	↑ LVEDD	No change in FS	Echo (<i>in vivo</i>)	↑ length	Direct measurement of freshly isolated myocytes	<i>Toischer et al 2010</i>	↑ cell length prior to ↓ FS
MI via ligation of circumflex coronary artery in adult pigs (gender not stated)	↑ LVEDD	↑ LVEDP	Echo (<i>in vivo</i>); catheter plus pressure transducer (<i>in vivo</i>)	No change in length	Direct measurement of myocytes from formalin-fixed tissue	<i>Yarbrough et al 2010</i>	↑ LVEDD & in HF (↑ LVEDP) but no change in cell length
Caspase inhibition to pigs with MI	↑ LVEDD, but < in absence of caspase inhibition	↑ LVEDP		↓ length			↑ LVEDD & in HF (↑ LVEDP) but ↓ cell length

↑, increase; ↓ decrease; echo, echocardiography; EF, ejection fraction; FS, fractional shortening; HF, heart failure; LV, left ventricle; LVEDD, left ventricular end diastolic diameter; LVEDP, left ventricular end diastolic pressure; LVSP, left ventricular systolic pressure; PCWP, pulmonary capillary wedge pressure; PWTd, posterior wall thickness in diastole; SHHF, spontaneously hypertensive heart failure; ↑, ↓ and no change are in comparison to control group unless otherwise stated

al. 1996), and cardiac myocyte length is strongly associated with age in SHHF rats (Tamura *et al.*, 1998) and with LV weight (Campbell *et al.* 1991; Capasso *et al.* 1992), the increases in cardiac myocyte length observed in the experimental groups may reflect age induced changes, rather than an association with adverse chamber remodelling (cardiac dilatation) and the development of heart failure.

Thirdly, data from various intervention studies failed to show changes in cardiac dimensions in parallel with changes in cardiac myocyte length. In intervention studies where increases in cardiac chamber diameter were prevented by thyroid hormone administration (Kuzman *et al.*, 2007) or intramyocardial delivery of mesenchymal stem cells (Li *et al.*, 2010), either no change (Kuzman *et al.*, 2007) or even increases in cardiac myocyte length (Li *et al.*, 2010) were noted. Alternatively, in one study decreases in cardiac myocyte length were noted subsequent to angiotensin II receptor blockade, but no changes in cardiac chamber dimensions were noted (Tamura *et al.*, 2000). Furthermore, in a study of the effects of long-term exercise in rats with heart failure, further increases in cardiac chamber dimensions due to exercise training were not accompanied by further increases in cardiac myocyte length (Schultz *et al.*, 2007). The results from the intervention studies discussed above, although different from each other, do not show parallel changes in cardiac chamber dimensions and cardiac myocyte length. Therefore the results of these studies do not support a role of changes in cardiac myocyte length in cardiac dilatation. Indeed, if increases in cardiac myocyte length were causally related to adverse cardiac remodelling, a reduction in cardiac myocyte length should be accompanied by a decrease in cardiac chamber dimensions. Hence the data provides no clear conclusion as to the possible role of cardiac myocyte length in adverse chamber remodelling. In fact, it could be concluded that there is no causal relationship.

However, the data need to be interpreted with caution in view of the use of load dependent measures of cardiac dimensions in these studies.

Lastly, few studies have made direct comparisons of animals with cardiac pathology which have heart failure to animals with the same cardiac pathology but without heart failure. The only studies which have used this study design have been done in SHHF rats (Gerdes *et al.*, 1996; Tamura *et al.*, 1998 and 2000). However, in these studies the rats in heart failure were from 12 to 22 months older than the rats not in heart failure. As discussed above, as cardiac myocyte length is associated with age (Tamura *et al.*, 1998), the increased cardiac myocyte length may reflect increased age rather than increased cardiac dimensions. Indeed, a study by Onodera *et al.* (1998) showed that cardiac myocyte lengthening increased with age and occurred well before the development of heart failure in SHHF rats. Although the study by Onodera *et al.* (1998) suggests that changes in cardiac myocyte length are not responsible for the development of heart failure, no measurements of cardiac dimensions were made in this study. To my knowledge no study to date has compared age-matched animals with the same cardiac pathology which have heart failure to those without heart failure.

Hence the data obtained from animal experimental models to date are equally confusing and hence the question of the relationship between cardiac myocyte length and adverse cardiac chamber remodelling remains unresolved.

1.5 PROBLEM STATEMENT AND STUDY OBJECTIVES

In summary, despite a plethora of studies aimed to address the relationship between cardiac dimensions and cardiac myocyte length, to date the data are controversial (Tables 1.1 and 1.2,

and Figure 1.4). As discussed the data are limited by the use of load dependent measures of cardiac dimensions; the comparison of hearts from humans of different gender and body size; the comparison of hearts from rat groups of different age and body size; and a failure to make direct comparisons between age-matched animals with cardiac pathology who are in heart failure and those who are not in heart failure. Hence, the role of cardiac myocyte length in adverse cardiac remodelling needs to be defined using load independent measures of chamber dimensions and in age-matched animals where direct comparisons are made between animals with cardiac pathology who are in heart failure and those who are not in heart failure.

To address the limitations discussed above, I chose to study two models of cardiac dilatation in pressure-overload induced cardiac hypertrophy in rats. The first model of cardiac dilatation was a **natural progression model** in that it involved the use of 23 month old SHR. In SHR older than 21 months of age, left ventricular hypertrophy is noted to progress to left ventricular decompensation, dilatation and heart failure in approximately half of the rats (Bing *et al.* 1995; Norton *et al.* 1997; Tsotetsi *et al.* 2001). The second model of cardiac dilatation, a **pharmacological model**, was induced in 14 month old SHR by chronic beta-adrenoreceptor activation [daily administration of the beta-adrenergic agonist isoproterenol (ISO) for a period of 4.5 months]. Chronic beta-adrenoreceptor activation in SHR, has been shown to enhance the progression from compensated left ventricular hypertrophy to left ventricular dilatation (Badenhorst *et al.* 2003b; Gibbs *et al.* 2004). In both of these models the rats in heart failure were age-matched to the rats not in heart failure and comparisons were made with an age-matched healthy control group. Importantly, in my studies I used load independent measures (determination of filling pressures at controlled volumes) to define cardiac dilatation.

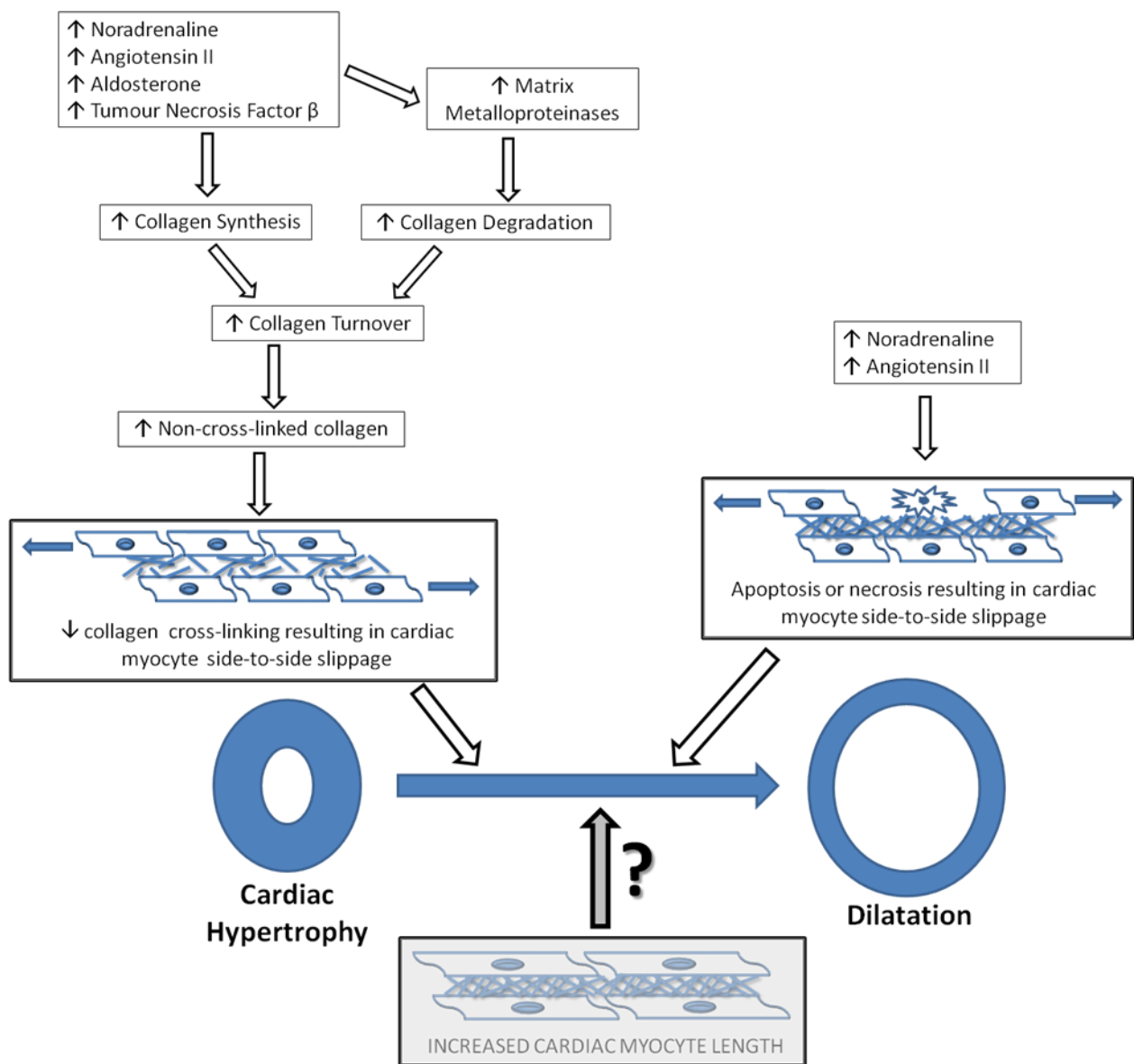


Figure 1.4 Schematic representation of the factors known to contribute to cardiac dilation; whereas the role of cardiac myocyte lengthening is still controversial.

The studies in this dissertation aimed to determine the role that cardiac myocyte lengthening in the development of adverse chamber remodelling (cardiac dilatation) that occurs in pressure-overload states in rats.

The specific objectives of my studies were:

- to compare the length of cardiac myocytes isolated from SHR rats in heart failure to those isolated from SHR rats without heart failure (natural progression model)
- to compare the length of cardiac myocytes isolated from SHR rats receiving isoproterenol (rats in heart failure) to those isolated from SHR rats not receiving isoproterenol (rats without heart failure) (pharmacological model)
- to compare the cardiac dimensions (measured using load independent measures), of SHR rats in heart failure to those isolated from SHR rats without heart failure (natural progression model)
- to compare the cardiac dimensions (measured using load independent measures), of SHR rats receiving isoproterenol (rats in heart failure) to those isolated from SHR rats not receiving isoproterenol (rats without heart failure) (pharmacological model)
- to determine the relationship between cardiac myocyte length and cardiac dimensions measured using load independent measures (both natural progression model and pharmacological model)

CHAPTER 2

2. METHODS

In order to assess the role that changes in cardiac myocyte dimensions have on the development of dilatation, two models of cardiac dilatation in pressure-overload induced cardiac hypertrophy in rats were used. All studies in this dissertation were approved by the Animal Ethics Screening Committee (AESC) of the University of the Witwatersrand (AESC Clearance Numbers 1997:44:5; 1999:01:2b; 2002:37:5; 2002:39:5 & 2006:41:5). The rats were obtained from the Central Animal Services (CAS) Unit of the University of the Witwatersrand, Johannesburg, South Africa.

2.1 RAT STRAINS AND GROUPS

For both models of cardiac dilatation in pressure-overload induced cardiac hypertrophy, I used spontaneously hypertensive rats (SHR), which are a strain of rats bred to have increased blood pressures (Gerdes *et al.* 1996; Tamura *et al.* 1998; Tsotetsi *et al.* 2001). As a consequence of chronically elevated blood pressures, SHR develop left ventricular hypertrophy after 11 months of age (Norton *et al.* 1997). The first model of cardiac dilatation was a **natural progression model** in that it involved the use of 23 month old SHR (n=18). In SHR older than 21 months of age, left ventricular hypertrophy is noted to progress to left ventricular decompensation, dilatation and heart failure in approximately half of the rats (Bing *et al.* 1995; Norton *et al.* 1997; Tsotetsi *et al.* 2001). The second model of cardiac dilatation, a **pharmacological model**, was induced in 14 month old SHR (n=9) by chronic beta-adrenoreceptor activation [daily administration of the beta-adrenergic agonist isoproterenol (ISO) for a period of 4.5 months]. Chronic beta-adrenoreceptor activation in SHR, has been shown to enhance the progression from compensated left ventricular

hypertrophy to left ventricular dilatation (Badenhorst *et al.* 2003b; Gibbs *et al.* 2004). In this arm of the study, an SHR group receiving twice daily administration of the vehicle of isoproterenol (saline) for a period of 4.5 months (SHR-Control, n=9), served as the ‘non-failure’ group (see Figure 2.1 below).

The control group for this study comprised of 23 month old Wistar Kyoto (WKY) rats (n = 9; Kleinterfarm Madorin Ltd, Germany). These rats are the genetic controls for SHR (Tsotetsi *et al.* 2001). The WKY control group acted as such for both the natural progression model as well as the pharmacological model of the study (see Figure 2.1 below), as these rats are normotensive, and are not known to develop heart failure. Although the WKY control group of rats were older (23 months old) than the SHR-Control and SHR-ISO rats (both 18.5 months old), in normotensive rats in which body weight and heart weight are stable, age has been shown to have no impact on myocyte dimensions (Bai *et al.* 1990; Onodera *et al.* 1998; Tamura *et al.* 1998). We have previously reported no differences in body weight or left ventricular weight in 21-22 month old WKY compared to 12 month old WKY (Badenhorst *et al.* 2003b). Moreover, as it has previously been shown that chronic administration of a beta-adrenergic agonist to the WKY strain of rats does not induce cardiac dilatation (Badenhorst *et al.* 2003b; Gibbs *et al.* 2004) I did not include a WKY group receiving chronic beta-adrenergic agonist administration.

The rats were housed in pairs in cages in the CAS Unit of the University of the Witwatersrand and given food and water *ad libitum* until termination at 18.5 or 23 months of age.

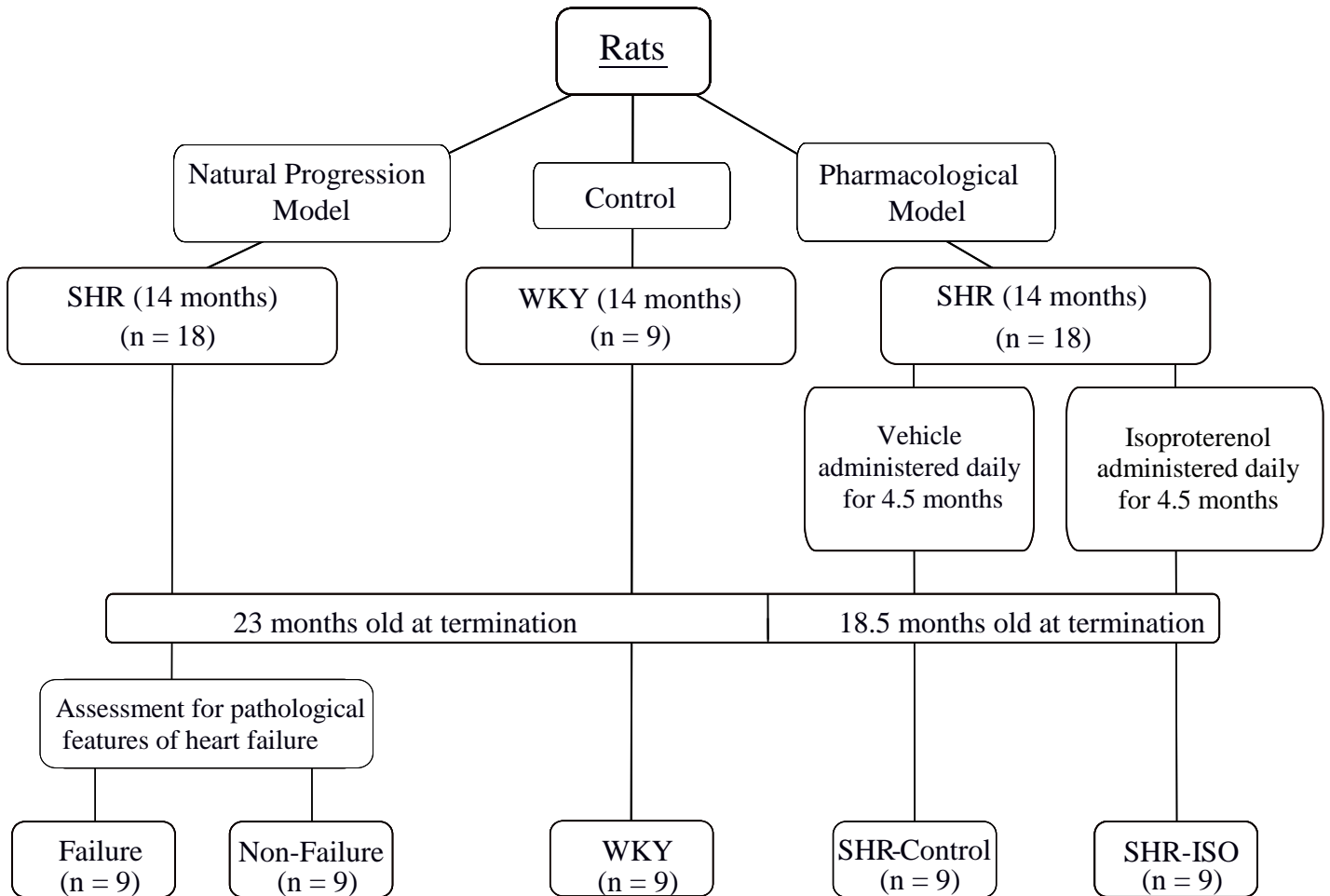


Figure 2.1 Flow chart detailing the groups of rats

The control group acted as such for both models. In the natural progression model, rats found to have pathological features of cardiac failure (see 2.2.1 below) were assigned to the failure group, and rats without any features of cardiac failure were assigned to the non-failure group.

In the pharmacological model, the beta-adrenergic agonist, isoproterenol (or its vehicle, saline) was administered from 14 months of age until termination at 18.5 months of age.

ISO, isoproterenol; SHR, spontaneously hypertensive rats; WKY, Wistar-Kyoto rats.

2.1.1 Natural Progression Model

Eighteen 14 month old SHR (OLAC, UK) were housed in the CAS Unit of the University of the Witwatersrand. At 23 months of age the rats were terminated. At the time of termination, the rats were assessed for signs and symptoms of cardiac failure (see 2.2.1 below). Rats noted to have pathological features of cardiac failure were assigned to the failure group (SHR Failure, n=9), and rats without any features of cardiac failure were assigned to the non-failure group (SHR Non-Failure, n=9).

2.1.2 Pharmacological Model

Eighteen 14 month old SHR (OLAC, UK) were randomly assigned to two groups of nine rats each. One group (SHR-ISO) received a twice daily intraperitoneal injection of the beta-adrenergic agonist isoproterenol (ISO) (Imuprel, Adcock Ingram), at a concentration of 0.02 mg/kg/injection, in a volume of approximately 0.2 ml for 4.5 months. The other group (SHR-Control) received a twice daily injection of the vehicle of ISO (0.2 ml of 0.9% saline) for 4.5 months. The rats were terminated at 18.5 months of age.

2.2 SYSTOLIC BLOOD PRESSURE

Non-invasive systolic blood pressures (SBP) were assessed in all rats prior to the end of the study using a tail-cuff technique. In the pharmacological model, these measurements were obtained at least 24-hours after the last dose of ISO. To familiarise the rats to the procedure, rats were placed in restrainers, the tail pre-warmed and the tail cuff inflated every 15 minutes for an hour a day on five separate days prior to the measurements. To determine SBP, rat tails were pre-warmed until the tail artery pulse could be detected with a photoelectric diode coupled to a Model 29 pulse amplifier (IITC Inc.). A tail-cuff coupled to a pressure

transducer was placed on the rat tail proximal to the photoelectric diode and inflated until the tail pulse disappeared. The tail cuff pressure was then slowly released until the tail artery pulse returned. Systolic BP was taken as the cuff BP at which the tail artery pulse returned. Recordings of the tail cuff pressure and the pulse were made on a Beckman dynograph model R511A recorder, the recordings of which were calibrated both before and after each recording.

2.3 LEFT VENTRICULAR GEOMETRY

Rats in the pharmacological model (at 18.5 months of age), rats in the natural progression model (at 23 months of age) and the WKY control rats (at 23 months of age) were anaesthetised using an intraperitoneal injection of ketamine (75 mg/kg) and xylazine (15 mg/kg) (Bayer HealthCare, Animal Health). Once anaesthetised, a 14-gauge needle was placed in the trachea for positive pressure ventilation using room air through a constant-volume respirator (Harvard Apparatus, South Natick, Massachusetts). The air in the ventilator was supplemented with oxygen to ensure adequate oxygen saturation.

The right carotid artery was catheterized using PP50 tubing. Placement of the carotid catheter allowed for the manual manipulation of ventricular filling as well as the measurement of systolic and diastolic arterial pressures and heart rate. A midline thoracotomy (sternotomy) was then performed.

Prior to performing a parietal pericardectomy, in the 23 month old rats (natural progression model), careful assessment was made for the presence of pleuropericardial effusions (the effusion was either in the pleura and/or the pericardium; see 2.2.1 below). Piezo-electric

ultra-sonic transducers, attached to a previously validated apparatus (Woodiwiss & Norton 1995; Trifunovic *et al.* 1995), were then placed across the short axis of the beating left ventricle (LV). These transducers emit ultra-sonic waves through one transducer (anteriorly, B in Figure 2.2) and receive the ultra-sonic waves through the other (posteriorly, C in Figure 2.2). The distance between the transducers was measured using a calibrated sonomicrometer (Triton Technology). The transducers were used to measure the external diameter of the left ventricle through the phases of the cardiac cycle over a range of left ventricular filling pressures (upper panel Figure 2.3).

The filling pressures were measured by means of the insertion of a 21-gauge needle through the apex of the heart (A in Figures 2.2 and 2.3). The 21-gauge needle was attached to a saline-filled PP25 polyethylene catheter which was coupled to a Gould P50 pressure transducer. The fluid filled catheter had amplitude-frequency responses which were uniform to 10Hz (Norton *et al.* 1997). Filling volumes were modified by the infusion of an iso-oncotic solution via the carotid catheter (Badenhorst *et al.* 2003b; Norton *et al.* 1997; Woodiwiss & Norton 1995; Tsotetsi *et al.* 2001). The frequent occurrence of extra systolic beats at filling pressures below 2 mm Hg prevented the collection of data at pressures below 2 mm Hg. The left ventricular end diastolic (LVED) diameters were therefore measured over a range of filling pressures between 2 mm Hg and 9 mm Hg.

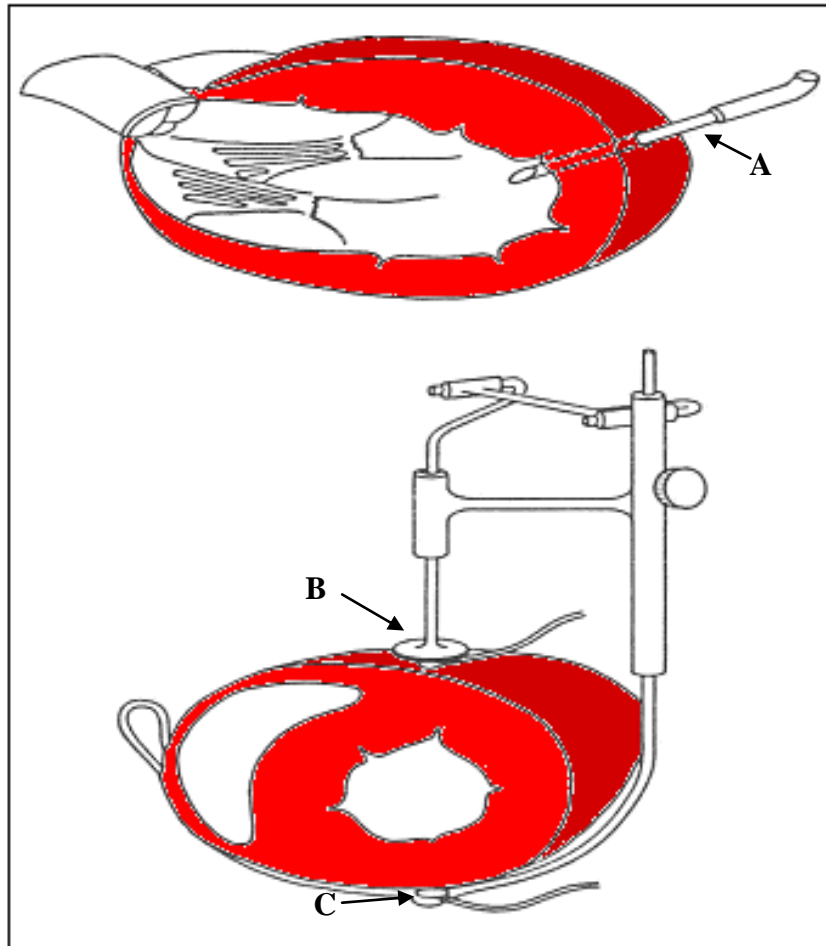


Figure 2.2 Intraventricular pressure monitoring and piezo-electric ultrasonic transducers

Diagrammatic representation of the apical catheter (A) and the apparatus used for the placement of the piezo-electric ultrasonic transducers (B and C) across the short axis of the left ventricle. A, apical catheter attached to 21-gauge needle; B, anterior (transmitting) transducer; C, posterior (receiving) transducer.

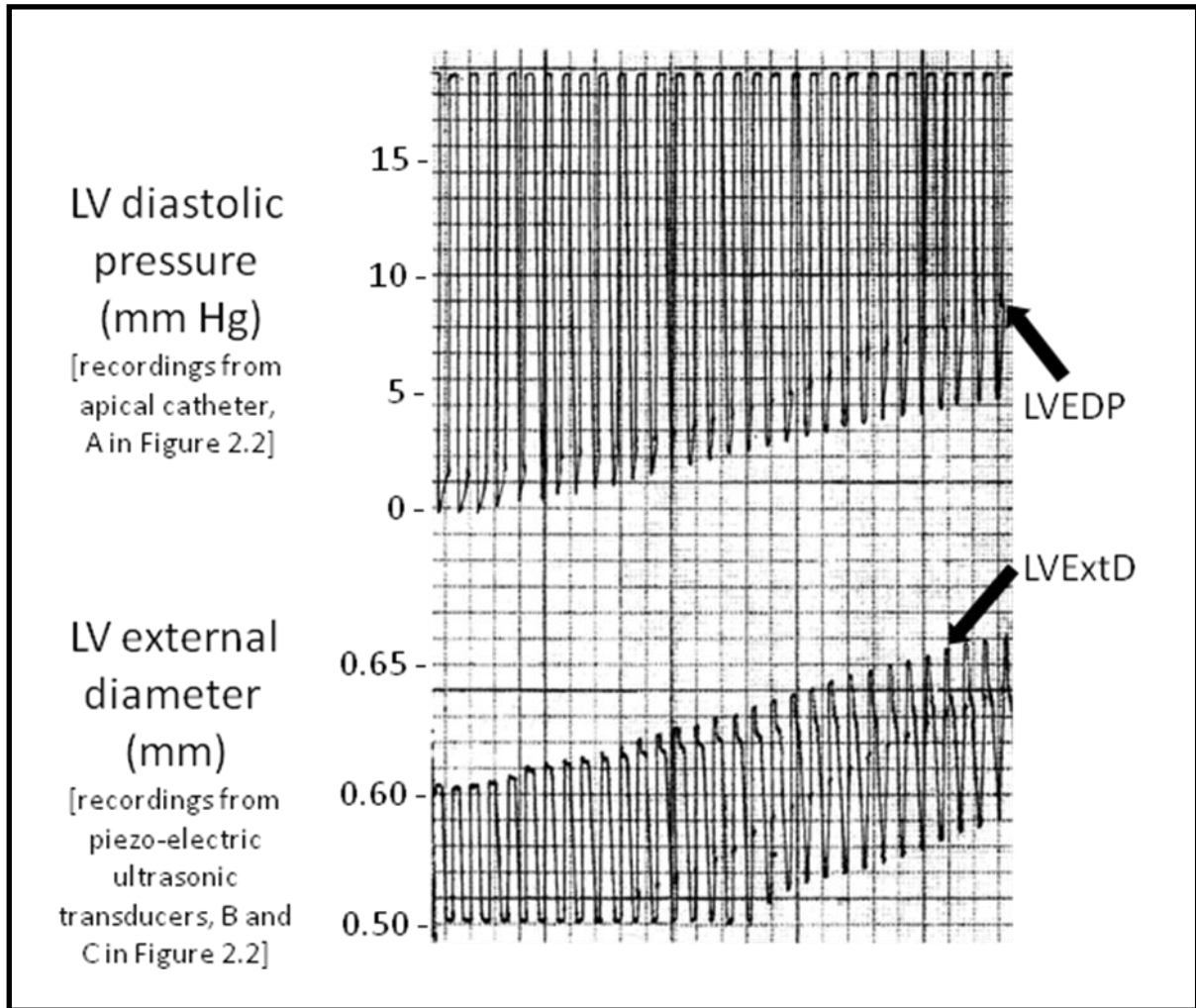


Figure 2.3 Example of recordings of left ventricular external diameter measurements

Example of recordings of LV external diameter (LVExtD) obtained from the piezo-electric ultrasonic transducers (B and C in figure 2.2) and of LV diastolic pressure obtained from the apical catheter (A in figure 2.2) inserted into the left ventricle.

LVEDP, LV end diastolic pressure

All recordings were made on a Beckman Dynograph Recorder (type R511A). Left ventricular end diastolic radius (LVEDr) was calculated from the LVED external diameter measurements, using the following equation (Weber *et al.* 1988),

$$\text{LVED radius} = \sqrt[3]{[\text{LVED external diameter} / 2]^3 - \text{LV wall Volume} [\frac{3}{4} \pi]}$$

where,

$$\text{LV wall volume} = 0.943 \times \text{LV wet weight}$$

and where 0.943 represents the density of cardiac tissue (Tsotetsi *et al.* 2001; Woodiwiss and Norton 1995).

Left ventricular end diastolic wall thickness (LVEDh), was then determined using the equation,

$$\text{LVEDh} = [(\text{LVED external diameter} - 2 \times \text{LVEDr}) / 2]$$

(Tsotetsi *et al.* 2001; Woodiwiss & Norton 1995); and from these measurements, LVED wall thickness to radius ratio (h/r) was calculated.

Using these values LVEDP-LVEDr and LVEDP-LVEDh/r relations were constructed in order to assess left ventricular geometry.

2.3.1 Identification of Failure and Non-failure Rats

In the natural progression model, rats were classified as in heart failure based upon the presence of pleuropericardial effusions and / or atrial thrombi. As stated above (see 2.2), at the time of thoracotomy and prior to pericardectomy careful assessment was made to identify

the presence or absence of pleuropericardial effusions. In addition, the presence or absence of atrial thrombi was identified at post-mortem (see 2.3 below).

Those animals that were found to have one or more of these pathological features of heart failure were assigned to the ‘SHR-Failure’ group (see Figure 2.1). Those rats that did not exhibit any pathological features of heart failure were assigned to the ‘SHR-Non-Failure’ group (see Figure 2.1). In order to confirm the presence of heart failure wet liver weights were determined in the SHR rats in the natural progression model and in the WKY control rats.

2.4 TISSUE SAMPLING

Once the collection of data to assess left ventricular geometry had been completed, a high dose (16mM) of potassium chloride (Hearse *et al.* 1975) was infused via the catheter into the carotid artery, hence arresting the heart in diastole. The heart was then removed, blotted dry and weighed. The right ventricular free wall was dissected away from the left ventricle and the left and right ventricles were weighed. During the dissection of the heart, the atria were removed and carefully inspected for the presence of thrombi (one of the features of heart failure).

Samples from the left ventricle were stored at -70°C for later analysis. The samples were carefully labelled so that cardiac myocytes could be isolated from the same region of each heart for accurate comparisons.

2.5 MYOCYTE ISOLATION

Cardiac myocytes were isolated from the frozen tissue samples using a modification of a technique previously described (Diffie & Nagle 2003; Gerdes *et al.* 1998; Tamura *et al.* 1998). A sharp blade was used to carefully section off a 20 mg (wet weight, for light microscopy) or 100 mg (wet weight, for flow cytometry) piece of the LV posterior wall from the same region of each rat heart. Each piece of LV tissue was of full thickness, in that it extended from epicardium to endocardium.

Calcium-free physiological saline solution (PSS) was made for the cardiac myocyte isolation process. PSS consisted of NaCl 120 mmol, KCl 10 mmol, KH_2PO_4 1.2 mmol, MgCl_2 2.6 mmol, glucose 10 mmol, taurine 20 mmol, pyruvate 6.2 mmol and HEPES (4-(2-hydroxyethyl)-piperazine-1-ethanesulfonic acid hemisodium salt) 4.8 mmol dissolved in 100 ml of distilled water (all chemicals obtained from Sigma Chemical Co., St. Louis, MO). 100ml of PSS was prepared for every 20mg of LV tissue. The PSS solution was titrated with 10 mM NaOH droplets until the pH of the solution was equal to a pH of 7.40 (physiological pH). The pH was measured using a pH meter (Beckman Φ 32 pH meter, Beckman Instruments, Inc. USA). For every 20 mg of LV tissue, 50 ml of incubation solution and 50 ml of wash solution were prepared as described below.

The incubation solution consisted of 15 mg Collagenase Type 2 (Worthington Biochemical Corporation, Lakewood NJ, USA) at a concentration of 317 U/mg, 14mg of Hyaluronidase (Worthington Biochemical Corporation, Lakewood NJ, USA) at a concentration of 581 U/mg, 125 mg of bovine serum albumin (Fraction V, Sigma Chemical Co., St. Louis, MO) and 0.0227 ml of 110 mM CaCl_2 dissolved in 50 ml of PSS. The CaCl_2 (Sigma Chemical

Co., St. Louis, MO) was prepared by dissolving 1.617g of CaCl₂ into 100 ml of distilled water.

The wash solution consisted of 0.045 ml of 110 mM CaCl₂ and 250 mg of bovine serum albumin.

The sample of LV tissue was minced and then placed in a tissue culture flask containing 10 ml of the incubation solution. The tissue culture flask was then placed in a preheated (37 °C) oscillating water bath. The sample was oscillated in the water bath at a rate of 60 cycles per minute (slow shake), for a period of ten minutes. The incubation solution was then aspirated and a further 10 ml of fresh incubation solution was added to the flask with the tissue, followed by a second ten minute period of oscillations at the same rate. The incubation was then aspirated, and a 10 ml of fresh incubation solution was added. For the third period of oscillations the cycle rate was increased to 120 cycles per minute for a period of 15 minutes. Throughout the oscillation procedure the incubation solution containing the tissue was gassed with 95% O₂ – 5% CO₂.

The flask was then removed from the water bath, two thirds of the incubation solution aspirated and the remainder of the contents of the flask (incubation solution containing digested tissue and tissue precipitants) were flushed through a 250-µm nylon mesh into a 15-ml polypropylene test tube. The remaining tissue was then gently flushed through the nylon mesh using ~10 ml of the wash solution. The sample was then left to settle for 15 minutes after which the top two thirds of the supernatant was aspirated and ~10 ml of fresh wash solution was added to the test tube. Following a second settling step of 15 minutes the supernatant was aspirated without disturbing the pellet of cells. The cells were then diluted in

PSS containing 0.01% bromophenyl blue (The Coleman and Bell Co., USA) which stains proteins, hence allowing for the easy identification of striations (sarcomere bands) within the cardiac myocytes (Figure 2.4). The diluted cell sample was then aliquoted into tissue culture dishes for analysis under light microscopy. Approximately 55-75% of the cells in the suspension were rod-shaped cardiac myocytes (Figure 2.4).

2.6 LIGHT MICROSCOPY

LV tissue from all rats in both models (natural progression and pharmacological) plus LV tissue from the WKY control group of the study, was assessed under light microscopy. Using an inverted light microscope (A, Figure 2.5), images seen under the microscope were relayed to a computer program using a digital camera (B, Figure 2.5) (Nikon Digital Sight DS-U1 & DS-5M, Nikon Corporation, Japan). The cells were viewed at 400x magnification and cardiac myocytes were selected based on the ability to see and count most of the sarcomere bands from one end of the cardiac myocyte to the other (Figure 2.6). Between 25 and 30 cardiac myocytes were selected from each LV tissue sample. Using the program, Act2U (Ver. 1.70 Nikon Corporation, Japan), the dimensions of each cardiac myocyte were measured. The software was calibrated using a $0.01 \times 100 = 1\text{mm}$ graticule (Graticules Ltd, Tonbridge, Kent, England). All images were saved on hard drive before being assessed. Saving of the images ensured that the cardiac myocyte images were not moving during the measurements and that the measurements could be reassessed at anytime. The dimensions measured were the length (A, Figure 2.6), width (B, Figure 2.6) and sarcomere length (distance between Z-bands) (C, Figure 2.6) of each cardiac myocyte. The length to width ratio of each cardiac myocyte was calculated. The 30-35 cardiac myocyte dimensions obtained were then averaged for each sample of LV tissue. From these group means were then calculated.

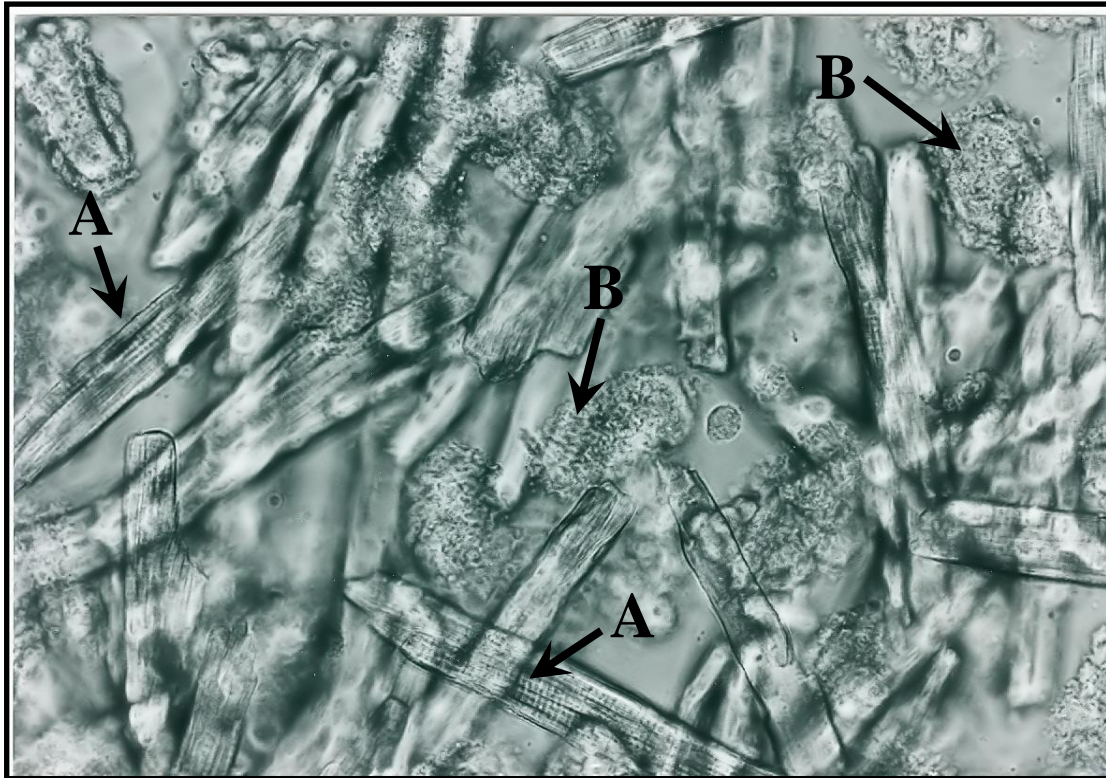


Figure 2.4 Examples of isolated cardiac myocytes

An example of ~70% rod-shaped isolated cardiac myocytes (A) surrounded by cell debris, non-viable cardiac myocytes or cells which are not cardiac myocytes (B) (upper panel) and a rod-shaped isolated cardiac myocyte (lower panel)



Figure 2.5 Photograph of digital camera and microscope

Photograph showing inverted microscope (A) to which digital camera (B) is attached. The digital camera is coupled to a computer running Act2U software and an image of a cardiac myocyte is displayed on the computer screen (C).

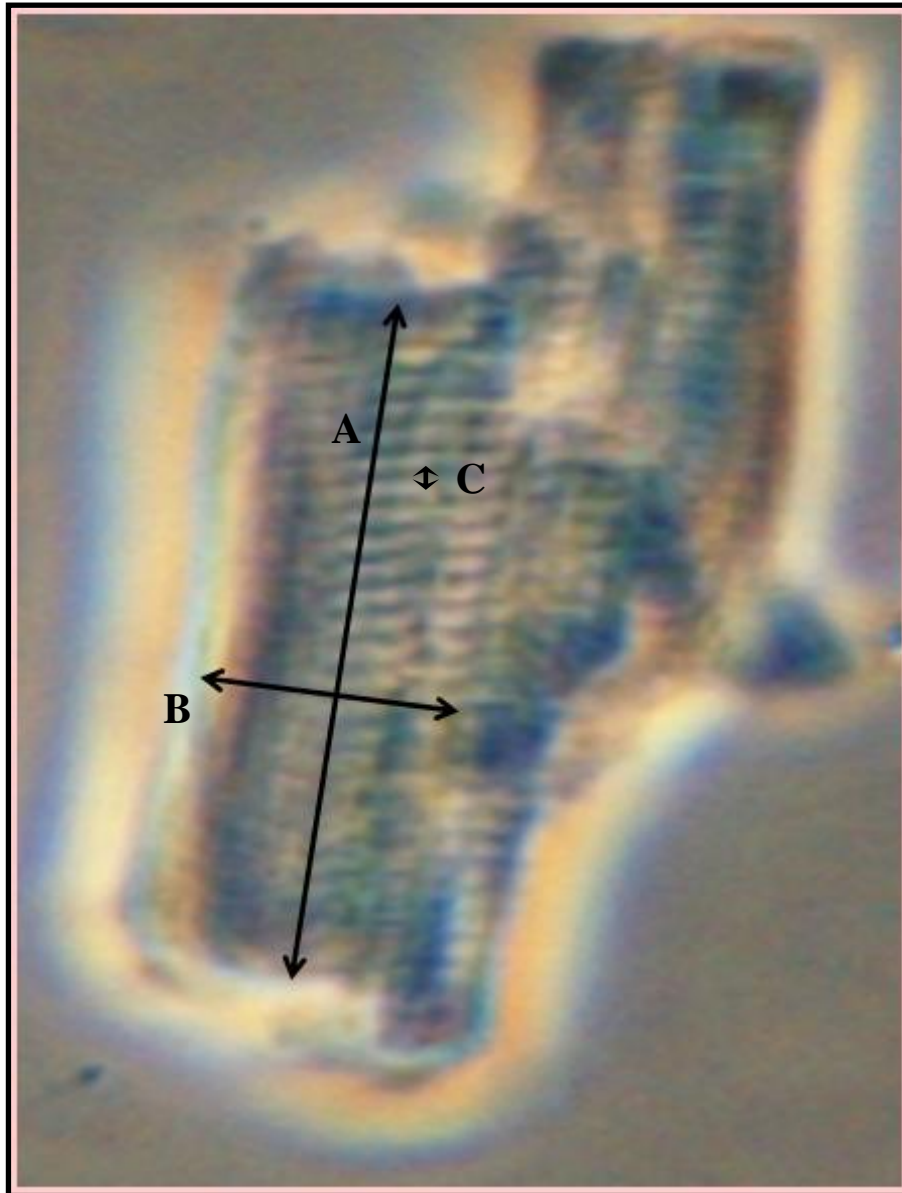


Figure 2.6 An example of striations of an isolated cardiac myocyte

Photograph of a cardiac myocyte showing striations and the measurement of length (A), width (B) and sarcomere length (C).

2.7 FLOW CYTOMETRY

As using light microscopy, relatively few cardiac myocytes can be measured in comparison to the total number of cardiac myocytes, I wished to also determine cardiac myocyte dimensions using a procedure which allows for the measurement of vast numbers of cells (~30 000 cells) in a short period of time. In order to do this I devised a method to measure cardiac myocyte dimensions using flow cytometry based upon previously described methods (Diez & Simm 1998; Nash *et al.* 1979). For the assessment of cardiac myocyte dimensions using flow cytometry, cardiac myocytes were isolated from 100mg of LV tissue from each of the rats (those in the natural progression model; those in the pharmacological model and the WKY control rats) using the same procedure as described above (see 2.4). However, after cardiac myocyte isolation, the cells were not stained with bromophenol blue; they were suspended in 1ml of PSS and placed in 5ml Polystyrene round bottom tubes (Falcon, Becton-Dickinson, USA) rather than in cell culture dishes.

Cardiac myocyte morphometry was assessed using a Becton-Dickinson flow cytometer (FACSCalibur[®], Franklin Lakes, NJ) (see Figure 2.7). Fluorescence in the FL1 channel was quantified at a single cell level and data were analysed using Cellquest[®] version 3.3 (Becton Dickinson software). The flow cytometer was preset to measure a maximum of 30 000 cells per sample. The cardiac myocytes were not stained as they autofluoresce, hence allowing for their detection and the assessment of their forward and side scatter. Side scatter gives an indication of cell granularity (number of intracellular organelles and/or proteins) and forward scatter a measure of relative cell size (based upon the shape of the cell and the degree of folding of the cell membrane). A dot plot of side versus forward scatter (Figure 2.8) was then drawn. The side versus forward scatter dot plot was then gated (A, Figure 2.8) to exclude

debris and cells which are not cardiac myocytes (cells with low granularity) (Strijdom H *et al.* 2004).

The measurement of cell length by the flow cytometer was achieved by the determination of the time of flight (FL1-W). The cardiac myocytes are passed through the flow chamber through which the excitation light source is shone at 90°. The longer the cardiac myocytes are, the greater is the period of time that the cardiac myocytes are in the path of the laser beam (called the time of flight) (Figure 2.9). Hence longer cardiac myocytes have a greater time of flight or FL1-W (Figure 2.10). In order for this measurement of cardiac myocyte length to be calibrated rod-shaped beads would be required. As at present only cylindrical calibration beads are available, I have indicated these cardiac myocyte length measurements as unitless. FL1-W measurements of ~15 000 to 20 000 cardiac myocytes were obtained for each LV specimen. From these measurements group means were calculated.

2.8 STATISTICAL ANALYSES

All data were compared between the five groups in the two models of dilatation; i.e. the SHR-Failure and SHR-Non-Failure for the natural progression model; the SHR-Control and SHR-ISO treated groups for the pharmacological model and the WKY control group. An analysis of variance (ANOVA) was performed followed by a Student-Newman-Keuls *post-hoc* test to assess for differences between the groups. The relations between cardiac myocyte length and LVED radius; light microscopy cardiac myocyte length and flow cytometry cardiac myocyte length; and cardiac myocyte length and LV weight normalised to 100g body weight were determined using linear correlation analysis (Pearson's). All data are represented as mean \pm SEM (standard error of the mean). The significance level was set at $p < 0.05$.



Figure 2.7 Flow cytometer

A photograph of the Becton-Dickinson flow cytometer (FACSCalibur®).

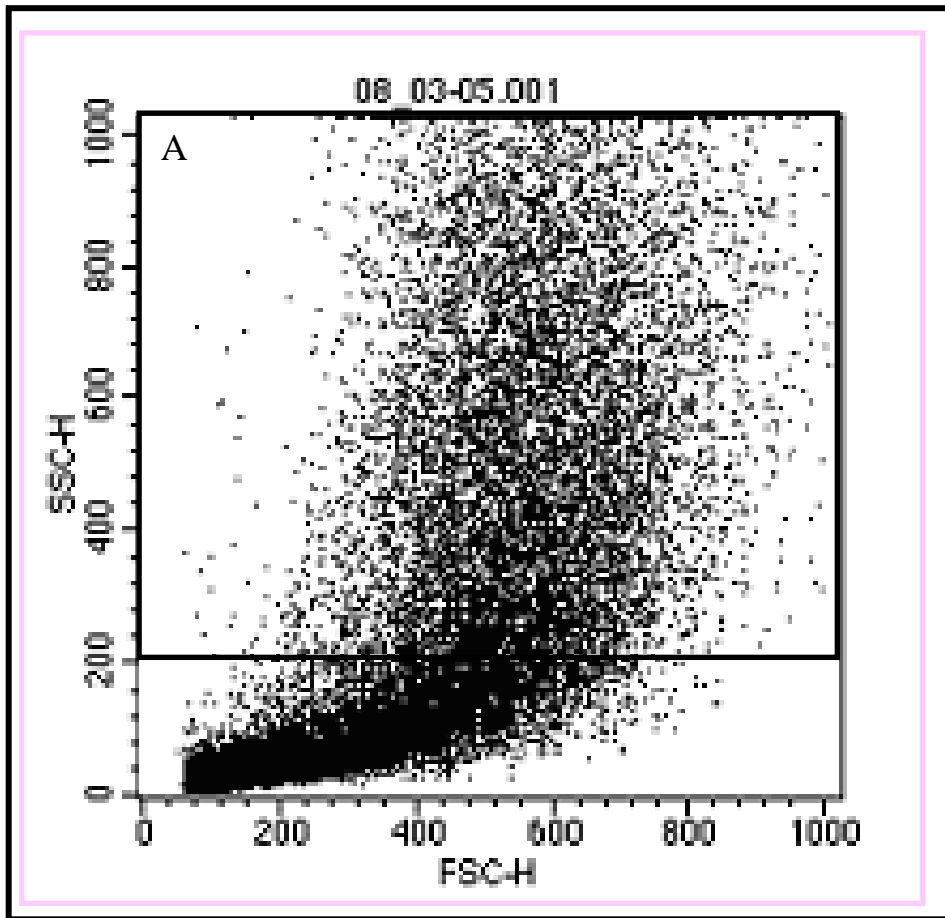


Figure 2.8 Example of flow cytometer dot plot

Dot plot of side scatter height (SSC-H) and forward scatter height (FSC-H) of cardiac myocytes. The dot plot was gated (A) from a SSC-H of above 200 in order to exclude debris and cells which are not cardiac myocytes [cells with low granularity (SSC-H)].

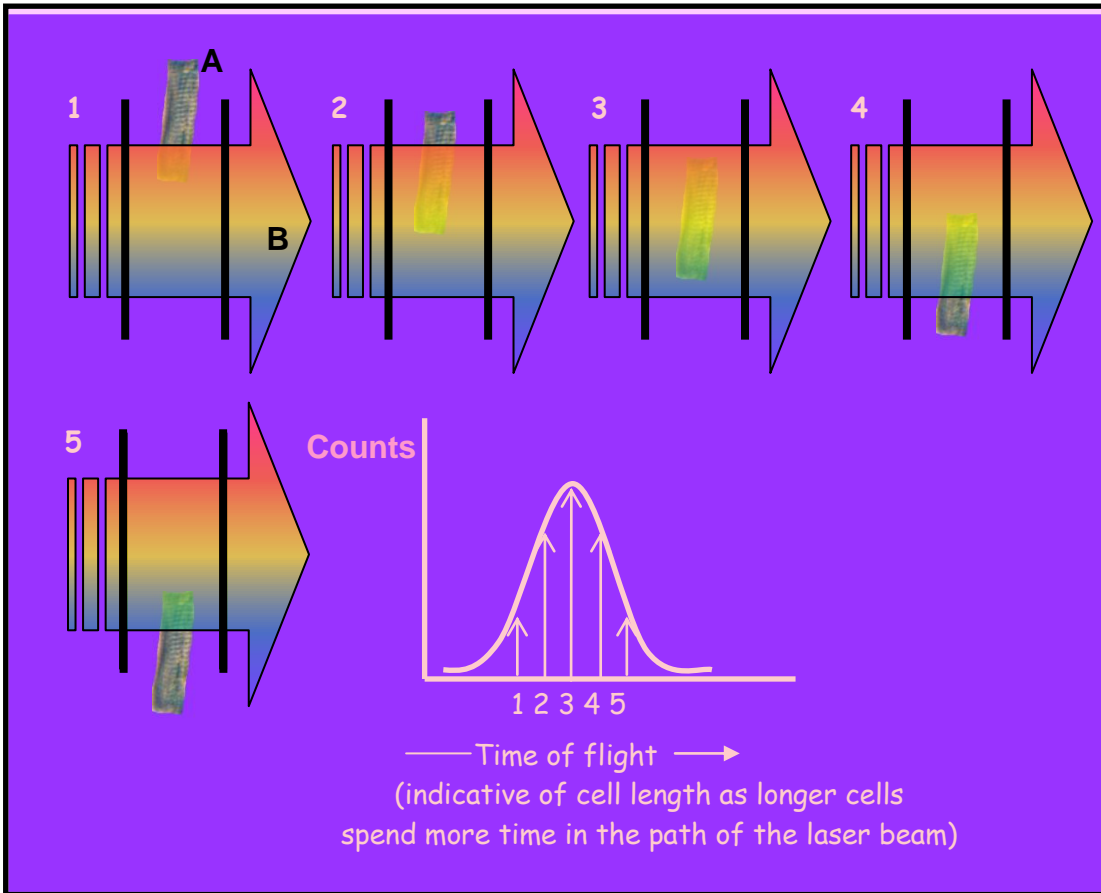


Figure 2.9 Diagrammatic representation of a cardiac myocyte in the path of the flow cytometer laser beam

Diagrammatic representation of a cardiac myocyte (A) in the path of the laser beam (B). As indicated in the graph, the time of flight counts (y-axis) increase as the cardiac myocyte passes from $\sim\frac{1}{3}$ (1) to the whole (3) of the cell being in the path of the laser beam.

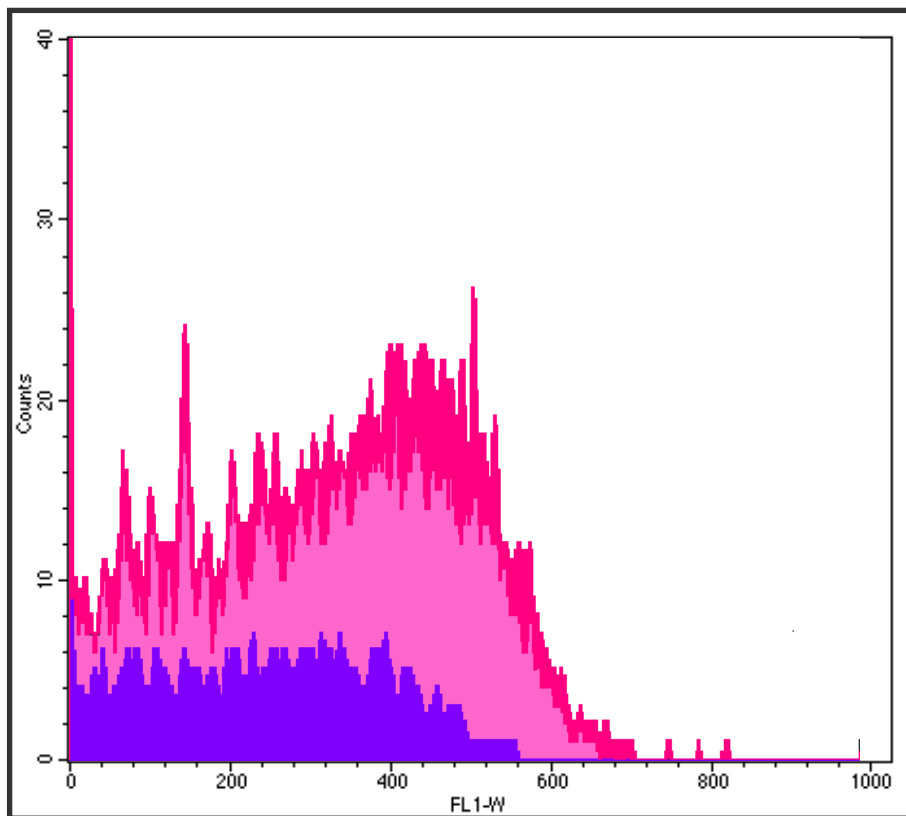


Figure 2.10 Plot of cardiac myocyte counts versus time of flight

Plot of counts versus time of flight (FL1-W) for cardiac myocytes from a normotensive WKY rat (purple), a SHR-NF rat (light pink) and a SHR-F rat (dark pink).

CHAPTER 3

3.0 RESULTS

3.1 LEFT VENTRICULAR GEOMETRY

3.1.1 Natural Progression Model

3.1.1.1 Body and Tissue Weights and Blood Pressures

Both heart weight and LV weight were increased in the SHR-Failure and SHR-Non-Failure groups when compared to the WKY control group (Table 3.1). However, the body weights of the WKY control group were greater than those of both the SHR-Failure and the SHR-Non-Failure groups. Nevertheless, LV weight standardised to 100g body weight remained increased in both the SHR-Failure and the SHR-Non-Failure groups compared to the WKY control group (Table 3.1). Consistent with the increased heart and LV weights, both SHR groups had increased SBP compared to the WKY group (Table 3.1).

Despite similar body weights; heart weight, LV weight and LV weight normalised to 100g body weight ratio were greater in the SHR-Failure group compared to the SHR-Non-Failure group. Consistent with the presence of heart failure, both RV weight and wet liver weight were increased in the SHR-Failure group compared to the SHR-Non-Failure group and the WKY control group (Table 3.1).

3.1.1.2 LV Dimensions

The LV end diastolic radius of the SHR-Failure group was significantly greater than that of the SHR-Non-Failure group throughout the measured LV end diastolic pressure range of 2 – 9 mm Hg (Figure 3.1, upper panel), but was only greater than that of the WKY control group at an LV end diastolic pressure of 9 mm Hg. Bearing in mind the increased body weight in the WKY control group, the LV end diastolic radius was normalised to 100g body weight. Throughout the measured LV end diastolic pressure range of 2-9 mm Hg, the LV end diastolic radius normalised to 100g body weight was greater in the SHR-Failure group

Table 3.1 Body and tissue weights in the natural progression model and in the pharmacological model

	Normotensive control	Natural progression model		Pharmacological model	
	WKY	SHR-Non-Failure	SHR-Failure	SHR-Control	SHR-ISO
Number	9	9	9	9	9
Body weight (g)	418±6	344±9***	336±8***	360±6***	353±10***
Heart weight (g)	1.35±0.03	1.75±0.03***	1.96±0.03***†‡	1.67±0.07**	2.01±0.13***##§
LV weight (g)	0.99±0.02	1.32±0.02***	1.50±0.02***†‡	1.29±0.06***	1.53±0.11***#§
LV weight / 100g body weight	0.238±0.006	0.383±0.009***	0.446±0.011***†‡	0.359±0.013***	0.437±0.034***##§
RV weight (g)	0.36±0.01	0.41±0.01	0.48±0.01***†‡‡‡	0.38±0.02	0.48±0.02***###§§
Liver weight (g)	13.10±0.38	13.48±0.48	15.41±0.75*†	-	-
Systolic blood pressure (mmHg)	128±8	188±7***	190±8***	186±6***	188±9***

Values are mean ± SEM. The WKY normotensive group was the control group for both models.

*p<0.05, **p<0.01, ***p<0.001 compared to the WKY control group; †p<0.05, ††p<0.001 compared to the SHR-Non-Failure group; #p<0.05, ##p<0.01, ###p<0.001 compared to the SHR-Control group; ‡p<0.05, ‡‡p<0.01 versus SHR-Control group; §p<0.05, §§p<0.01 versus SHR-Non-Failure group.

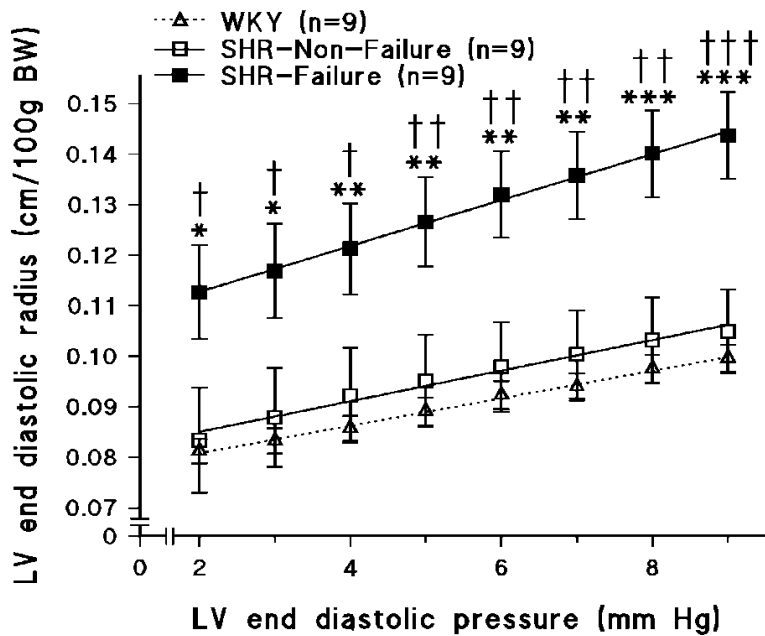
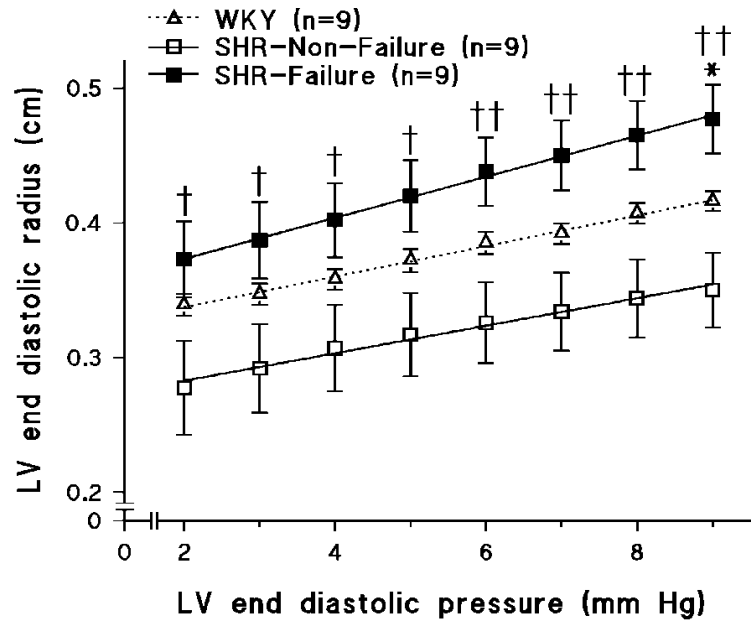


Figure 3.1 Left ventricular end diastolic radius – pressure relations in the natural progression model

Left ventricular (LV) end diastolic radius – pressure relations (upper panel) and these relations after normalising LV radius to 100g body weight (BW) (lower panel) for the three groups in the natural progression model.

*p<0.05, **p<0.01, ***p<0.001 compared to the WKY control group; †p<0.05, ††p<0.01, †††p<0.001 compared to the SHR-Non-Failure group.

compared to those of the SHR-Non-Failure group and the WKY control group (Figure 3.1, lower panel). The increased LV end diastolic radius normalised to 100g body weight in the SHR-Failure group is indicative of the presence of LV dilatation.

Throughout the measured LV end diastolic pressure range of 2-9 mm Hg, the LV end diastolic wall thickness to radius ratio was higher in the SHR-Non-Failure group compared to that of the WKY control group, consistent with compensatory concentric geometry (Figure 3.2). Moreover the LV end diastolic wall thickness to radius ratio in the SHR-Failure group was decreased compared to that of the SHR-Non-Failure group and was no different to that of the WKY controls (Figure 3.2). The decreased LV end diastolic wall thickness to radius ratio in the SHR-Failure group is consistent with the presence of LV decompensation and dilatation.

3.1.2 Pharmacological Model

3.1.2.1 Body and Tissue Weights

Body weight was lower but heart weight and LV weight were greater in the SHR-Control and SHR-ISO groups when compared to the WKY control group (Table 3.1). In addition, the SHR-ISO group had significantly greater heart weight and LV weight than the SHR-Control group (Table 3.1). Furthermore, the LV weight normalised to 100g body weight of the SHR-Control and SHR-ISO groups was greater than that of the WKY control group. Moreover, the LV weight normalised to 100g body weight of the SHR-ISO group was greater than that of the SHR-Control group (Table 3.1). In the SHR-ISO group, RV weight was increased compared to both the SHR-Control and the WKY groups, consistent with the presence of LV failure in the SHR-ISO group.

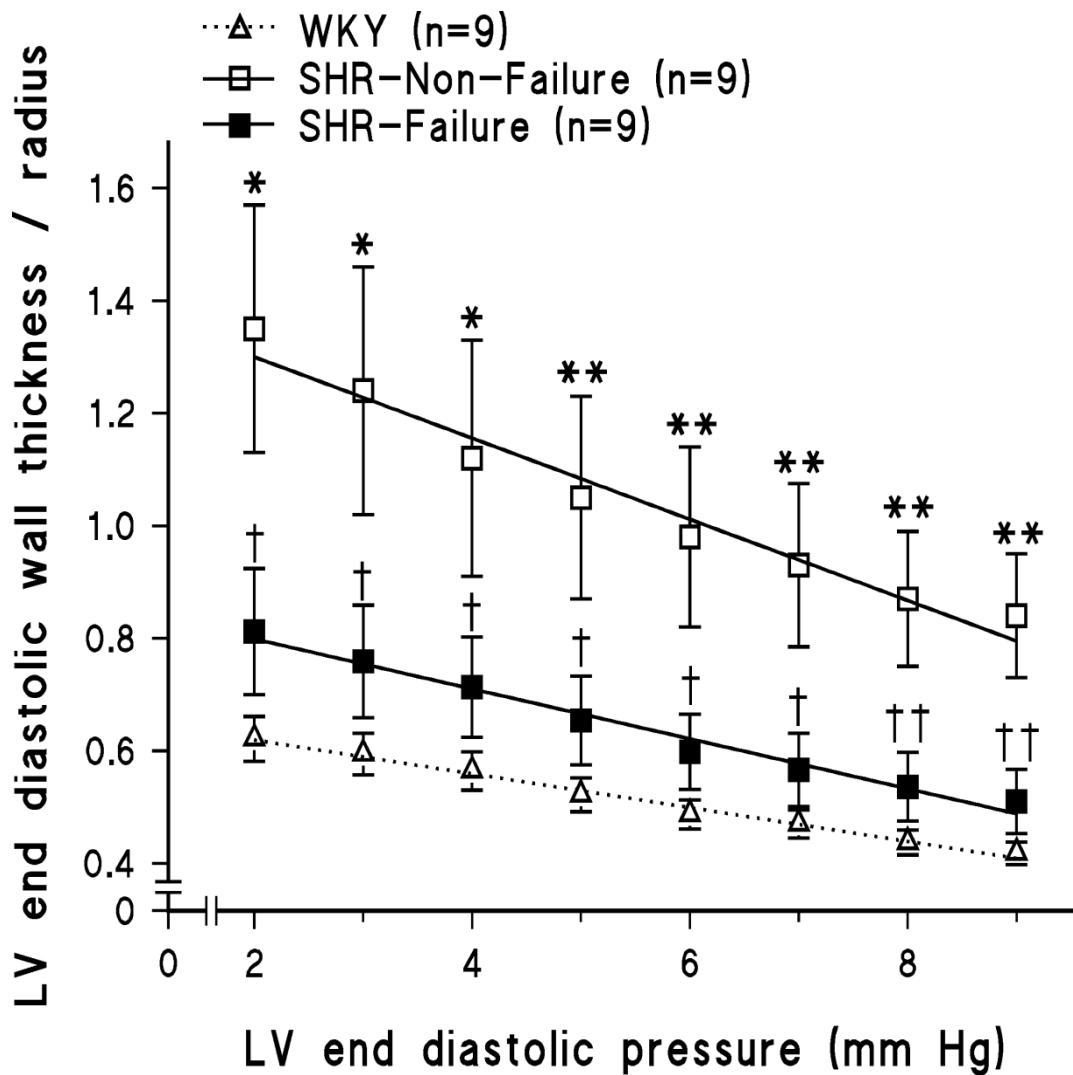


Figure 3.2 Left ventricular end diastolic wall thickness to radius ratio – pressure relations in the natural progression model

Left ventricular (LV) end diastolic wall thickness to radius ratio – pressure relations for the three groups in the natural progression model.

*p<0.05, **p<0.01 compared to the WKY control group; †p<0.05, ††p<0.01 compared to the SHR-Non-Failure group.

3.1.2.2 LV Dimensions

The LV end diastolic radius of the SHR-ISO group were increased compared to those of both the WKY control and the SHR-Control groups throughout the measured LV end diastolic pressure range of 2 – 9 mm Hg (Figure 3.3, upper panel), indicative of the presence of LV dilatation in the SHR-ISO group. Similarly, the LV end diastolic radius normalised to 100g body weight was increased in the SHR-ISO group compared to both the SHR-Control and the WKY control groups throughout the measured LV end diastolic pressure range of 2-9 mm Hg (Figure 3.3, lower panel). No differences were noted between the SHR-Control and WKY control groups.

Indicative of the presence of compensatory concentric geometry, the LV end diastolic wall thickness to radius ratio at LV end diastolic pressures of 2-6 mm Hg was increased in the SHR-Control group (Figure 3.4). In comparison, at LV end diastolic pressures of 2-6 mm Hg, the LV end diastolic wall thickness to radius ratio in the SHR-ISO group was lower than that of the SHR-Control group and was no different from that of the WKY control group (Figure 3.4). The decreased LV end diastolic wall thickness to radius ratio in the SHR-ISO group is indicative of LV decompensation and dilatation.

3.2 MYOCYTE DIMENSIONS

3.2.1 Natural Progression Model

3.2.1.1 Light microscopy

There was a significant increase in the length of the cardiac myocytes of the hypertensive groups (SHR-Failure and SHR-Non-Failure groups) when compared to the normotensive (WKY) group (Figure 3.5, upper panel). Importantly, there was no difference in the cardiac myocyte lengths between the two hypertensive groups. Hence, despite the presence of LV

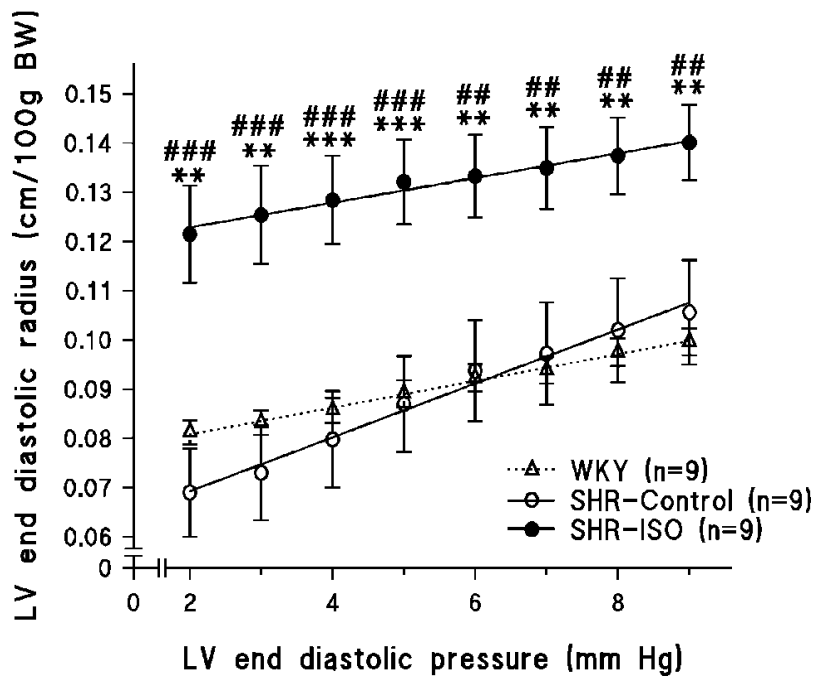
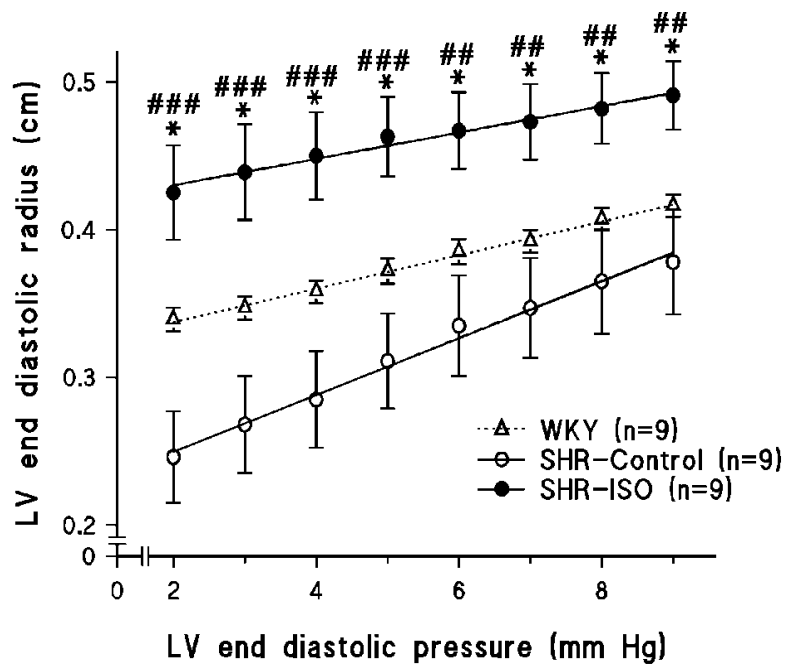


Figure 3.3 Left ventricular end diastolic radius – pressure relations in the pharmacological model

Left ventricular (LV) end diastolic radius – pressure relations (upper panel) and these relations after normalising LV radius to 100g body weight (BW) (lower panel) for the three groups in the pharmacological model.

*p<0.05, **p<0.01, ***p<0.001 compared to the WKY control group; ##p<0.01, ###p<0.001 compared to the SHR-Control group.

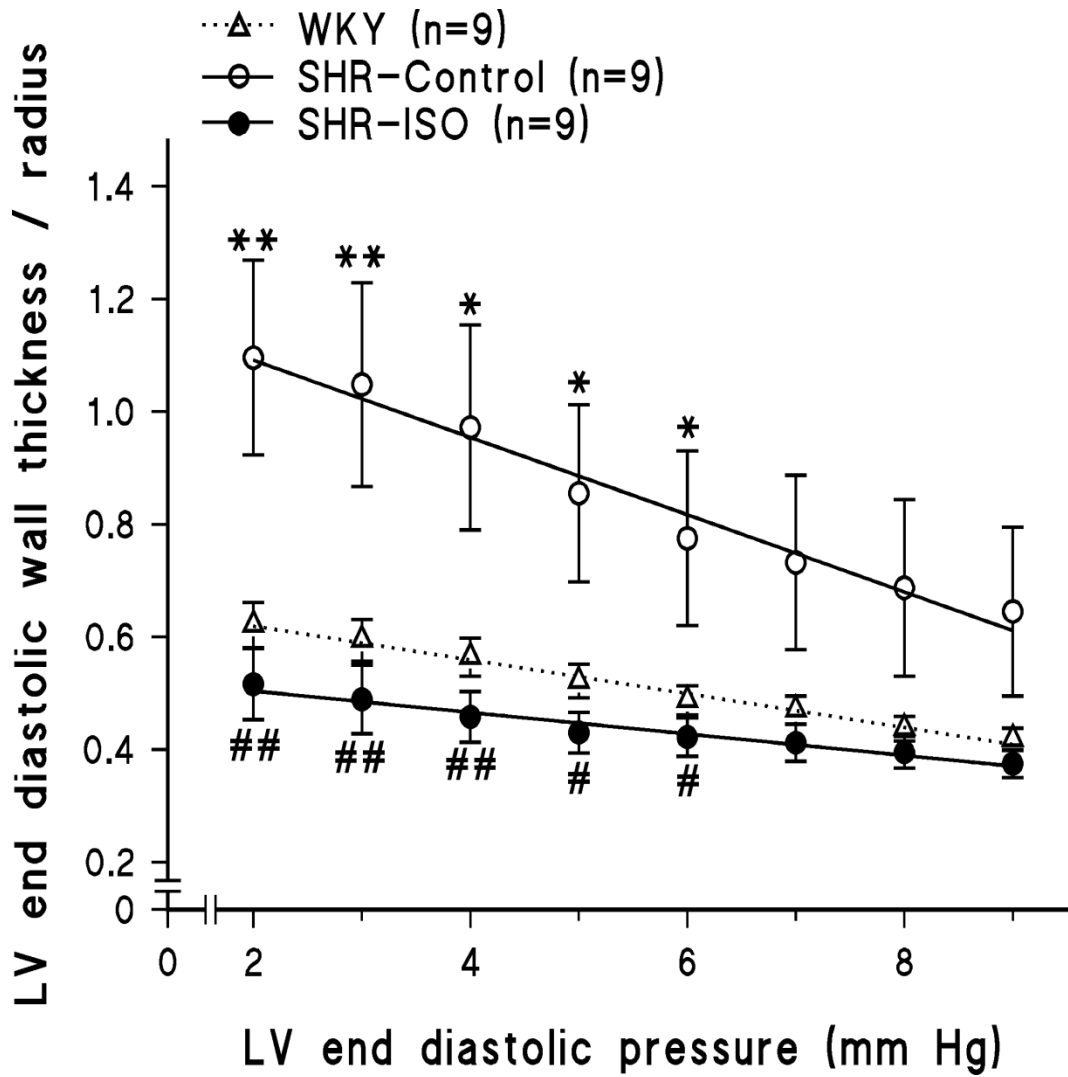


Figure 3.4 Left ventricular end diastolic wall thickness to radius ratio – pressure relations in the pharmacological model

Left ventricular (LV) end diastolic wall thickness to radius ratio – pressure relations for the three groups in the pharmacological model.

*p<0.05, **p<0.01 compared to the WKY control group; #p<0.05, ##p<0.01 compared to the SHR-Control group.

dilatation, the SHR-Failure rats had cardiac myocytes of similar length to those of the SHR-Non-Failure rats (absence of LV dilatation) (Figure 3.5, upper panel). Consistent with an increased cardiac myocyte length in the hypertensive groups, a right shift in the frequency distribution of cardiac myocyte lengths was noted in the SHR-Non-Failure and SHR-Failure groups in comparison to the WKY control group (Figure 3.5, lower panel).

No differences were noted for either cardiac myocyte width (Figure 3.6, upper panel) or the cardiac myocyte length to width ratio (Figure 3.6, lower panel) between the SHR-Failure, SHR-Non-Failure and WKY groups. In addition no differences in sarcomere length (μm) (WKY: 1.87 ± 0.04 ; SHR-Non-Failure: 1.99 ± 0.04 ; SHR-Failure: 2.00 ± 0.04) or sarcomere number (WKY: 45 ± 2 ; SHR-Non-Failure: 46 ± 2 ; SHR-Failure: 46 ± 2) were noted between the three groups.

3.2.1.2 Flow Cytometry

The data collected from the same rat hearts using flow cytometry indicated a similar pattern as that shown with light microscopy. The length (FL1W) of the WKY cardiac myocytes was significantly decreased as compared to that of the two hypertensive groups, SHR-Failure and SHR-Non-Failure (Figure 3.7). Moreover, no differences in cardiac myocyte length (FL1W) were noted between the SHR-Failure and the SHR-Non-Failure groups (Figure 3.7), indicating that despite differences in LV dimensions (Figures 3.1 and 3.2), no differences in cardiac myocyte length (FL1W) were noted.

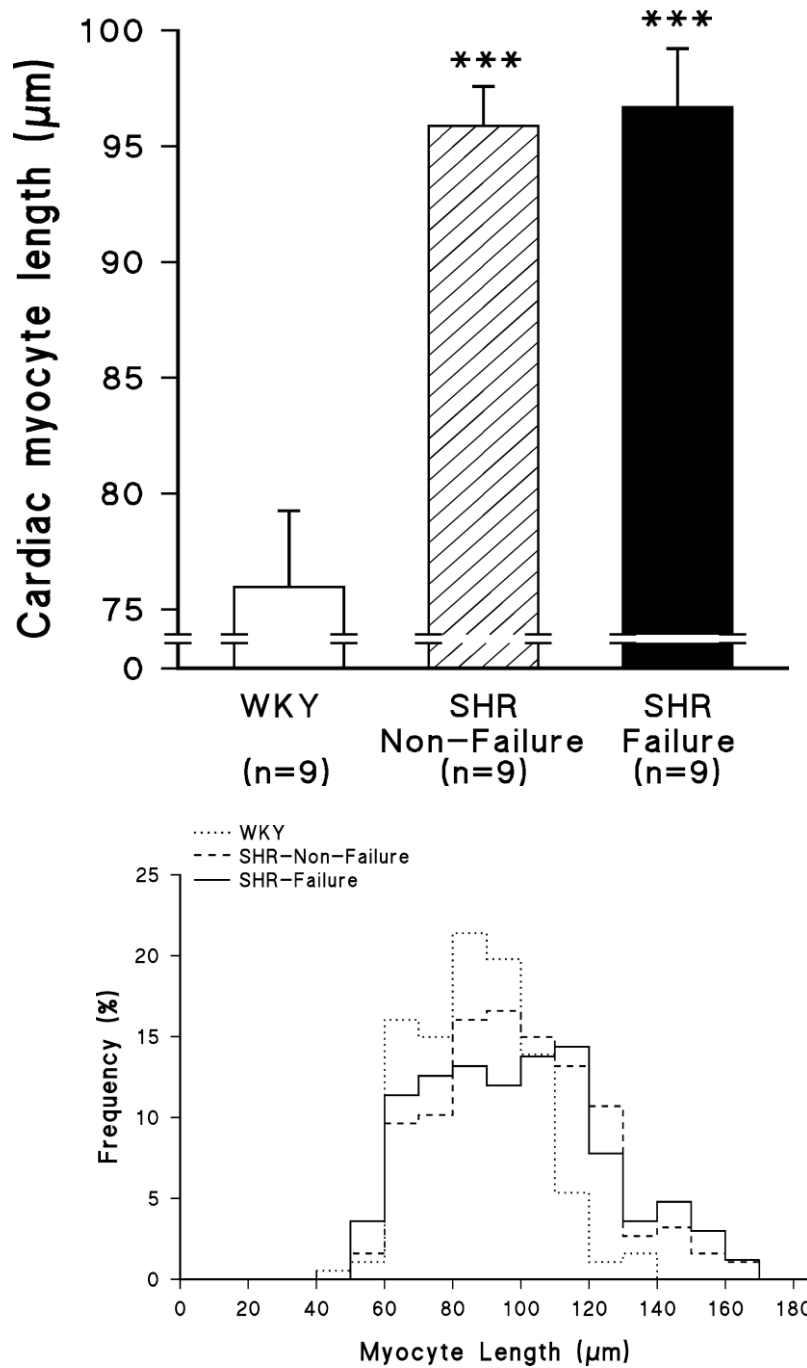


Figure 3.5 Cardiac myocyte lengths and frequency distribution of cardiac myocyte lengths in the natural progression model

Cardiac myocyte lengths (upper panel) and frequency distribution of cardiac myocyte lengths (lower panel) as assessed by light microscopy in the three groups of the natural progression model.

***p<0.001 compared to the WKY control group.

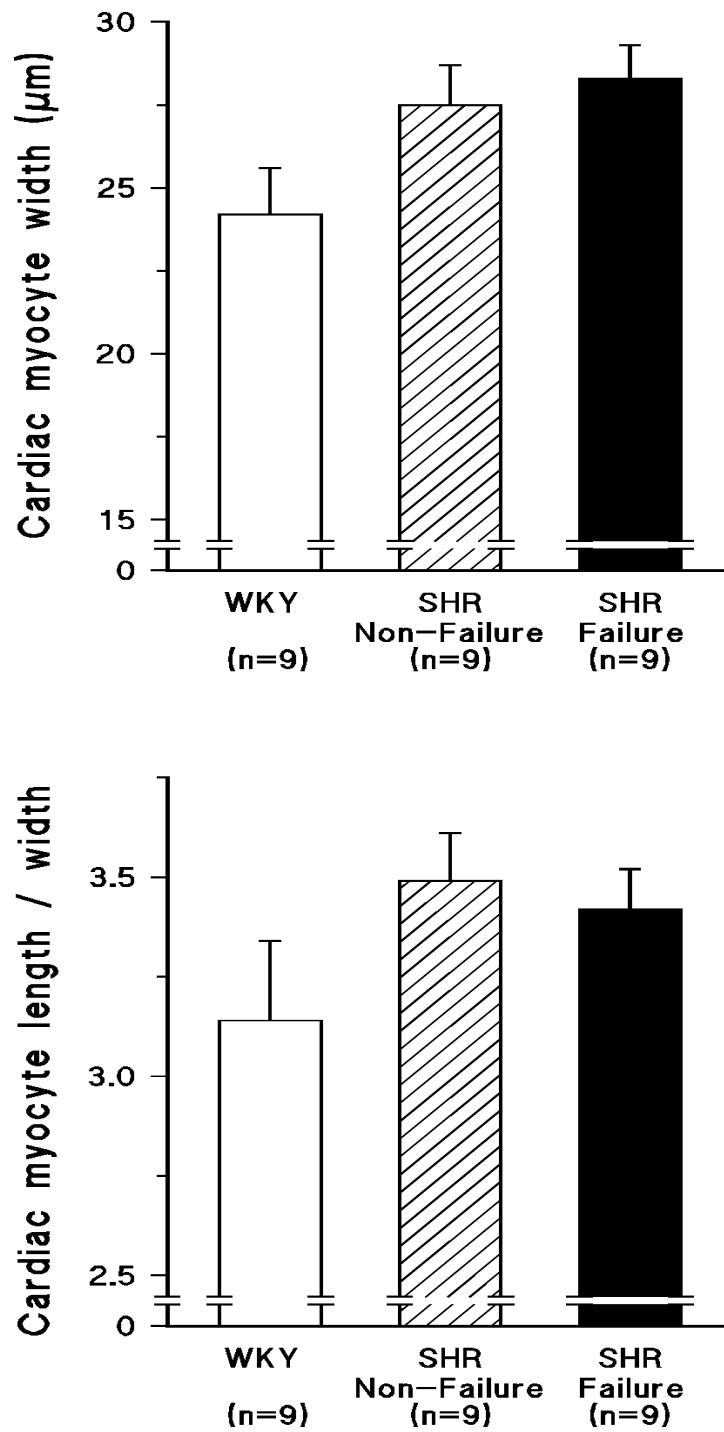


Figure 3.6 Cardiac myocyte widths and length to width ratios in the natural progression model

Cardiac myocyte widths (upper panel) and length to width ratios (lower panel) as assessed by light microscopy in the three groups of the natural progression model.

No significant differences were noted between the three groups.

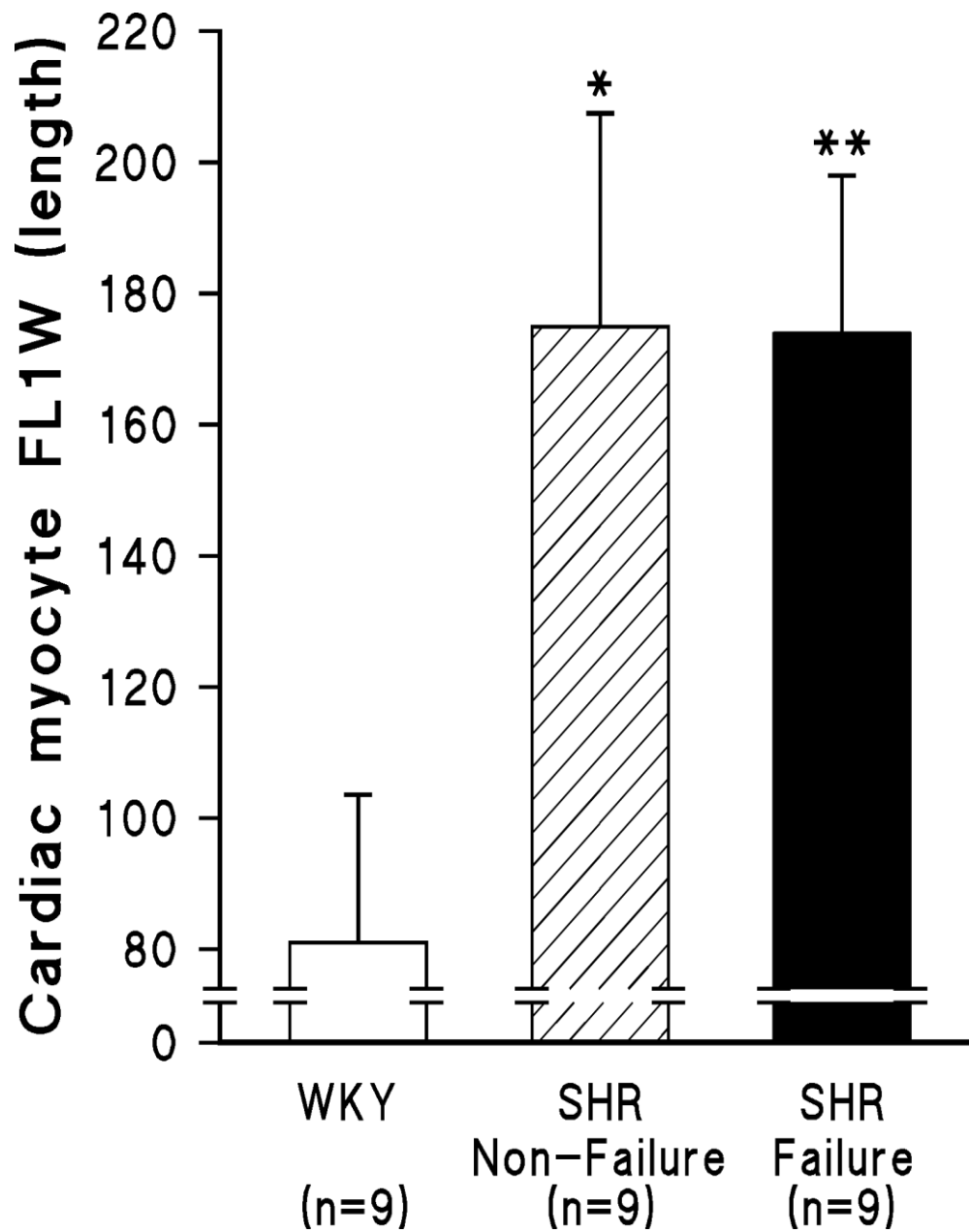


Figure 3.7 Cardiac myocyte lengths as assessed by flow cytometry in the natural progression model

Cardiac myocyte lengths as assessed by flow cytometry (FL1W) in the three groups of the natural progression model.

* $p < 0.05$, ** $p < 0.01$ compared to the WKY control group.

3.2.2 Pharmacological model

3.2.2.1 Light microscopy

There was a significant increase in the length of the cardiac myocytes of the SHR-Control and SHR-ISO groups when compared to those of the normotensive WKY control group (Figure 3.8, upper panel). Importantly, there was no difference in the length of the cardiac myocytes of the SHR-ISO group compared to those of the SHR-Control groups (Figure 3.8, upper panel). Hence, despite the presence of cardiac dilatation in the SHR-ISO group, but not in the SHR-Control group, the cardiac myocyte length was no different between these two groups. Consistent with an increased cardiac myocyte length in the hypertensive groups, a right shift in the frequency distribution of cardiac myocyte lengths was noted in the SHR-Control and SHR-ISO groups in comparison to the WKY control group (Figure 3.8, lower panel).

The cardiac myocyte widths of the SHR-ISO and SHR-Control groups were no different from those of the WKY control group (Figure 3.9, upper panel). In addition, no differences in the cell length to width ratios were noted between the three groups (Figure 3.9, lower panel). A modest increase ($p < 0.05$) in sarcomere length (μm) was noted in SHR-Control (2.10 ± 0.04) and SHR-ISO (2.13 ± 0.04) in comparison to WKY (1.87 ± 0.04). However, no differences in sarcomere number (WKY: 45 ± 2 ; SHR-Control: 40 ± 2 ; SHR-ISO: 40 ± 2) were noted between the three groups.

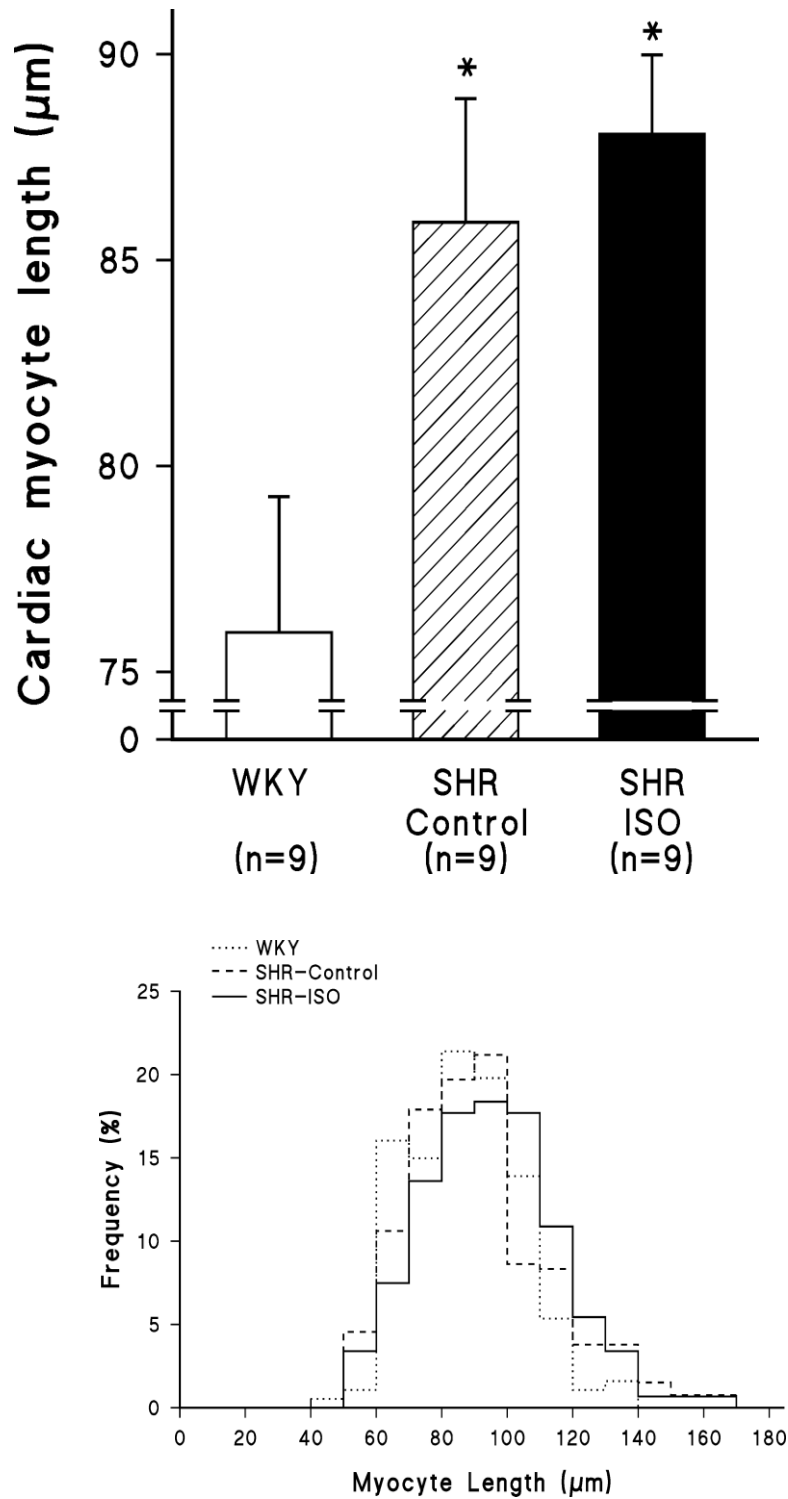


Figure 3.8 Cardiac myocyte lengths and frequency distribution of cardiac myocyte lengths in the pharmacological model

Cardiac myocyte lengths (upper panel) and frequency distribution of cardiac myocyte lengths (lower panel) as assessed by light microscopy in the three groups of the pharmacological model.

*p<0.05 compared to the WKY control group.

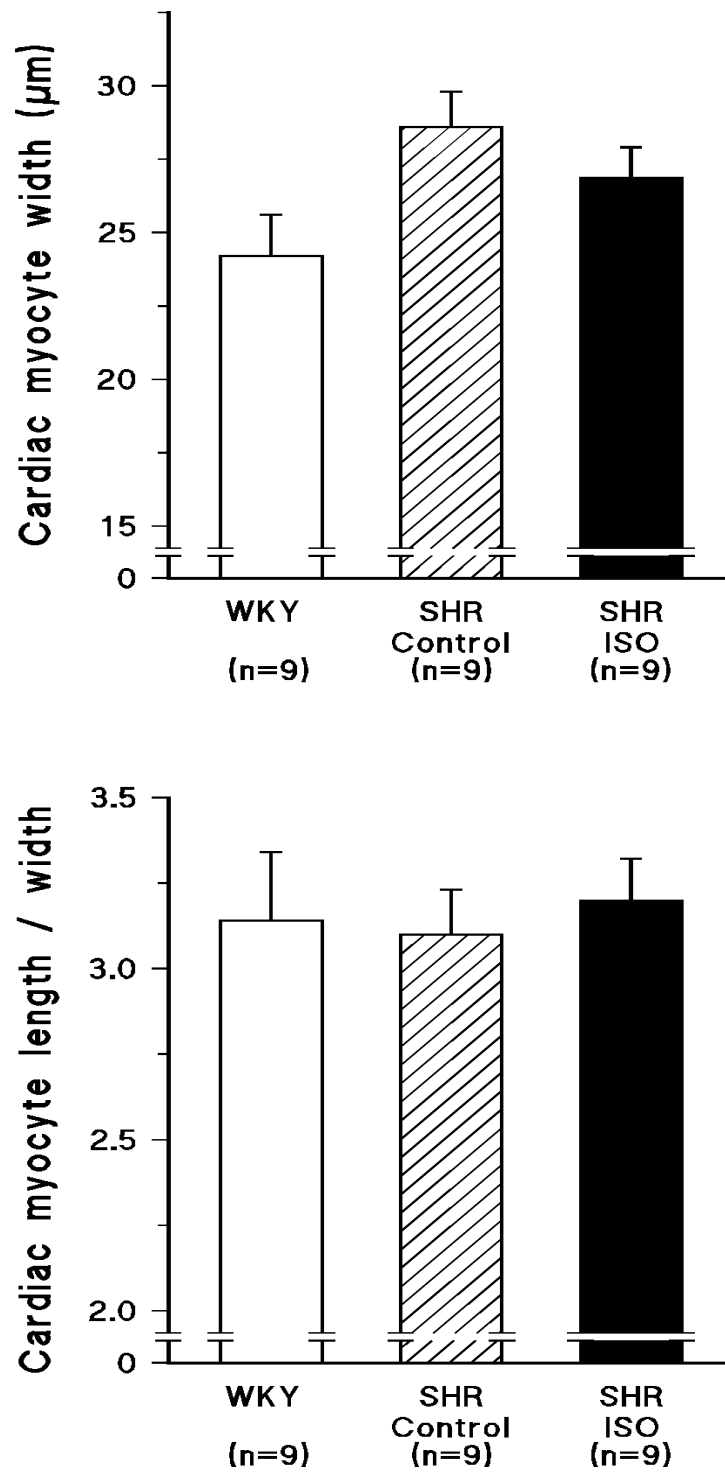


Figure 3.9 Cardiac myocyte widths and length to width ratios in the pharmacological model

Cardiac myocyte widths (upper panel) and length to width ratios (lower panel) as assessed by light microscopy in the three groups of the pharmacological model.

No significant differences were noted between the three groups.

3.2.2.2 Flow Cytometry

The data collected from the same rat hearts using flow cytometry indicated a similar pattern as that shown with light microscopy. The length (FL1W) of the WKY cardiac myocytes was significantly shorter as compared to that of the SHR-Control and SHR-ISO groups (Figure 3.10). Importantly, despite differences in LV dimensions (Figures 3.3 and 3.4) no difference in cardiac myocyte length (FL1W) was evident between the SHR-ISO and SHR-Control groups (Figure 3.10).

3.3 CORRELATIONS

3.3.1 Left ventricular end diastolic radius and cardiac myocyte length

Linear correlation analyses between LV end diastolic radius and cardiac myocyte length (Figure 3.11, light microscopy, upper panel and flow cytometry, lower panel) were performed using data from all groups (SHR-Non-Failure, SHR-Failure, WKY, SHR-Control, SHR-ISO). Despite a range of light microscopy mean myocyte lengths (~70-110 μm) and mean LV end diastolic radii (~0.1-0.6 cm), no correlation was observed (Figure 3.11, upper panel). Furthermore, no correlation was observed between flow cytometry myocyte lengths and LV end diastolic radii (Figure 3.11, lower panel).

3.3.2 Cardiac myocyte lengths obtained using light microscopy versus flow cytometry

The two techniques used to measure cardiac myocyte length were linearly correlated (Figure 3.12). The cardiac myocytes from the WKY control rats were the smallest (in the left of Figure 3.12) and no differences between the four SHR groups were evident (there is considerable overlap of the data obtained in these four groups, Figure 3.12). Using these two techniques the same differences were shown between the groups (compare figures 3.5 and 3.7; compare Figures 3.8 and 3.10). Hence, although absolute measurements of cell length

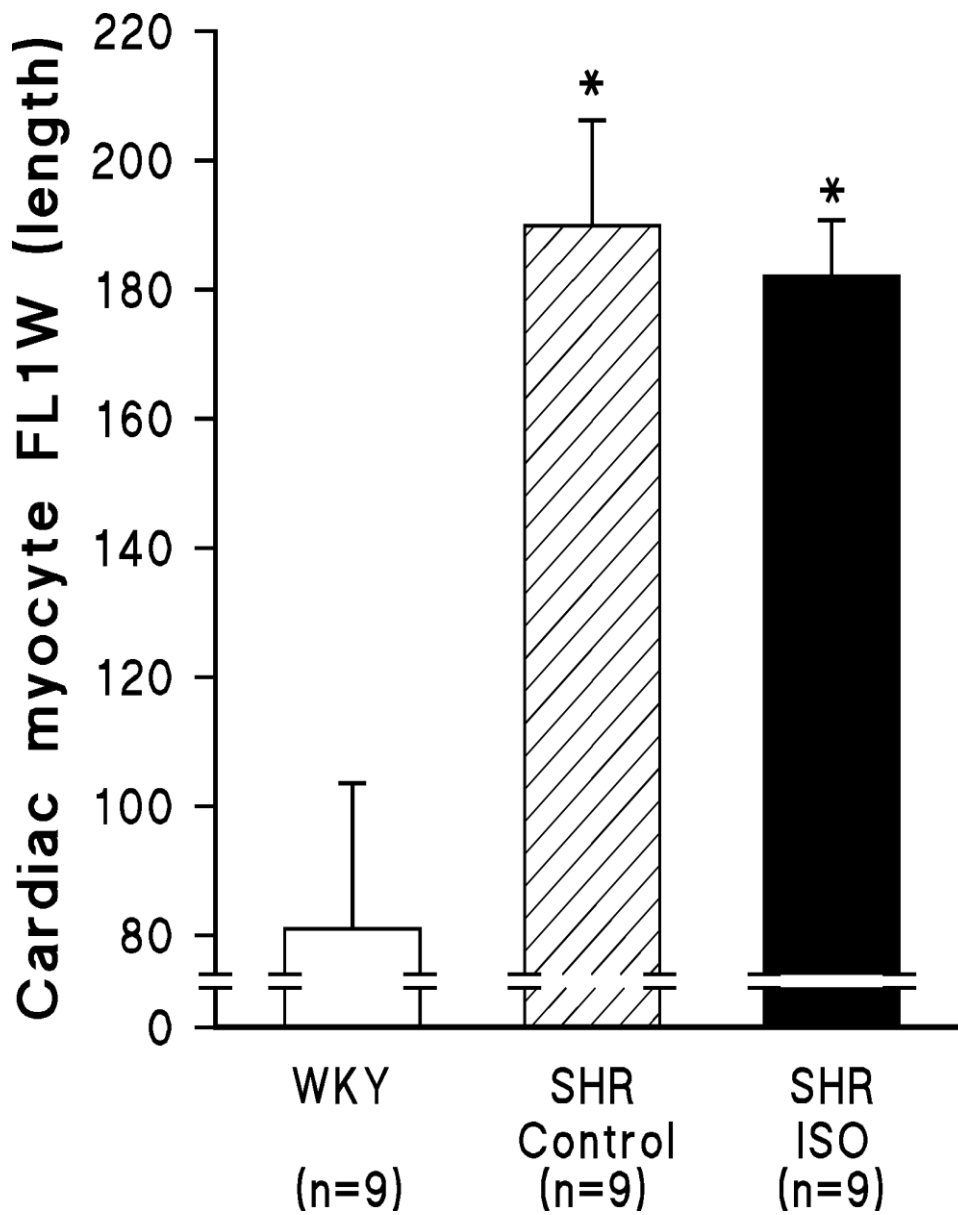


Figure 3.10 Cardiac myocyte lengths as assessed by flow cytometry in the pharmacological model

Cardiac myocyte lengths as assessed by flow cytometry (FL1W) in the three groups of the pharmacological model.

*p<0.05 compared to the WKY control group.

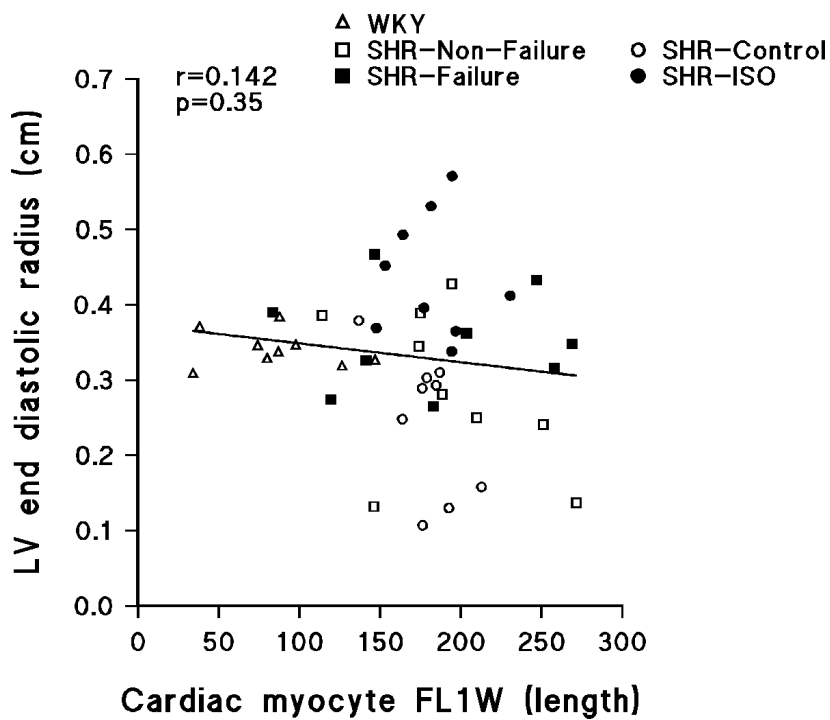
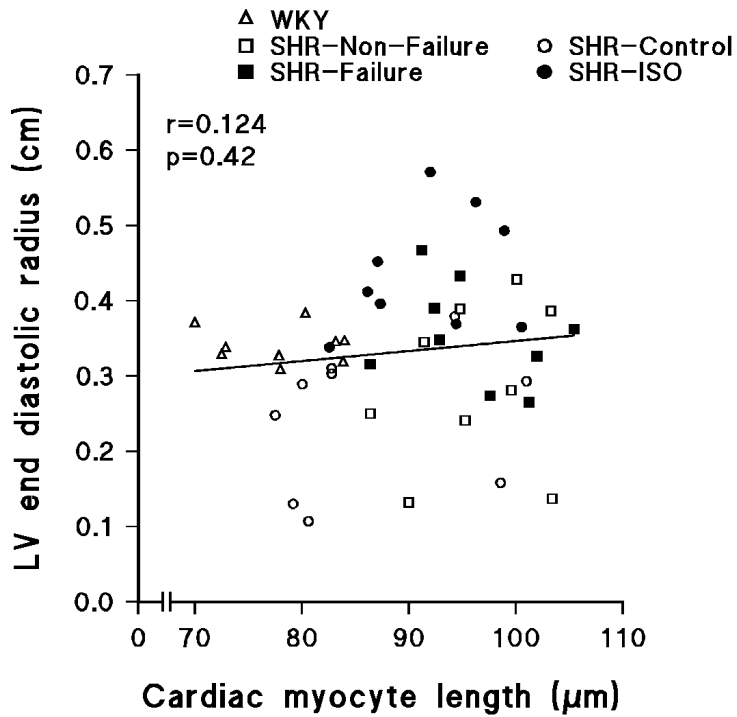


Figure 3.11 Linear correlation analyses between left ventricular end diastolic radius and cardiac myocyte length

Linear correlation analyses between left ventricular (LV) end diastolic radius and cardiac myocyte length as assessed by light microscopy (upper panel) and flow cytometry (lower panel) using data obtained in all groups.

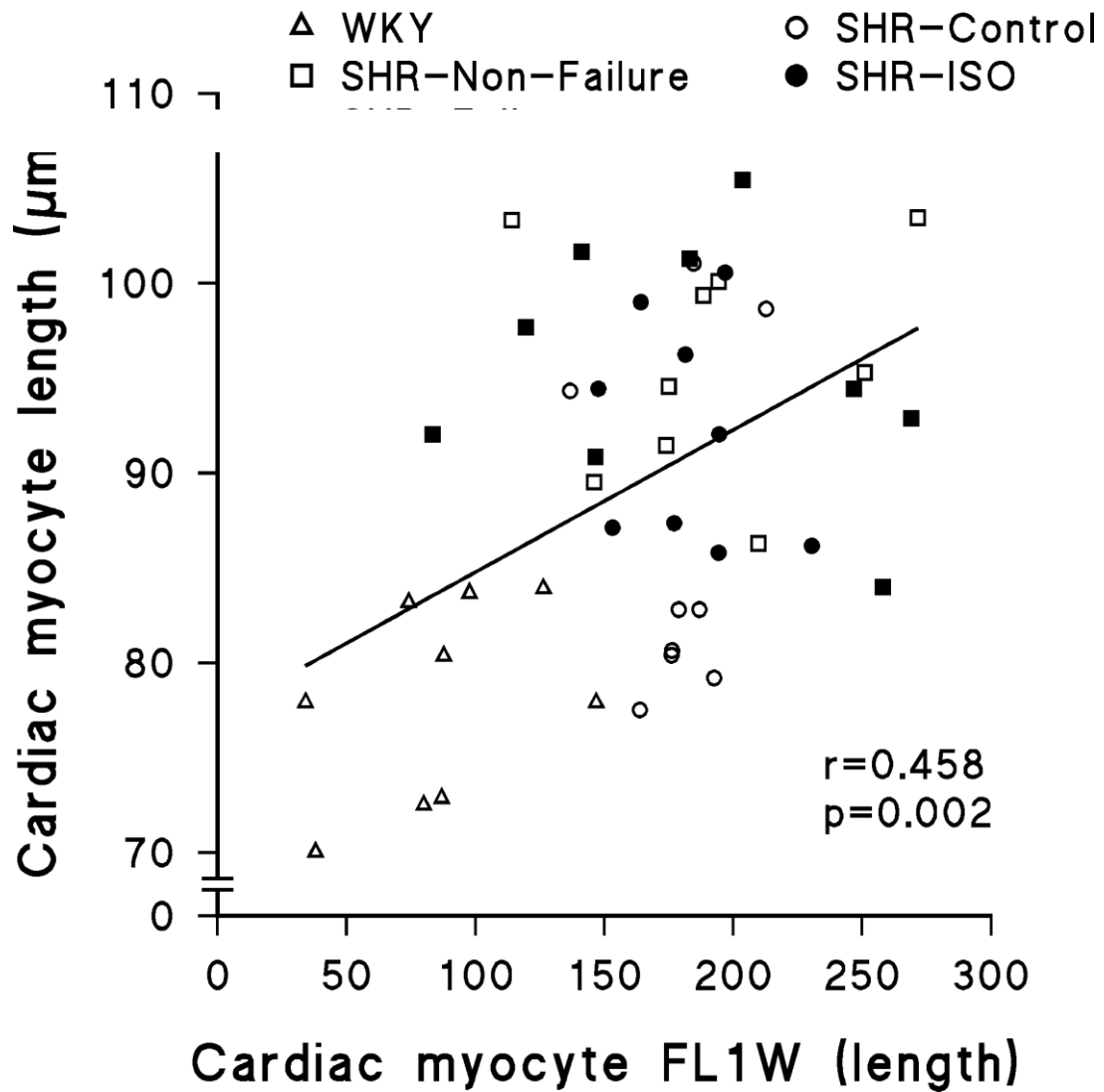


Figure 3.12 Linear correlation analysis between cardiac myocyte length measured using light microscopy and flow cytometry

Linear correlation analysis between cardiac myocyte length measured using light microscopy (y-axis) and cardiac myocyte length assessed using flow cytometry (FL1W, x-axis) using data obtained in all groups.

cannot be obtained using flow cytometry, due to the inability to calibrate at present, differences in cardiac myocyte length between groups can be assessed using this technique.

3.3.3 Left ventricular weight (mg/100g body weight) versus cardiac myocyte length

A strong association was noted between LV weight normalised to 100g body weight and cardiac myocyte length measured using either light microscopy (Figure 3.13, upper panel) or flow cytometry (Figure 3.13, lower panel).

CHAPTER 4

4.0 DISCUSSION

The main findings of the present study are as follows: The length of cardiac myocytes isolated from rats with LV dilatation (SHR-Failure and SHR-ISO) was no different from the length of cardiac myocytes isolated from rats without LV dilatation (SHR-Non-Failure and SHR-Control). The two models of LV dilatation used [natural progression model (SHR-Failure) and pharmacological model (SHR-ISO)] revealed the same outcome that LV dilatation (increased LV end diastolic radius and decreased LV wall thickness to radius ratio) is not associated with an increase in cardiac myocyte length. Furthermore, the data were confirmed using two methods (light microscopy and flow cytometry) to determine cardiac myocyte length. However, the hypertensive rats (SHR-Non-Failure; SHR-Failure; SHR-Control; SHR-ISO) did have an increased cardiac myocyte length compared to that of normotensive rats (WKY control).

The present study clarifies that although alterations in cardiac myocyte dimensions accompany hypertension-induced cardiac hypertrophy (Bishop *et al.* 1979; McCrossan *et al.* 2004; Olivetti *et al.* 1994; Zierhut *et al.* 1991), further increases in cardiac myocyte length are not a mechanism of the development of cardiac dilatation and heart failure. The present study is the first study to assess cardiac myocyte dimensions in age-matched animals with cardiac dilatation and to accurately determine LV dilatation using load independent measurements. Our data showing that LV dilatation is not associated with increases in cardiac myocyte length are in contrast to a number of studies mostly from the same group (Chen *et al.*, 2010; Gerdes *et al.* 1996; Onodera *et al.* 1998; Schultz *et al.*, 2007; Tamura *et al.* 1998, 1999 and 2000) that report increases in cardiac myocyte length in rats in heart failure.

As a model of heart failure, Gerdes and his colleagues (Gerdes *et al.* 1996; Onodera *et al.* 1998; Tamura *et al.* 1998, 1999 and 2000) have used rats that are genetically predisposed to the development of heart failure with increasing age (spontaneously hypertensive heart failure, SHHF). Consequently, in all of their studies the rats with heart failure were 3 to 16 months older than those rats not in heart failure (Gerdes *et al.* 1996: 24 versus 12 months; Onodera *et al.* 1998: 12 versus 9 months; Tamura *et al.* 1998, 1999 and 2000: 18 versus 2, 16 versus 6 and 22 versus 18 months respectively). As cardiac myocyte length is strongly correlated with age in SHHF rats (Tamura *et al.* 1998) and with LV weight (Campbell *et al.* 1991; Capasso *et al.* 1992; current study), and LV weight increases with age in hypertensive rats (Gerdes *et al.* 1996), the increased cardiac myocyte length observed in the SHHF rats with heart failure may be attributed to the increased age and hence LV weight of these rats rather than the presence of increased LV dimensions and heart failure. Moreover, in a study to assess reverse remodelling, an angiotensin II type 1 receptor blocker resulted in a decrease in myocyte length associated with a decrease in heart weight but no change in LV internal dimensions in age-matched SHHF rats (Tamura *et al.* 2000). In addition, although differences in cardiac myocyte length and heart weight between the angiotensin II type 1 receptor blocker treatment group and the hydralazine treatment group were noted, no differences in LV internal dimensions between these two groups were evident (Tamura *et al.* 2000).

Few previous studies have simultaneously measured cardiac myocyte length and LV dimensions. Most studies reporting increases in cardiac myocyte length in rats with heart failure compared to rats without heart failure have failed to measure LV dimensions (Gerdes *et al.* 1996; Onodera *et al.* 1998; Tamura *et al.* 1998 and 1999). Hence, whether increases in cardiac myocyte length accompany LV dilatation is not evident from these studies. Moreover, the few studies which have assessed LV dimensions have used *in vivo* echocardiography,

which is dependent on loading conditions and heart rate. Hence the increases in LV dimensions reported previously (Tamura *et al.* 2000) may be as a consequence of increases in loading conditions rather than the presence of LV remodelling and dilatation. Indeed in SHHF rats increases in LV internal dimensions are accompanied by increases in LV systolic wall stress (afterload) (Tamura *et al.* 2000) and decreases in LV internal dimensions occurred when LV systolic wall stress was reduced (Tamura *et al.* 2000). Similarly, in both aortic banded guinea pigs (Wang *et al.* 1999) and supraventricular tachycardia-induced cardiomyopathy in pigs (Spinale *et al.* 1996), increases in LV internal dimensions were measured in the presence of increases in afterload (systolic wall stress) and preload (LV end diastolic pressure). Furthermore, the reductions in LV end diastolic diameter reported following LV assist device support are likely to be due to the decreases in pulmonary capillary wedge pressure (preload) as a consequence of LV assist device support (Zafeiridis *et al.* 1998). Although, one previous study did not use echocardiography, they measured LV dimensions of cardiac rings following perfusion fixation (Kajstura *et al.* 1995), in which the perfusion pressure was maintained equal to the LV end diastolic pressure measured *in vivo*. As the LV filling pressure was increased in the dogs with pacing-induced heart failure, the increased LV dimensions reported are likely to be attributed to the increased preload (Kajstura *et al.* 1995). Moreover, reductions in cardiac myocyte length have been reported when cardiac preload and/or afterload are decreased (Campbell *et al.* 1991; Cooper *et al.* 1982 and 1984; Thompson *et al.* 1984). In contrast in the present study, LV dilatation was defined as the presence of an increased LV end diastolic radius and a decreased LV end diastolic wall thickness to radius ratio determined over a range of controlled LV filling volumes *in vivo*. Hence, the increases in LV dimensions in the current study are an accurate indication of the presence of LV dilatation independent of loading conditions.

A further explanation for the discrepancy between our data and that of others may be the difference in the strain of rats used. In the studies by Gerdes and colleagues (Gerdes *et al.* 1996; Onodera *et al.* 1998; Tamura *et al.* 1998, 1999 and 2000) the SHHF model has been used predominantly. However, the genetic background of the SHHF rat strain differs from that of the SHR and WKY rat strains (McCune *et al.* 1990; 1995a and 1995b). Moreover, the SHHF rat strain is reported to have longer cardiac myocytes than normal adult rats (Gerdes *et al.* 1996), a difference that was noted long before the development of the clinical signs and decreased hemodynamic function associated with heart failure (Onodera *et al.* 1998). Typically SHHF rats not in heart failure have cardiac myocyte lengths of ~140 to 150 μm (Capasso *et al.* 1992; Tamura *et al.* 1999), whereas mean cardiac myocyte lengths of 109 to 145 μm and 94 to 110 μm have been reported in the Sprague-Dawley (Bai *et al.* 1990; Korecky & Rakusan 1978; Nash *et al.* 1979) and Fischer (Bishop & Drummond 1979) strains of rats respectively. Similar to the results of the present study, previous studies reported longer cardiac myocytes in SHR compared to WKY rats (Aiello *et al.* 2004; Bishop *et al.* 1979; Brooksby *et al.* 1992; McCrossan *et al.* 2004). In these previous studies cardiac myocyte lengths ranged from 93 to 140 μm in WKY and from 105 to 150 μm in SHR (Aiello *et al.* 2004; Bishop *et al.* 1979; Brooksby *et al.* 1992; McCrossan *et al.* 2004) and in the present study we report mean cardiac myocyte lengths of 76 μm in WKY rats and 86 to 96 μm in SHR. Hence, even within rat strain there is a wide range of cardiac myocyte lengths. Differences within strain may be related to differences in the origin of the rats, as those SHR and WKY obtained from the same source have similar cardiac myocyte lengths (Bishop *et al.* 1979: WKY=93 μm and SHR=105 μm ; Brooksby *et al.* 1992: WKY=95 μm and SHR=115 μm ; both from Charles River Breeding Laboratory); whereas WKY and SHR from a different source (bred in the researchers own facility as opposed to from Charles River Breeding Laboratory) have different cardiac myocyte lengths (WKY=136 μm and SHR=147 μm ;

Aiello *et al.* 2004). Similarly, Sprague-Dawley rats obtained from different sources (Bio-Breeding Laboratories: Korecky & Rakusan 1978 versus Holtman Company: Bai *et al.* 1990) have different cardiac myocyte lengths (120 μm : Korecky & Rakusan 1978; 145 μm : Bai *et al.* 1990). In this regard the SHR used in the present study were bred in the Central Animal Services at the University of the Witwatersrand. The original breeding pairs were obtained over 20 years ago from OLAC, UK. It has also been reported that differences in cardiac myocyte size can be present in different shipments of a given strain of rats (Campbell *et al.* 1991). In addition, cardiac myocyte lengths vary across species. Mean cardiac myocyte lengths of 122 to 137 μm have been reported in normal adult hamsters (Sorenson *et al.* 1985) and in normal adult guinea pigs mean cardiac myocyte length is 168 μm (Wang *et al.* 1999).

It may also be argued that the method of cell isolation may impact upon cardiac myocyte dimensions. Fixation after isolation does not appear to impact upon cardiac myocyte length (freshly isolated: 109 μm ; fixed: 109 μm ; Nash *et al.* 1979); however, plated cardiac myocytes are longer (147 μm , Fraticelli *et al.* 1989) than those freshly isolated (110 μm , Sorenson *et al.* 1985) from the same strain of rat of the same age (Wistar). Nevertheless, Diffie and Nagle (2003), who used a similar method of isolation as in the present study (ie. from frozen tissue) report cardiac myocyte lengths of 123 μm which are no different from those of cardiac myocytes freshly isolated (120 μm , Korecky and Rakusan 1978) from the same strain (Sprague Dawley) of rats of the same age. Hence it is unlikely that the method of cell isolation used in the present study had an impact on the cardiac myocyte lengths recorded. Furthermore, the slack (relaxed) sarcomere lengths of 1.87 μm (WKY) and 1.99 to 2.13 μm (SHR) recorded in the present study are similar to those recorded in previous studies 1.60 μm (Fischer: Bishop and Drummond, 1979), 1.62 μm (Wistar, WKY and SHR: Bishop *et al.* 1979), 1.80 μm (Sprague-Dawley: Korecky & Rakusan 1978) 1.81 μm (WKY) and 1.85

μm (SHR) (McCrossan *et al.* 2004), 1.83 μm (Wistar: Fraticelli *et al.* 1989), 1.88 μm (SHHF: Gerdes *et al.* 1996), 1.90 μm (Sprague-Dawley: Diffie & Nagle 2003; SHHF: Tamura *et al.* 1998) and 1.95 μm (WKY and SHR: Brooksby *et al.* 1992).

Lastly, the discrepancy between the results of our study and that of previous studies may be related to differences in the models of LV dilatation and heart failure. Besides the SHHF rat model (Gerdes *et al.* 1996; Onodera *et al.* 1998; Tamura *et al.* 1998, 1999 and 2000), cardiac myocyte lengths have been assessed in two other models of heart failure, namely supraventricular tachycardia-induced cardiomyopathy in pigs (Spinale *et al.* 1996) and dogs (Kajstura *et al.* 1995), and constriction of the descending thoracic aorta in guinea pigs (Wang *et al.* 1999). Consistent with the SHHF model, in these two models increases in cardiac myocyte length have been reported in the group with increased LV end diastolic dimensions (Kajstura *et al.* 1995; Spinale *et al.* 1996; Wang *et al.* 1999). However, as cardiac dilatation has been attributed to alterations in both cardiac myocyte dimensions and myocardial fibrosis in dilated cardiomyopathy in humans (Beltrami *et al.* 1995), and changes in myocyte volume are reported to correlate with alterations in heart mass unless there is extensive fibrosis (Gerdes, 2002), it is important to assess the relative contribution of each of these factors to LV remodelling. In this regard, Campbell *et al.* (1991) attribute increases in heart weight despite no change in cardiac myocyte size to increases in myocardial fibrosis. Importantly, in the SHHF model only modest increases in myocardial collagen content (an increase from 1.9 to 2.5%; Onodera *et al.* 1998; Tamura *et al.* 1998) have been noted. Similarly, there is a lack of myocardial fibrosis in the aortic banding model (Wang *et al.* 1999), and in tachycardia-induced cardiomyopathy myocardial collagen concentrations are either decreased (Spinale *et al.* 1996) or modestly increased (from 0.5 to 6%, Kajstura *et al.* 1995). In contrast, in both the natural progression (SHR-Failure) and the pharmacological (SHR-ISO) model used in the

present study, we have previously shown that alterations in the characteristics of myocardial collagen play a major role in determining LV remodelling and dilatation (Anamourlis *et al.* 2006; Badenhorst *et al.* 2003a and 2003b; Tsotetsi *et al.* 2001; Veliotes *et al.* 2005; Woodiwiss *et al.* 2001), data which is supported by studies showing increased fibrosis in SHR in heart failure (Boluyt *et al.* 1995; Conrad *et al.* 1995; Engelmann *et al.* 1987). Hence it is not surprising that we found no contribution of cardiac myocyte length to LV dilatation; whereas in models in which fibrosis plays little role (Kajstura *et al.* 1995; Onodera *et al.* 1998; Spinale *et al.* 1996; Tamura *et al.* 1998; Wang *et al.* 1999), alterations in cardiac myocyte length were observed.

In agreement with previous studies conducted in SHR (Boluyt *et al.* 1995; Conrad *et al.* 1995; Engelmann *et al.* 1987), no changes in cardiac myocyte dimensions were noted in SHR with LV dilatation in the present study. In this regard, Engelmann *et al.* (1987) report no change in cardiac myocyte cross-sectional area but substantial increases in myocardial fibrosis in SHR with decreased LV wall thickness. Similarly, Boluyt *et al.* (1995) and Conrad *et al.* (1995) report decreases in cardiac myocyte fractional area and increased myocardial fibrosis in SHR in heart failure.

Furthermore, in support of the lack of association between cardiac myocyte length and LV dimensions observed in the present study; Schultz *et al.* (2007) showed that 16 months of exercise in SHHF rats resulted in a 21% increase in LV diastolic diameter, but no change in myocyte length. The deleterious effects of exercise on cardiac remodelling (enhanced LV dilatation) were however associated with a profound increase in cardiac fibrosis (~140%). Similarly, the prevention of increases in cardiac chamber diameter, by thyroid administration in cardiomyopathic hamsters, was associated with no change in cardiac myocyte length

(Kuzman *et al.*, 2007). In a study assessing the impact of TNF- α overexpression on cardiac remodelling; although cardiac myocyte length was increased in both male and female rats, increases in LV diastolic diameter were only observed in the male rats (Janczewski *et al.* 2003). Moreover, Tamura *et al.*, (2000) reported decreases in cardiac myocyte length subsequent to angiotensin II receptor blockade; however no changes in cardiac dimensions were noted. Lastly, increases rather than decreases in cardiac myocyte length were reported in a recent study in which intramyocardial delivery of mesenchymal stem cells resulted in the prevention of cardiac dilatation following myocardial infarction in mice (Li *et al.*, 2010).

Although a limitation of the present study may be the use of cardiac myocytes isolated from frozen tissue, this is unlikely. As previously discussed the lengths of cardiac myocytes isolated from frozen tissue (123 μm , Diffie & Nagle, 2003) are no different from those of freshly isolated cardiac myocytes (120 μm , Korecky & Rakusan 1978). In addition, the method used to isolate cardiac myocytes is more likely to impact on absolute length measurements than on comparisons between groups. Hence, the lack of difference in cardiac myocyte lengths between rats with LV dilatation (SHR-Failure and SHR-ISO) and those without LV dilatation (SHR-Failure and SHR-Control) is not likely to be as a consequence of the method of cardiac myocyte isolation. In contrast, the strengths of the present study include the use of two methods of measurement of cardiac myocyte length; the investigation of two models of cardiac dilatation; and the assessment of LV dimensions using load and heart rate independent measures.

From a clinical perspective the present study suggests that in hypertension-induced and beta-adrenergic induced heart failure, models in which the cardiac interstitium plays a major role, alterations in cardiac myocyte dimensions do not contribute to LV dilatation. Hence, in these

models therapy should be aimed at targeting the extracellular matrix rather than growth or hypertrophy of cardiac myocytes.

In conclusion, the present study indicates that although cardiac hypertrophy (in both hypertension-induced and beta-adrenergic-induced models) is associated with increases in cardiac myocyte length, cardiac dilatation in these models is not attributed to alterations in cardiac myocyte dimensions.

CHAPTER 5

5.0 REFERENCES

1. Agabiti-Rosei E, Muiesan ML, Romanelli G, Castellano M, Beschi M, Alicandri C & Muiesan G (1987). Cardiac function as related to adrenergic activity in hypertensive left ventricular hypertrophy. *J Clin Hypertens* **3**, 203-210.
2. Aiello EA, Villa-Abrille MC, Escudero EM, Portiansky EL, Pérez NG, de Hurtado MC & Cingolani HE (2004). Myocardial hypertrophy of normotensive Wistar-Kyoto rats. *Am J Physiol Heart Circ Physiol* **286**, H1229-H1235.
3. American Heart Association (2010). Heart Disease and Stroke Statistics – 2010 Update. Dallas, Texas: American Heart Association.
4. Anamourlis C, Badenhorst D, Gibbs M, Correia R, Veliotes D, Osadchii O, Norton GR & Woodiwiss AJ (2006). Phosphodiesterase inhibition promotes the transition from compensated hypertrophy to cardiac dilatation in rats. *Eur J Physiol* **451**, 526–533.
5. Anand IS, Fisher LD, Chiang YT, Latini R, Masson S, Maggioni AP, Glazer RD, Tognoni G & Cohn JN (2003). Changes in brain natriuretic peptide and norepinephrine over time and mortality and morbidity in the Valsartan Heart Failure Trial (Val-HeFT). *Circulation* **107**, 1278-1283.
6. Anker SD & Coats AJ (2002). How to RECOVER from RENAISSANCE? The significance of the results of RECOVER, RENAISSANCE, RENEWAL and ATTACH. *Int J Cardiol* **85**, 195-197.
7. Anversa P, Loud AV, Levicky V & Guideri G (1985). Left ventricular failure induced by myocardial infarction. Myocyte hypertrophy. *Am J Physiol Heart Circ Physiol* **248**, H876-H882.
8. Badenhorst D, Maseko M, Tsotetsi OJ, Naidoo A, Brooksbank R, Norton GR & Woodiwiss AJ (2003a). Cross-linking influences the impact of quantitative changes

- in myocardial collagen on cardiac stiffness and remodelling in hypertension in rats. *Cardiovasc Res* **57**, 632-641.
9. Badenhorst D, Veliotes D, Maseko M, Tsotetsi OJ, Brooksbank R, Naidoo A, Woodiwiss AJ & Norton GR (2003b). β -adrenergic activation initiates chamber dilatation in concentric hypertrophy. *Hypertension* **41**, 499–504.
 10. Bai SL, Campbell SE, Moore JA, Morales MC & Gerdes AM (1990). Influence of age, growth, and sex on cardiac myocyte size and number in rats. *Anat Rec* **226**, 207-212.
 11. Banfi C, Cavalca V, Veglia F, Brioschi M, Barcella S, Mussoni L, Boccotti L, Temoli E, Biglioloi P & Agostoni PG (2005). Neurohumoral activation is associated with increased levels of plasma matrix metalloproteinase-2 in human heart failure. *Eur Heart J* **26**, 481-488.
 12. Baumgarten G, Knuefermann P & Mann DL (2000). Cytokines as emerging targets in the treatment of heart failure. *Trends Cardiovasc Med* **10**, 216-223.
 13. Beltrami CA, Finato N, Rocco M, Feruglio GA, Puricelli C, Cigola E, Quaini EH, Sonnenblick EH, Olivetti G & Anversa P (1994). Structural basis of end-stage failure in ischemic cardiomyopathy in humans. *Circulation* **89**, 151-163.
 14. Beltrami CA, Finato N, Rocco M, Feruglio GA, Puricelli C, Cigola E, Sonnenblick EH, Olivetti G & Anversa P (1995). The cellular basis of dilated cardiomyopathy in humans. *J Mol Cell Cardiol* **27**, 291-305.
 15. Bing OH, Brooks WW, Robinson KG, Slawsky MT, Hayes JA, Litwin SE, Sen S & Conrad CH (1995). The spontaneously hypertensive rat as a model of the transition from compensated left ventricular hypertrophy to failure. *J Mol Cell Cardiol* **27**, 383-396.

16. Bishop SP, Oparil S, Reynolds RH & Drummond JL (1979). Regional myocyte size in normotensive and spontaneously hypertensive rats. *Hypertension* **1**, 378-383.
17. Bishop SP & Drummond JL (1979). Surface morphology and cell size measurement of isolated rat cardiac myocytes. *J Mol Cell Cardiol* **11**, 423-433.
18. Boluyt MO, Bing OH & Lakatta EG (1995). The ageing spontaneously hypertensive rat as a model of the transition from stable compensated hypertrophy to heart failure. *Eur Heart J* **16**, 19-30.
19. Brilla CG, Zhou G, Matsubara L & Weber KT (1994). Collagen metabolism in cultured adult rat cardiac fibroblasts: Response to angiotensin II and aldosterone. *J Mol Cell Immunol* **26**, 809-820.
20. Bristow MR (1997). Mechanism of action of beta-blocking agents in heart failure. *Am J Cardiol.* **80**, 26L-40L.
21. Brooksby P, Levi AJ & Jones JV (1992). Contractile properties of ventricular myocytes isolated from spontaneously hypertensive rat. *J Hypertens* **10**, 521-527.
22. Campbell SE, Korecky B & Rakusan K (1991). Remodeling of myocyte dimensions in hypertrophic and atrophic rat hearts. *Circ Res* **68**, 984-996.
23. Capasso JM, Robinson TF & Anversa P (1989). Alterations in collagen cross-linking impair myocardial contractility in the mouse heart. *Circ Res* **65**, 1657-1664.
24. Capasso JM, Fitzpatrick D & Anversa P (1992). Cellular mechanisms of ventricular failure: myocyte kinetics and geometry with age. *Am J Physiol Heart Circ Physiol* **262**, H1770-1781.
25. Chen YF, Redetzke RA, Sivertson RM, Coburn TS, Cypher LR & Gerdes AM (2010). Post-myocardial infarction left ventricular myocyte remodeling: are there gender differences in rats? *Cardiovasc Pathol* Nov 15 (Epub ahead of print).

26. Cohn JN, Ferrari R & Sharpe N (2000). Cardiac remodeling - concepts and clinical implications: A consensus paper from an International Forum on Cardiac Remodeling. *J Am Coll Cardiol* **35**, 569–582.
27. Cohn JN, Levine TB, Olivari MT, Garberg V, Lura D, Francis GS, Simon AB & Rector T (1984). Plasma norepinephrine as a guide to prognosis in patients with chronic congestive heart failure. *N Engl J Med* **311**, 819-823.
28. Coker ML, Jolly JR, Joffs C, Etoh T, Holder JR, Bond BR & Spinale FG (2001). Matrix metalloproteinase expression and activity in isolated myocytes after neurohormonal stimulation. *Am J Physiol Heart Circ Physiol* **281**, H543-H551.
29. Communal C, Singh K, Pimentel DR & Colucci WS (1998). Norepinephrine stimulates apoptosis in adult rat ventricular myocytes by activation of the beta-adrenergic pathway. *Circulation* **98**, 1329-1334.
30. Conrad CH, Brooks WW, Hayes JA, Sen S, Robinson KG & Bing OH (1995). Myocardial fibrosis and stiffness with hypertrophy and heart failure in the spontaneously hypertensive rat. *Circulation* **91**, 161-170.
31. Cooper G 4th & Marino TA (1984). Complete reversibility of cat right ventricular chronic progressive pressure overload. *Circ Res* **54**, 323-331.
32. Cooper G 4th & Tomanek RJ (1982). Load regulation of the structure, composition, and function of mammalian myocardium. *Circ Res* **50**, 788-798.
33. Danser AHJ, van Kesteren CAM, Bax WA, Tavenier M, Derkx FH, Saxena PR & Schalekamp MA (1997). Prorenin, renin, angiotensinogen, and angiotensin-converting enzyme in normal and failing human hearts. Evidence for renin binding. *Circulation* **96**, 220-236.
34. De Angelis N, Fiordaliso F, Latini R, Calvillo L, Funicello M, Gobbi M, Mennini T & Masson S (2002). Appraisal of the role of angiotensin II and aldosterone in

- ventricular myocyte apoptosis in adult normotensive rat. *J Mol Cell Cardiol* **34**, 1655-1665.
35. Diez C & Simm A (1998). Gene expression in rod shaped cardiac myocytes, sorted by flow cytometry. *Cardiovasc Res* **40**, 530-537.
36. Diffie GM & Nagle GF (2003). Exercise training alters length dependence of contractile properties in rat myocardium. *J Appl Physiol* **94**, 1137-1144.
37. Engelmann GL, Vitullo JC & Gerrity RG (1987). Morphometric analysis of cardiac hypertrophy during development, maturation, and senescence in spontaneously hypertensive rats. *Circ Res* **60**, 487-494.
38. Ertl G, Gaudron P, Eilles C, Schorb W & Kochsiek K (1991). Compensatory mechanisms for cardiac dysfunction in myocardial infarction. *Basic Res Cardiol* **86**, 159-165.
39. Esler M, Kaye D, Lambert G, Esler D & Jennings G (1997). Adrenergic nervous system in heart failure. *Am J Cardiol* **80**, 7L-14L.
40. Fedak PWM, Verma S, Weisel RD, Skrtic M & Li RK (2005). Cardiac remodelling and failure. From molecules to man (Part III). *Cardiovasc Path* **14**, 109-119.
41. Ferrari R, Ceconi C, Campo G, Cangiano E, Cavazza C, Secchiero P & Tavazzi L (2009). Mechanisms of remodelling. A question of life (stem cell production) and death (myocyte apoptosis). *Circ J* **73**, 1973-1982.
42. Francis GS, Cohn JN, Johnson G, Rector TS, Goldman S & Simon A (1993). Plasma norepinephrine, plasma renin activity, and congestive heart failure. Relations to survival and the effects of therapy in V-HeFT II. The V-HeFT VA Cooperative Studies Group. *Circulation* **87**, VI40-48.
43. Fraticelli A, Josephson R, Danziger R, Lakatta E & Spurgeon H (1989). Morphological and contractile characteristics of rat cardiac myocytes from maturation to senescence. *Am J Physiol Heart Circ Physiol* **257**, H259- H265.

44. Frey N, Katus HA, Olson EN & Hill JA (2004). Hypertrophy of the heart: a new therapeutic target? *Circulation* **109**, 1580-1589.
45. Frigerio M & Roubina E (2005). Drugs for left ventricular remodelling in heart failure. *Am J Cardiol* **96**(suppl), 10L-18L.
46. Gaudron P, Eilles C, Kugler I & Ertl G (1993). Progressive left ventricular dysfunction and remodelling after myocardial infarction. Potential mechanisms and early predictors. *Circulation* **87**, 755-763.
47. Gerdes AM (2002). Cardiac myocyte remodeling in hypertrophy and progression to failure. *J Card Fail* **8**, S264-S268.
48. Gerdes AM & Capasso JM (1995). Structural remodeling and mechanical dysfunction of cardiac myocytes in heart failure. *J Mol Cell Cardiol.* **27**, 849-856.
49. Gerdes AM & Iervasi G (2010). Thyroid replacement therapy and heart failure. *Circulation* **122**, 385-393.
50. Gerdes AM, Kellerman SE, Moore JA, Muffly KE, Clark LC, Reaves PY, Malec KB, McKeown PP & Schoken DD (1992). Structural remodelling of cardiac myocytes in patients with ischemic cardiomyopathy. *Circulation* **86**, 426-430.
51. Gerdes AM, Onodera T, Tamura T, Said S, Bohlmeyer TJ, Abraham WT & Bristow MR (1998). New method to evaluate myocyte remodelling from formalin-fixed biopsy and autopsy material. *J Card Fail* **4**, 343-348.
52. Gerdes AM, Onodera T, Wang X & McCune SA (1996). Myocyte remodelling during the progression to failure in rats with hypertension. *Hypertension* **28**, 609-614.
53. Gerson MC, Craft LL, McGuire N, Suresh DP, Abraham WT & Wagoner LE (2002). Carvedilol improves left ventricular function in heart failure patients with idiopathic dilated cardiomyopathy and a wide range of sympathetic nervous system function as measured by iodine 123 metaiodobenzylguanidine. *J Nucl Cardiol* **9**, 608-615.

54. Gibbs M, Veliotos DG, Anamourlis C, Badenhorst D, Osadchii O, Norton GR & Woodiwiss AJ (2004). Chronic beta-adrenoreceptor activation increases cardiac cavity size through chamber remodeling and not via modifications in myocardial material properties. *Am J Physiol Heart Circ Physiol* **287**, H2762-H2767.
55. Gilbert JC & Glantz SA (1989). Determinants of left ventricular filling and of the diastolic pressure-volume relation. *Circ Res* **64**, 827-852.
56. Greenberg B, Quinones MA, Koilpillai C, Limacher M, Shindler D, Benedict C & Shelton B (1995). Effects of long-term enalapril therapy on cardiac structure and function in patients with left ventricular dysfunction. Results of the SOLVD echocardiography substudy. *Circulation* **91**, 2573-2581.
57. Grossman W, Jones D & McLaurin LP (1975). Wall Stress and patterns of hypertrophy in the human left ventricle. *J Clin Invest* **56**, 56-64.
58. Gunasinghe SK, Ikonomidis J & Spinale FG (2001). Contributory role of matrix metalloproteinases in cardiovascular remodeling. *Curr Drug Targets Cardiovasc Haematol Disord* **1**, 75-91.
59. Gunja-Smith Z, Morales AR, Romanelli R & Woessner JF Jr (1996). Remodeling of human myocardial collagen in idiopathic dilated cardiomyopathy. Role of metalloproteinases and pyridinoline cross-links. *Am J Pathol* **148**, 1639-1648.
60. Hasking GJ, Esler MD, Jennings GL, Burton D, Johns JA & Korner PI (1986). Norepinephrine spillover to plasma in patients with congestive heart failure: evidence of increased overall and cardiorenal sympathetic nervous activity. *Circulation* **73**, 615-621.
61. Hearse DJ, Stewart DA & Braimbridge MV (1975). Hypothermic arrest and potassium arrest: metabolic and myocardial protection during elective cardiac arrest. *Circ Res* **36**, 481-489.

62. Hein S, Amon E, Kostin S, Schönburg M, Elsässer A, Polyakova V, Bauer EP, Klövekorn WP & Schaper J (2003). Progression from compensated hypertrophy to failure in the pressure-overloaded human heart. Structural deterioration and compensatory mechanisms. *Circulation* **107**, 984-991.
63. Hermida N, López B, González A, Dotor J, Lasarte JJ, Sarobe P, Borrás-Cuesta F & Díez J (2009). A synthetic peptide from transforming growth factor-beta1 type III receptor prevents myocardial fibrosis in spontaneously hypertensive rats. *Cardiovasc Res* **81**, 601-609.
64. Hill JA & Olson EN (2008). Cardiac plasticity. *N Engl J Med* **358**, 1370-1380.
65. Inoko M, Kihara Y, Morii I, Fujiwara H, Sasayama S (1994). Transition from compensatory hypertrophy to dilated, failing left ventricles in Dahl salt-sensitive rats. *Am J Physiol Heart Circ Physiol* **267**, H2471-H2482.
66. Iwai N, Shimoike H & Kinoshita M (1995). Cardiac rennin-angiotensin system in the hypertrophied heart. *Circulation* **92**, 2690-2696.
67. Janczewski AM, Kadokami T, Lemster B, Frye CS, McTiernan CF & Feldman AM (2003). Morphological and functional changes in cardiac myocytes isolated from mice overexpressing TNF- α . *Am J Physiol Heart Circ Physiol* **284**, H960-H969.
68. Janicki JS, Brower GL, Gardner JD, Chancey AL & Stewart JA Jr (2004). The dynamic interaction between Matrix Metalloproteinase Activity and adverse myocardial remodeling. *Heart Failure Reviews* **9**, 33-42.
69. Kai H, Kuwahara F, Tokuda K & Imaizumi T (2005). Diastolic dysfunction in hypertensive hearts: Roles of perivascular inflammation and reactive myocardial fibrosis. *Hypertens Res* **28**, 483-490.

70. Kajstura J, Zhang X, Liu Y, Szoke E, Cheng W, Olivetti G, Hintze TH & Anversa P (1995). The cellular basis of pacing-induced dilated cardiomyopathy. Myocyte cell loss and myocyte cellular reactive hypertrophy. *Circulation* **92**, 2306-2317.
71. Kang PM & Izumo S (2000). Apoptosis and heart failure: A critical review of the literature. *Circ Res* **86**, 1107-1113.
72. Katz AM (2002). Proliferative signalling and disease progression in heart failure. *Circ J* **66**, 225-231.
73. Kelm M, Schafer S, Mingers S, Heydthausen M, Vogt M, Motz W & Strauer BE (1996). Left ventricular mass is linked to cardiac noradrenaline in normotensive and hypertensive patients. *J Hypertens* **14**, 1365-1367.
74. King MK, Coker ML, Goldberg A, McElmurray JH, 3rd, Gunasinghe HR, Mukherjee R, Zile MR, O'Neill TP & Spinale FG (2003). Selective matrix metalloproteinase inhibition with developing heart failure: effects on left ventricular function and structure. *Circ Res* **92**, 177-185.
75. Kluger, J., Cody, R. J. & Laragh, J. H. (1982). The contributions of sympathetic tone and the renin-angiotensin system to severe chronic congestive heart failure: response to specific inhibitors (prazosin and captopril). *Am J Cardiol* **49**, 1667-1674.
76. Konstam MA, Rousseau MF, Kronenberg MW, Udelson JE, Melin J, Stewart D, Dolan N, Edens TR, Ahn S, Kinan D, Howe DM, Kilcoyne L, Metherall J, Benedict C, Yusuf S & Pouleur H (1992). Effects of the angiotensin converting enzyme inhibitor enalapril on the long-term progression of left ventricular dysfunction in patients with heart failure. SOLVD Investigators. *Circulation* **86**, 431-438.
77. Kudoh S, Komuro I, Mizuno T, Yamazaki T, Zou Y, Shiojima I, Takekoshi N & Yazaki Y (1997). Angiotensin II stimulates c-Jun NH₂-terminal kinase in cultured cardiac myocytes of neonatal rats. *Circ Res* **80**, 139-146.

78. Korecky B & Rakusan K (1978). Normal and hypertrophic growth of the rat heart: changes in cell dimensions and number. *Am J Physiol Heart Circ Physiol* **234**, H123-H128.
79. Kuwahara F, Kai H, Tokuda K, Takeya M, Takeshita, Egashira K & Imaizumi T (2004). Hypertensive myocardial fibrosis and diastolic dysfunction: another model of inflammation? *Hypertension* **43**, 739-745.
80. Kuzman JA, Tang Y, Vogelsang KA, Said S, Anderson BE, Morkin E & Gerdes AM (2007). Thyroid hormone analog, diiodothyropropionic acid (DITPA), exerts beneficial effects on chamber and cellular remodelling in cardiomyopathic hamsters. *Can J Physiol Pharmacol* **85**, 311-318.
81. Laskey WK, St. John Sutton M, Zeevi G, Hirshfeld JW & Reichek N (1984). Left ventricular mechanics in dilated cardiomyopathy. *Am J Cardiol* **54**, 620-625.
82. Levy D, Garrison RJ, Savage DD, Kannel WB & Castelli WP (1990). Prognostic implications of echocardiographically determined left ventricular mass in the Framingham Heart Study. *N Engl J Med* **322**, 1561-1566.
83. Li YY, Feng Y, McTiernan CF, Pei W, Moravec CS, Wang P, Rosenblum W, Kormos RL & Feldman AM (2001). Downregulation of matrix metalloproteinases and reduction in collagen damage in the failing human heart after support with left ventricular assist devices. *Circulation* **104**, 1147-1152.
84. Li Q, Turdi S, Thomas DP & Ren J (2010). Intra-myocardial delivery of mesenchymal stem cells ameliorates left ventricular and cardiomyocyte contractile dysfunction following myocardial infarction. *Toxicology Letters* **195**, 119-126.
85. Linzbach AJ (1960). Heart failure from the point of view of quantitative anatomy. *Am J Cardiol* **5**, 370-382.
86. Lorell BH (1997). Transition from hypertrophy to failure. *Circulation* **96**, 3824-3827.

87. Mann DL & Spinale FG (1998). Activation of matrix metalloproteinases in the failing human heart: breaking the tie that binds. *Circulation* **98**, 1699-1702.
88. Matsui T & Rosenzweig A (2005). Convergent signal transduction pathways controlling cardiomyocyte survival and function: the role of PI-3-kinase and Akt. *J Mol Cell Cardiol* **38**, 63-71.
89. Mayosi BM, Flisher AJ, Lalloo UG, Sitas F, Tollman SM & Bradshaw D (2009). The burden of non-communicable diseases in South Africa. *Lancet* **374**, 934-947.
90. McCrossan ZA, Billeter R & White E (2004). Transmural changes in size, contractile and electrical properties of SHR left ventricular myocytes during compensated hypertrophy. *Cardiovasc Res* **63**, 283-292.
91. McCune SA, Baker PB & Stills HF Jr (1990). SHHF/Mcc-cp rat: model of obesity, non-insulin-dependent diabetes, and congestive heart failure. *ILAR News* **32**, 23-27.
92. McCune SA, Radin MJ, Jenkins JE, Chu YY & Park S (1995a). SHHF/Mcc-fa cp rat model: effects of gender and genotype on age of expression of metabolic complications and congestive heart failure and on response to drug therapy. In: Shafir E, ed. Lessons From Animal Diabetes V. *Smith-Gordon*, 255-270.
93. McCune SA, Park S, Radin MJ & Jurin RR (1995b). The SHHF/Mcc-fa^{cp} rat model: a genetic model of congestive heart failure. In: Singal PK, Dixon IMC, Beamish RE, Dhalla NS, eds. Mechanisms of Heart Failure. *Kluwer Academic Publishers*, 91-106.
94. Metra M, Nodari S, Parrinello G, Giubbini R, Manca C & Dei Cas L (2003). Marked improvement in left ventricular ejection fraction during long-term beta-blockade in patients with chronic heart failure: clinical correlates and prognostic significance. *Am Heart J* **145**, 292-299.

95. Mizuno Y, Yoshimura M, Yasue H, Sakamoto T, Ogawa H, Kugiyama K, Harada E, Nakayama M, Nakamura S, Ito T, Shimasaki Y, Saito Y & Nakao K (2001). Aldosterone production is activated in failing ventricle in human. *Circulation* **103**, 72-77.
96. Mujundar VS & Tyagi SC (1999). Temporal regulation of extracellular matrix components in transition from compensatory hypertrophy to decompensatory heart failure. *J Hypertens* **17**, 261-270.
97. Mukherjee R, Brinsa TA, Dowdy KB, Scott AA, Baskin JM, Deschamps AM, Lowry AS, Escobar GP, Lucas DG, Yarbrough WM, Zile MR & Spinale FG (2003). Myocardial infarct expansion and matrix metalloproteinase inhibition. *Circulation* **107**, 618-625.
98. Nash GB, Tatham PE, Powell T, Twist VW, Speller RD & Loverock LT (1979). Size measurements on isolated rat heart cells using Coulter analysis and light scatter flow cytometry. *Biochim Biophys Acta* **587**, 99-111.
99. Norton GR, Tsotetsi OJ & Woodiwiss AJ (1993). Hydrochlorothiazide improves ventricular compliance and thus performance without reducing hypertrophy in renal artery stenosis in rats. *Hypertension* **21**, 638-645.
100. Norton GR, Tsotetsi J, Trifunovic B, Hartford C, Candy GP & Woodiwiss AJ (1997). Myocardial stiffness is attributed to alterations in cross-linked collagen rather than total collagen or phenotypes in spontaneously hypertensive rats. *Circulation* **96**, 1991-1998.
101. Norton GR, Woodiwiss AJ, Gaasch WH, Mela T, Chung ES, Aurigemma GP & Meyer TE (2002). Heart failure in pressure overload hypertrophy: The relative roles of ventricular remodeling and myocardial dysfunction. *J Am Coll Cardiol* **39**, 664-671.

102. Olivetti G, Capasso JM, Sonnenblick EH & Anversa P (1990). Side-to-side slippage of myocytes participates in ventricular wall remodelling acutely after myocardial infarction in rats. *Circ Res* **67**, 23-34.
103. Olivetti G, Melissari M, Balbi T, Quaini F, Cigola E, Sonnenblick EH & Anversa P (1994). Myocyte cellular hypertrophy is responsible for ventricular remodelling in the hypertrophied heart of middle aged individuals in the absence of cardiac failure. *Cardiovasc Res* **28**, 1199-1208.
104. Onodera T, Tamura T, Said S, McCune SA & Gerdes AM (1998). Maladaptive remodelling of cardiac myocyte shape begins long before failure in hypertension. *Hypertension* **32**, 753-757.
105. Opie LH, Commerford PJ & Pfeffer MA (2006). Controversies in cardiology 4. Controversies in ventricular remodelling. *Lancet* **367**. 356-367.
106. Packer M, Bristow MR, Cohn JN, Colucci WS, Fowler MB, Gilbert EM & Shusterman NH (1996). The effect of carvedilol on morbidity and mortality in patients with chronic heart failure. U.S. Carvedilol Heart Failure Study Group. *N Engl J Med* **334**, 1349-1355.
107. Papadimitriou JM, Hopkins BE & Taylor RR (1974). Regression of left ventricular dilation and hypertrophy after removal of volume overload: morphological and ultrastructural study. *Circ Res* **35**, 127-135.
108. Pangonyte D, Stalioraityte E, Ziuraitiene R, Kazlauskaite D, Palubinskiene J & Balnyte I (2008). Cardiomyocyte remodelling in ischemic heart disease. *Medicina (Kaunas)* **44**, 848-854.
109. Patterson JH & Adams KF, Jr (1996). Pathophysiology of heart failure: changing perceptions. *Pharmacotherapy* **16**, 27S-36S.

110. Peterson JT, Hallak H, Johnson L, Li H, O'Brien PM, Sliskovic DR, Bocan TMA, Coker ML, Etoh T & Spinale FG (2001). Matrix metalloproteinase inhibition attenuates left ventricular remodeling and dysfunction in a rat model of progressive heart failure. *Circulation* **103**, 2303-2309.
111. Pfeffer MA, Braunwald E, Moye LA, Basta L, Brown EJ Jr, Cuddy TE, Davis BR, Geltman EM, Goldman S, Flaker GC, Klein M, Lamas GA, Packer M, Rouleau J, Rouleau JL, Rutherford J, Wertheimer JH & Hawkins CM on behalf of SAVE investigators (1992). Effect of captopril on mortality and morbidity in patients with left ventricular dysfunction after myocardial infarction. Results of the Survival and Ventricular Enlargement Trial. *N Engl J Med* **327**, 669-677.
112. Polyakova V, Hein S, Kostin S, Ziegelhoeffer T & Schaper J (2004). Matrix metalloproteinases and their tissue inhibitors in pressure-overloaded human myocardium during heart failure progression. *J Am Coll Cardiol* **44**, 1609-1618.
113. Reddy HK, Tjahja IE, Campbell SE, Janicki JS, Hayden MR & Tyagi SC (2004). Expression of matrix metalloproteinase activity in idiopathic dilated cardiomyopathy: a marker of cardiac dilatation. *Mol Cell Biochem* **264**, 183-191.
114. Remme WJ (2003). Pharmacological modulation of cardiovascular remodelling. A guide to heart failure therapy. *Cardiovasc Drugs Ther* **17**, 349-360.
115. Rohde LE, Ducharme A, Arroyo LH, Aikawa M, Sukhova GH, Lopez-Anaya A, McClure KF, Mitchell PG, Libby P & Lee RT (1999). Matrix metalloproteinase inhibition attenuates early left ventricular enlargement after experimental myocardial infarction in mice. *Circulation* **99**, 3063-3070.
116. Roten L, Nemoto S, Simsic J, Coker ML, Rao V, Baicu S, Defreyte G, Soloway PJ, Zile MR & Spinale FG (2000). Effects of gene deletion of the tissue inhibitor of the

- matrix metalloproteinase-type 1 (TIMP-1) on left ventricular geometry and function in mice. *J Mol Cell Cardiol* **32**, 109-120.
117. Russell B, Curtis MW, Koshman YE & Samarel AM (2010). Mechanical stress-induced sarcomere assembly for cardiac muscle growth in length and width. *J Mol Cell Cardiol* **48**, 817-823.
118. Sabbah HN & Sharov VG (1998). Apoptosis in heart failure. *Prog Cardiovasc Dis* **40**, 549-562.
119. Sadoshima J & Izumo S (1997). The cellular and molecular response of cardiac myocytes to mechanical stress. *Annu Rev Physiol* **59**, 551-571.
120. Sakata Y, Yamamoto K, Mano T, Nishikawa N, Yoshida J, Hori M, Miwa T & Masuyama T (2004) Activation of matrix metalloproteinases precedes left ventricular remodeling in hypertensive heart failure rats: its inhibition as a primary effect of angiotensin-converting enzyme inhibitor. *Circulation* **109**, 2143-2149.
121. Sallin EA (1969). Fiber orientation and ejection fraction in the human left ventricle. *Biophys J* **9**, 954-964.
122. Scheinin SA, Capek P, Radovancevic B, Duncan JM, McAllister HA & Frazier OH (1992). The effect of prolonged left ventricular support on myocardial histopathology in patients with end-stage cardiomyopathy. *ASAIO Journal* **38**, M271-M274.
123. Schultz RL, Swallow JG, Waters RP, Kuzman JA, Redetzke RA, Said S, Morreale de Escobar G & Gerdes AM (2007). Effects of excessive long-term exercise on cardiac function and myocyte remodelling in hypertensive heart failure rats. *Hypertension* **50**, 410-416.

124. Schunkert H, Jackson B, Tang SS, Schoen FJ, Smits JF, Apstein CS & Lorell BH (1993). Distribution and functional significance of cardiac angiotensin converting enzyme in hypertrophied rat hearts. *Circulation* **87**, 1328-1339.
125. Seneri GG, Modesti PA, Boddi M, Cecioni I, Paniccia R, Coppo M, Galanti G, Simonetti I, Vanni S, Papa L, Bandinelli B, Migliorini A, Modesti A, Maccherini M, Sani G & Toscano M (1999). Cardiac growth factors in human hypertrophy: Relations with myocardial contractility and wall stress. *Circ Res* **85**, 57-67.
126. Sigurdsson A, Amtorp O, Gundersen T, Nilsson B, Remes J & Swedberg K (1994). Neurohormonal activation in patients with mild or moderately severe congestive heart failure and effects of ramipril. The Ramipril Trial Study Group. *Br Heart J* **72**, 422-427.
127. Singh K, Xiao L, Remondino A, Sawyer DB & Colucci WS (2001). Adrenergic regulation of cardiac myocyte apoptosis. *J Cell Physiol* **189**, 257-265.
128. Sorenson AL, Tepper D, Sonnenblick EH, Robinson TF & Capasso JM (1985). Size and shape of enzymatically isolated ventricular myocytes from rats and cardiomyopathic hamsters. *Cardiovasc Res* **19**, 793-799.
129. Spann JF Jr, Buccino RA, Sonnenblick EH, Braunwald E (1967). Contractile state of cardiac muscle obtained from cats with experimentally produced ventricular hypertrophy and heart failure. *Circ Res* **21**, 341-343.
130. Spinale FG (2002). Matrix metalloproteinases: regulation and dysregulation in the failing heart. *Circ Res* **90**, 520-530.
131. Spinale FG, Coker ML, Heung LJ, Bond BR, Gunasinghe HR, Etoh T, Goldberg AT, Zellner JL & Crumbley AJ (2000). A matrix metalloproteinase induction/activation system exists in the human left ventricular myocardium and is upregulated in heart failure. *Circulation* **102**, 1944-1949.

132. Spinale FG, Coker ML, Krombach SR, Mukherjee R, Hallak H, Houck WV, Clair MJ, Kribbs SB, Johnson LL, Peterson JT & Zile MR (1999). Matrix metalloproteinase inhibition during the development of congestive heart failure: effects on left ventricular dimensions and function. *Circ Res* **85**, 364-376.
133. Spinale FG, Coker ML, Thomas CVT, Walker JD, Mukherjee R & Hebbar (1998). Time dependent changes in matrix metalloproteinase activity and expression during the progression of congestive heart failure: relation to ventricular and myocyte function. *Circ Res* **82**, 482-495.
134. Spinale FG, Crawford, Jr. FA, Hewett KW & Carabello BA (1991). Ventricular failure and cellular remodeling with chronic supraventricular tachycardia. *J Thorac Cardiovasc Surg* **102**, 874-882.
135. Spinale FG, Zellner JL, Johnson WS, Eble DM & Munyer PD (1996). Cellular and extracellular remodeling with the development and recovery from tachycardia-induced cardiomyopathy: changes in fibrillar collagen, myocyte adhesion capacity and proteoglycans. *J Mol Cell Cardiol* **28**, 1591-1608.
136. Stewart S, Wilkinson D, Hansen C, Vaghela V, Mvungi R, McMurray J & Sliwa K (2008). Predominance of heart failure in the heart of Soweto study cohort. *Circulation* **118**, 2360-2367.
137. St John Sutton M, Pfeffer MA, Moye L, Plappert T, Rouleau JL, Lamas G, Rouleau J, Parker JO, Arnold MO, Sussex B & Braunwald E (1997). Cardiovascular death and left ventricular remodeling two years after myocardial infarction: baseline predictors and impact of long-term use of captopril: information from the Survival and Ventricular Enlargement (SAVE) trial. *Circulation* **96**, 3294-3299.

138. Strijdom H, Muller C & Lochner A (2004). Direct intracellular nitric oxide detection in isolated adult cardiomyocytes: flow cytometric analysis using the fluorescent probe, diaminofluorescein. *J Mol Cell Cardiol* **37**, 897-902.
139. Swedberg K, Eneroth P, Kjeksus J & Wilhelmsen L (1990). Hormones regulating cardiovascular function in patients with severe congestive heart failure and their relation to mortality. CONSENSUS Trial Study Group. *Circulation* **82**, 1730-1736.
140. Tamura T, Onodera T, Said S & Gerdes AM (1998). Correlation of myocyte lengthening to chamber dilation in spontaneously hypertensive heart failure (SHHF) rat. *J Mol Cell Cardiol* **30**, 2175-2181.
141. Tamura T, Said S & Gerdes AM (1999). Gender-related differences in myocyte remodeling in progression to heart failure. *Hypertension* **33**, 676-680.
142. Tamura T, Said S, Harris J, Lu W & Gerdes AM (2000). Reverse remodelling of cardiac myocyte hypertrophy in hypertension and failure by targeting of the Renin-Angiotensin System. *Circulation* **102**, 253-259.
143. Tarone G & Lembo G (2003). Molecular interplay between mechanical and humoral signalling in cardiac hypertrophy. *Trends Mol Med* **9**, 376-382.
144. Thompson EW, Marino TA, Uboh CE, Kent RL & Cooper G 4th (1984). Atrophy reversal and cardiocyte redifferentiation in reloaded cat myocardium. *Circ Res* **54**, 367-377.
145. Toischer K, Rokita AG, Unsold B, Zhu W, Kararigas G, Sossalla S, Reuter SP, Becker A, Teucher N, Seidler T, Grebe C, Preub L, Gupta SN, Schmidt K, Lehnart SE, Kruger M, Linke WA, Backs J, Regitz-Zagrosek V, Schafer K, Filed LJ, Maier LS & Hasenfuss (2010). Differential cardiac remodelling in preload versus afterload. *Circulation* **122**, 993-1003.

146. Toyama T, Hoshizaki H, Seki R, Isobe N, Adachi H, Naito S, Oshima S & Taniguchi K (2003). Efficacy of carvedilol treatment on cardiac function and cardiac sympathetic nerve activity in patients with dilated cardiomyopathy: comparison with metoprolol therapy. *J Nucl Med* **44**, 1604-1611.
147. Trifunovic B, Norton GR, Duffield MJ, Avraam P & Woodiwiss AJ (1995). An androgenic steroid decreases left ventricular compliance in rats. *Am J Physiol Heart Circ Physiol* **268**, H1096-H1105.
148. Tsoetsi OJ, Woodiwiss AJ, Netjhardt M, Qubu D, Brooksbank R & Norton GR (2001). Attenuation of cardiac failure, dilatation, damage, and detrimental interstitial remodeling without regression of hypertrophy in hypertensive rats. *Hypertension* **38**, 846-851.
149. Udelson JM & Konstam MA (2002). Relation between left ventricular remodelling and clinical outcomes in heart failure patients with left ventricular systolic dysfunction. *J Card Fail* **8**, 465-471.
150. Vasan RS, Larson MG, Benjamin EJ, Evans JC & Levy D (1997). Left ventricular dilatation and the risk of congestive heart failure in people without myocardial infarction. *N Engl J Med* **336**, 1350-1355.
151. Veliotis DGA, Woodiwiss AJ, Deftereos DAJ, Gray D, Osadchii O & Norton GR (2005). Aldosterone receptor blockade prevents the transition to cardiac pump dysfunction induced by β -Adrenoreceptor activation. *Hypertension* **45**, 914-920.
152. Waagstein F (1993a). Beta blockers in heart failure. *Cardiology* **82** Suppl 3, 13-18.
153. Waagstein F, Bristow MR, Swedberg K, Camerini F, Fowler MB, Silver MA, Gilbert, EM, Johnson MR, Goss FG & Hjalmarson A (1993b). Beneficial effects of metoprolol in idiopathic dilated cardiomyopathy. Metoprolol in Dilated Cardiomyopathy (MDC) Trial Study Group. *Lancet* **342**, 1441-1446.

154. Wang X, Li F & Gerdes AM (1999). Chronic pressure overload cardiac hypertrophy and failure in guinea pigs: I. Regional hemodynamics and myocyte remodeling. *J Mol Cell Cardiol* **31**, 307-317.
155. Weber KT & Brilla CG (1991). Pathological hypertrophy and cardiac interstitium. Fibrosis and renin-angiotensin-aldosterone system. *Circulation* **83**, 1849-1865.
156. Weber KT, Brilla CG, Campbell SE, Guarda E, Zhou G & Sririam K (1993). Myocardial fibrosis: role of angiotensin II and aldosterone. *Basic Res Cardiol* **88** (suppl I), 129-137.
157. Weber KT, Brilla CG & Janicki JS (1990). Structural remodeling of myocardial collagen in systemic hypertension: Functional consequences and potential therapy. *Heart Failure* **6**, 129-137.
158. Weber KT, Janicki JS, Shroff SG, Pick R, Chen RM & Bashey RI (1988). Collagen remodeling of the pressure-overloaded, hypertrophied nonhuman primate myocardium. *Circ Res* **62**, 757-765.
159. Weisman HF, Bush DE, Mannisi JA, Weisfeldt ML & Healy B (1988). Cellular mechanisms of myocardial infarct expansion. *Circulation* **78**, 186-201.
160. Woodiwiss AJ & Norton GR (1995). Exercise-induced cardiac hypertrophy is associated with an increased myocardial compliance. *J Appl Physiol* **78**, 1303-1311.
161. Woodiwiss AJ, Tsotetsi OJ, Sprott S, Lancaster EJ, Mela T, Chung ES, Meyer TE & Norton GR (2001). Reduction in myocardial collagen cross-linking parallels left ventricular dilatation in rat models of systolic chamber dysfunction. *Circulation* **103**, 155-160.
162. Yarbrough WM, Mukherjee R, Stroud RE, Meyer EC, Escobar GP, Sample JA, Hendrick JW, Mingoia JT & Spinale FG (2010). Caspase inhibition modulates left

- ventricular remodelling following myocardial infarction through cellular and extracellular mechanisms. *J Cardiovasc Pharmacol* **55**, 408-416.
163. Yousef ZR, Redwood SR & Marber MS (2000). Postinfarction left ventricular remodelling: where are the theories and trials leading us? *Heart* **83**, 76-80.
164. Yussman MG, Toyokawa T, Odley A, Lynch RA, Wu G, Colbert MC, Aronow BJ, Lorenz JN & Dorn GW, 2nd (2002). Mitochondrial death protein Nix is induced in cardiac hypertrophy and triggers apoptotic cardiomyopathy. *Nat Med* **8**, 725-730.
165. Zafeiridis A, Jeevanandam V, Houser SR & Margulies KB (1998). Regression of cellular hypertrophy after left ventricular assist device support. *Circulation* **98**, 656-662.
166. Zierhut W, Zimmer H-G & Gerdes AM (1991). Effect of Angiotensin Converting Enzyme inhibition on pressure-induced left ventricular hypertrophy in rats. *Circ Res* **69**, 609-617.
167. Zimmer H-G, Gerdes AM, Lortet S & Mall G (1990). Changes in heart function and cardiac cell size with chronic myocardial infarction. *J Mol Cell Cardiol* **22**, 1231-1243.

APPENDICES
(Animal Ethics Screening Committee Clearance Certificates)

UNIVERSITY OF THE WITWATERSRAND, JOHANNESBURG

STRICTLY CONFIDENTIAL

ANIMAL ETHICS SCREENING COMMITTEE (AESC)

CLEARANCE CERTIFICATE NO. 2006/41/05

APPLICANT: Mr RJ Correia

SCHOOL: Physiology

DEPARTMENT:

LOCATION: Medical School

PROJECT TITLE: Do alterations in cardiac myocyte dimensions contribute to the development of cardiac dilation?


Number and Species

45 SHR and 45 WKY rats (all male)

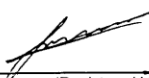
Approval was given for to the use of animals for the project described above at an AESC meeting held on 20060425. This approval remains valid until 20080224.

The use of these animals is subject to AESC guidelines for the use and care of animals, is limited to the procedures described in the application form and to the following additional conditions:

The minimum time between the two procedures must be 7 days

Signed:  Date: 04/05/06
(Chairperson, AESC)

I am satisfied that the persons listed in this application are competent to perform the procedures therein, in terms of Section 23 (1) (c) of the Veterinary and Para-Veterinary Professions Act (19 of 1982)

Signed:  Date: 04/05/06
(Registered Veterinarian)

cc: Supervisor: Professor AJ Woodiwiss
Director: CAS

Works 2000/1ain0015/AESCCert.wps

AESC 3

STRICTLY CONFIDENTIAL

UNIVERSITY OF THE WITWATERSRAND, JOHANNESBURG

ANIMAL ETHICS SCREENING COMMITTEE

CLEARANCE CERTIFICATE NO:

2002	39	5
------	----	---

APPLICANT: Professor G Norton

DEPARTMENT: School of Physiology

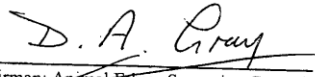
PROJECT TITLE: Effect of Antioxidant and an Aldosterone Receptor Antagonist On Cardiac Remodeling In Adrenergic- Mediated Cardiac Dilatation In Rats

Species	Number	Expiry Date
SHR (rats)	72	2004
WKY (rats)	48	2004

i) Approval is hereby given for the experiment described in the above application.

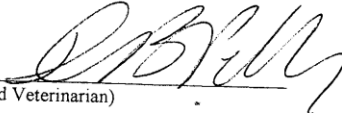
The use of these animals is subject to AESC Guidelines for the use and care of animals, is limited to the procedures specified in the application form, and to:

APPROVED

SIGNED 
(Chairman: Animal Ethics Screening Committee)

DATE: 2 May 2002

ii) I am satisfied that the persons listed in this application are competent to perform the procedures therein, in terms of Section 23(1)(c) of the Veterinary and Para-veterinary Professions Act (19 of 1982)

SIGNED 
(Registered Veterinarian)

DATE: 2 May 2002

NOTE:

First-time users of the CAS should contact the Director of the CAS in order to familiarise themselves with the facilities available, and the procedures required by the CAS for the carrying out of experiments.

UNIVERSITY OF THE WITWATERSRAND, JOHANNESBURG

ANIMAL ETHICS SCREENING COMMITTEE

CLEARANCE CERTIFICATE NO:

2002	37	5
------	----	---

APPLICANT: Professor G Norton

DEPARTMENT: School of Physiology

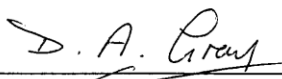
PROJECT TITLE: Effect of Pentoxifylline On Cardiac Remodeling In Adrenergic-Mediated Cardiac Dilatation In Rats

Species	Number	Expiry Date
Sprague dawley	48	2004
SHRs (rats)	48	2004
WKYs (rats)	48	2004

i) Approval is hereby given for the experiment described in the above application.

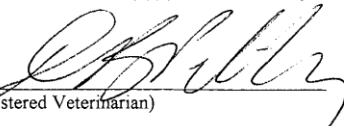
The use of these animals is subject to AESC Guidelines for the use and care of animals, is limited to the procedures specified in the application form, and to:

APPROVED

SIGNED 
(Chairman: Animal Ethics Screening Committee)

DATE: 2 May 2002

ii) I am satisfied that the persons listed in this application are competent to perform the procedures therein, in terms of Section 23(1)(c) of the Veterinary and Para-veterinary Professions Act (19 of 1982)

SIGNED 
(Registered Veterinarian)

DATE: 2 May 2002

NOTE:

First-time users of the CAS should contact the Director of the CAS in order to familiarise themselves with the facilities available, and the procedures required by the CAS for the carrying out of experiments.

AESC 3

STRICTLY CONFIDENTIAL

UNIVERSITY OF THE WITWATERSRAND, JOHANNESBURG

ANIMAL ETHICS SCREENING COMMITTEE

CLEARANCE CERTIFICATE NO:

99	1	2b
----	---	----

APPLICANT: Dr G Norton

DEPARTMENT: Physiology

PROJECT TITLE: Isoprenaline-induced cardiac remodelling: Role of myocardial cross-linked collagen

Species	Number	Expiry Date
Sprague-Dawley rats	90	27 January 2001
SHR rats	80	27 January 2001
WKY rats	80	27 January 2001

i) Approval is hereby given for the experiment described in the above application.

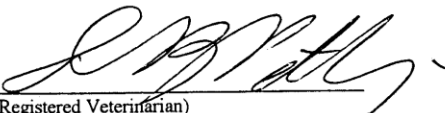
The use of these animals is subject to AESC Guidelines for the use and care of animals, is limited to the procedures specified in the application form, and to:

Nil.

SIGNED 
(Chairman: Animal Ethics Screening Committee)

DATE: 27 January 1999

ii) I am satisfied that the persons listed in this application are competent to perform the procedures therein, in terms of Section 23(1)(c) of the Veterinary and Para-veterinary Professions Act (19 of 1982)

SIGNED  DATE:

(Registered Veterinarian)

NOTE:

First-time users of the CAS should contact the Director of the CAS in order to familiarise themselves with the facilities available, and the procedures required by the CAS for the carrying out of experiments.

AESC 3

STRICTLY CONFIDENTIAL

UNIVERSITY OF THE WITWATERSRAND, JOHANNESBURG

ANIMAL ETHICS SCREENING COMMITTEE

CLEARANCE CERTIFICATE NO:

97	44	5
----	----	---

APPLICANT: Dr G Norton

DEPARTMENT: Physiology

PROJECT TITLE: The influence of an atriopeptidase inhibitor on cardiac morphology and performance in hypertensive heart disease


Species	Number	Expiry Date
Spontaneously hypertensive rats	40	29 May 1999
Wistar Kyoto rats	20	29 May 1999
SD rats	90	29 May 1999

First-time users of the CAS should contact the Director of the CAS in order to familiarise themselves with the facilities available.

The use of these animals is subject to AESC Guidelines for the use and care of animals, to the procedures specified in the application form, and to:

- a) the animals being monitored daily for the first three weeks of the experimental period, and thereafter once weekly;
- b) the end-point regarding weight loss being that should a rat lose more than 15% of its body weight, it will be euthanased.

SIGNED


(Chairman: Animal Ethics Screening Committee)

DATE: 29 May 1997

Please see attachment: